Exploring the role of AIB1 and FOXA1 in mammary tumorigenesis using transgenic mouse models
Ву
Sierra Mariette Lusson
A thesis submitted to McGill University in partial fulfillment of the requirements of the degree of Master of Science in Biochemistry
©Sierra Mariette Lusson 2022
Department of Biochemistry
McGill University
August 2022

# TABLE OF CONTENTS

ABSTRACT	
RÉSUMÉ	6
ACKNOWLEDGEMENTS	8
CONTRIBUTION OF AUTHORS	10
LIST OF FIGURES AND TABLES.	11
LIST OF ABBREVIATIONS	12
1. INTRODUCTION	16
1.1 Breast cancer	16
1.1.1 Breast Cancer Prevalence	
1.1.2 Mammary gland structure and development	
1.1.3 Histological subtypes of breast cancer	
1.1.4 Molecular Subtypes of Breast cancer	19
1.2 ER in Luminal Breast Cancers	21
1.2.1 ER Structure and Function	
1.2.2 Isoforms of ER	22
1.2.3 ER Signaling	23
1.2.4 ER Targeted Therapies	23
1.2.5 Drug Resistance and ER Positive Tumor Relapse	
1.2.5.1 Alteration of Regulatory Elements	
1.2.5.2 Mutations in ER	26
1.3 AIB1 in Breast Cancer	27
1.3.1 AIB1 Structure and Function	27
1.3.2 Posttranslational Modifications of AIB1	28
1.3.3 AIB1 and ER Transcriptional Activity	29
1.3.4 AIB1 in Luminal Breast	29
1.3.4.1 AIB1 Overexpression	29
1.3.4.1.1 Hormone-Independent AIB1 Signaling	30
1.3.4.1.2 AIB1 and Tamoxifen Resistance	30
1.3.5 Mouse Models of AIB1	31
1.4 FOXA1 in Breast Cancer.	32
1.4.1 FOXA1 Structure and Function	32
1.4.1.1 FOXA1 Function in Mammary Glands	33
1.4.2 Regulation of FOXA1	
1.4.3 FOXA1 in Luminal Breast Cancer	
1.4.3.1 FOXA1 and ER Signaling	
1.4.3.2 FOXA1 and Breast Cancer Patient Survival	
1.4.4 Mouse models of FOXA1	
1.5 Mouse Models of Breest Cancer	37

1.5.1 MMTV	37
1.5.1.1 MMTV-PyMT	
1.5.2 Cre Recombinase/loxP System.	
1.5.3 rtTA/TetO System	
1.5.4 Mouse Models of ER	
1.5.4.1 TetO-ER	
1.5.4.2 KI ESR1 Y541S	
1.6 Experimental Rational	40
2. RESULTS AND DISCUSSION	42
2.1 Characterizing novel AIB1 and FOXA1 overexpression mouse models AIC and FIC	42
2.1.1 Experimental Rational and Generation of AIC and FIC Constructs	
2.1.2 Generating Transgenic AIC and FIC Founder Animals	
2.1.3 Early Characterization of Novel AIC Founder Lines	
2.1.3.1 Exploring longer Dox inductions in different AIC founder lines	
2.1.4 Early Characterization of Novel FIC Founder Lines	
2.1.4.1 Exploring longer Dox inductions in FIC model	
2.1.4.2 Exploring FOXA1 overexpression in organoid culture	
2.2 Future Directions	
2.2.1 Further characterization of AIC and FIC mouse models	
2.2.2 Exploring the role of overexpressed AIB1 and FOXA1 in mammary gland develop	
2.2.3 Exploring the role of overexpressed AIB1 and FOXA1 in the context of a mutant E	
2.2.4 Exploring genes involved in AIB1 and FOXA1 driven tumorigenesis	76
3. MATERIALS & METHODS	77
3.1 Transgenic Animals.	
3.1.1 Mouse Husbandry	
3.1.2 Doxycycline Induction	
3.1.3 Mammary Tumor Monitoring	
3.1.4 Tissue Sample Processing	
3.1.4.1 Wholemounts	
3.2 DNA Analysis	
3.2.1 Tail DNA Extraction	
3.2.2 Genotyping	79
3.3 Tissue Culture	80
3.3.1 General Cell Culture	
3.3.2 Tissue Dissociation and Epithelial Cell Isolation	
3.3.3 FACS analysis	
3.3.4 Organoid Culture	
3.4 Protein Analysis.	
3.4.1 Protein extraction	
3.4.2 Immunoblotting	
3.4.3 Immunohistochemistry (IHC)	
3.4.4 Immunofluorescence (IHF).	83

3.5 RNA Analysis	84
3.5.1 RNA extraction and cDNA synthesis	
3.5.2 RT-qPCR	
3.6 Statistical Analysis	
4. REFERENCES	0.4

#### **ABSTRACT**

Worldwide, breast cancer is the leading malignancy diagnosed in women accounting for roughly 23% of all cancer cases. Furthermore, breast cancer is the leading cause of cancer related death in women; ER-positive breast cancers being the most lethal of the subtypes. Currently, endocrine treatment is available for breast cancers over expressing the ER, however, patients often develop a resistance to this therapy and relapse after prolonged exposure with high rates of ESR1 mutation occurrences. Mutant ERs have enhanced levels of ER transcriptional activity leading to increased cell proliferation and tumor development. AIB1, a steroid receptor coactivator, interacts with ER in a ligand-dependent fashion to enhance estrogen-dependent transcription and overexpression of AIB1 in AIB1-tg mice was sufficient to drive tumorigenesis. Additionally, transfection studies identified AIB1 as a molecular player in endocrine resistance whereby tamoxifen behaves like an estrogen agonist in ER-positive breast cancer cells that express elevated levels of AIB1, and knockdown of AIB1 restores antitumor effects of tamoxifen. ERdriven transcription is also heavily regulated by pioneer factor FOXA1 whereby knockdown of FOXA1 in MCF-7 tumor cells significantly reduced ER chromatin binding events. Silencing FOXA1 in tamoxifen resistant breast cancer cells significantly reduced ER binding and proliferation suggesting FOXA1 is necessary for hormone independent growth in tamoxifen resistant cancers. In our study, we aim to elucidate the role of ER in luminal breast cancer, specifically exploring members of the ER transcriptome; AIB1 and FOXA1. To understand the role of oncoproteins AIB1 and FOXA1 in early ER positive breast cancer, we have generated two novel inducible mouse models overexpressing AIB1 and FOXA1. AIB1 and FOXA1 genes are expressed under the Tet-Operon and linked to Cre recombinase via IRES then subsequently crossed into the MTB construct to generate AIC/MTB and FIC/MTB mice. Early characterization of the novel models shows positive expression of our transgene within multiple founder strains. Within AIC/MTB mice, RT-qPCR and western blotting analysis show AIB1 mRNA and protein overexpression in our founder lines 1 and 3 following dox induction. AIC virgin mice overexpressing AIB1 had abnormal mammary gland development with significantly greater alveolar budding following

8-week dox induction. Overexpression of FOXA1 mRNA and protein have been shown within founder lines 1 and 3 of our FIC/MTB cohorts. FIC mice show abnormal mammary gland development in virgin glands following a 1-week induction, where glands have reduced ductal development. Additionally, FIC models show tumorigenic capacity, whereby FOXA1 overexpression within FIC mammary-derived organoids drove organoid hypertrophy. While much more characterization work remains to be done, my thesis shows a promising start to successful AIB1 and FOXA1 overexpression luminal breast cancer mouse models. The AIC and FIC models will eventually be crossed into the ESR1 Y541S model to investigate the role of AIB1 and FOXA1 in endocrine resistance in the context of a mutated ER. This exploration will hopefully provide a better understanding of escape mechanisms adopted by mutant ER.

# RÉSUMÉ

Le cancer du sein est le cancer le plus diagnostiqué chez les femmes du monde entier, représentant environ 23% de tous les cas. De plus, le cancer du sein est la principale cause de mortalité lié au cancer chez les femmes. Les cancers du sein ER (récepteur d'estrogène) -positifs est le plus mortel des sous-types. Actuellement, un traitement endocrinien est disponible pour les cancers du sein sur-exprimant l'ER, cependant, les patientes développent souvent une résistance à cette thérapie et rechutent après une exposition prolongée avec des taux élevés d'apparition de mutations ESR1. Les ER mutants ont des niveaux accrus d'activité transcriptionnelle, conduisant à une prolifération cellulaire accrue et au développement de tumeurs. AIB1, un coactivateur des récepteurs stéroïdiens, interagit avec ER de manière dépendante du ligand pour améliorer la transcription dépendante à l'œstrogène et la surexpression de AIB1 chez les souris AIB1-tg est suffisante pour entraîner l'apparition de tumeurs. De plus, des études de transfection ont identifié AIB1 comme un acteur moléculaire de la résistance endocrinienne pour lequel le tamoxifène se comporte comme un agoniste l'œstrogène dans les cellules cancéreuses ER-positives qui expriment des niveaux élevés d'AIB1. En plus, l'inactivation d'AIB1 dans ces cellules restaure les effets antitumoraux du tamoxifène. La transcription dirigée par les ER est également fortement régulée par le facteur pionnier FOXA1. Inactivation de FOXA1 dans les cellules tumorales MCF-7 a considérablement réduit les événements de liaison à la chromatine des ER. Enlever l'expression FOXA1 dans les cellules cancéreuses du sein résistantes au tamoxifène a considérablement réduit la liaison et la prolifération des ER, ce qui suggère que FOXA1 est nécessaire à la croissance indépendante des hormones dans les cancers résistants au tamoxifène. Dans notre étude, nous visons à élucider le rôle de ER dans le cancer du sein luminal, en explorant spécifiquement les membres du transcriptome de l'ER; AIB1 et FOXA1. Pour comprendre le rôle des oncoprotéines AIB1 et FOXA1 dans le cancer du sein précoce ER positif, nous avons généré deux nouveaux modèles murins inductibles surexprimant AIB1 et FOXA1. Les gènes AIB1 et FOXA1 sont exprimés sous l'opéron Tet et liés à la recombinase Cre via IRES puis ensuite croisés dans la construction MTB pour générer des souris

AIC/MTB et FIC/MTB. La caractérisation précoce des nouveaux modèles montre une expression positive de notre transgène au sein de plusieurs souches fondatrices. Chez les souris AIC/MTB, les analyses RTqPCR et IHC montrent une surexpression de l'ARNm et des protéines AIB1 dans nos lignées fondatrices 1 et 3 après induction de la doxicycline (dox). Les souris vierges AIC surexprimant AIB1 présentent un développement anormal de leurs glandes mammaires avec un bourgeonnement alvéolaire significativement plus important après une induction à la dox de 8 semaines. La surexpression de l'ARNm et de la protéine FOXA1 a été démontrée dans les lignées fondatrices 1 et 3 de nos cohortes FIC/MTB. Les souris FIC présentent un développement anormal des glandes mammaires vierges après une induction d'une semaine, où les glandes présentent une réduction de leur développement canalaire. De plus, les modèles FIC montrent une capacité tumorigène, la surexpression de FOXA1 dans les organoïdes dérivés du sein FIC entraînant une hypertrophie organoïde. Bien qu'il reste encore beaucoup de travail de caractérisation à faire, ma thèse montre un début prometteur pour des modèles réussis de cancer du sein luminal de surexpression de AIB1 et FOXA1. Les modèles AIC et FIC seront éventuellement croisés avec le modèle ESR1 Y541S pour étudier le rôle de AIB1 et FOXA1 dans la résistance endocrinienne dans le contexte d'un ER muté. Cette exploration fournira une meilleure compréhension des mécanismes d'échappement adoptés par le mutant ER.

#### **ACKNOWLEDGEMENTS**

My thesis would not have been possible without the support and guidance of countless people within my community. To begin I would like to acknowledge my supervisor Bill, you have welcomed me into your lab during the mayhem of COVID. I am deeply grateful to you for accepting me into your lab and allowing me the opportunity to exercise my scientific curiosity. I am additionally thankful for your guidance and support throughout my MSc. Next, I would like to express my gratitude to the members of my research advisory committee; Dr. Vincent Giguère and Dr. Daniela Quail. I sincerely appreciate your feedback and guidance of my research.

To acknowledge my University of Alberta undergraduate advisors and professors Dr. Adrienne Wright, Dr Rachel Milner, and Dr. Jonathan Parrish, who have counseled my decision to continue my career in academia. Thank you for inspiring my curiosity of biochemistry, for encouraging determination, and guiding me towards such a rewarding program.

My most earnest appreciation and gratitude to the Muller lab for which my MSc would not have been possible. Foremost to Bin, thank you for sharing your passion for cancer and research with me. I am incredibly grateful for your mentorship and guidance of my project. Thank you for making my MSc such a rewarding experience and I look forward to destroying you in badminton in the future. To Ippy, my mentor and dear friend; I can honestly say that without you I could not have completed my thesis so smoothly. From your supportive counsel to invaluable friendship, you have made my time here that much more enjoyable. Thank you for inspiring me with your compassion and enthusiasm and for sharing your nerdom; you're a nat 20 to me <3 To Gabriella, thank you for mentoring me and integrating me into the lab. To Alice, thank you for always making me laugh, and for all your help with this project. To Adeline, I've enjoyed sharing our French heritage and a big thank you for your help editing the French abstract of this thesis. To Hailey, for your willingness to help me out in a time crunch. To Linshan and Tung, thank you for your contributions to this project, your organoid expertise and your counsel are invaluable. To Vasilios, thank you for integrating me into the lab, and for all your help with my mouse work. To

Virginie, thank you for practicing French with me, and for all your work in my project. To Dongmei, for your expert advice and counsel in IHC and for all your sweet compliments. To the other members of the lab, I have not personally mentioned, you have all helped with this project in some manner, whether giving me advise, helping me with an experiment, teaching me the layout of the lab, sharing your stories and your passions, and being so welcoming, I would like to express my sincerest and profound gratitude.

Lastly, I would like to express my gratitude to my family and friends, who have always supported my passions and ambitions. Mom, thank you for being my rock, my biggest fan, and for your unconditional love and support. Your selflessness, dedication, and resilience will always be my greatest inspiration, I love you forever. Papa, thank you for supporting me in all my endeavors, and for teaching me endurance, grit, and hard work. Your diligent work ethic and enduring love has encouraged me to keep forging ahead, je t'aime toujours. To my siblings; Nadine, Francis, Felix, Coco, and Taya, thank you for being my most loyal supporters and for shaping the character I am today. From inspiring my creativity to encouraging fearlessness and ambition through all our crazy adventures on the farm, I am incredibly grateful and proud to be your sister. Thank you all for always having my back, love you guys always. To my dear friends, thank you for being a source of love, encouragement, and inspiration, I am so fortunate to share your friendship.

My MSc. experience, while at times incredibly challenging, has been a highly rewarding and enriching experience. Thank you to everyone who made this possible. Moving forward, I am excited to exercise my newly obtained knowledge, and skills achieved throughout my degree.

### CONTRIBUTION OF AUTHORS

I hereby state that I have carried out the work presented in this thesis unless stated otherwise.

#### **Animal models**

Dr. Bin Xiao and Gabriella Johnson carried out much of the cloning work for both the FIC and AIC constructs, generating TetO-IRES-Cre-SV40 construct for the AIB1 and FOXA1 models.

ESR1 Y541S mutant mice were inherited from Gabriella Johnsons original cohort.

McGill transgenic animal core injected FVB mice with FIC and AIC constructs and weaned the first litter of transgenic pups.

Dr. Chen Ling generated the ESR1Y541S mouse model.

Dr. Bin Xiao helped expand founder 3 AIC/MTB cohort and helped necropsy 8-week induction experimental mice.

Alice Nam helped wean and genotype litters of the AIC-3/MTB cohort.

Dr. Lewis Chodosh provided the MTB strain.

### Technical assistance and data analysis

Vasilios Papavasiliou extracted sperm from founder 1 and founder 3 AIC and FIC founders.

Hailey Proud and Dongmei Zuo performed AIB1 and FOXA1 IHF staining (Fig. 2-5B., Fig. 2-7C)

Linshan Liu grew AIC and FIC organoids and performed staining (Fig. 2-10)

Paraffin-embedding, sectioning, and H&E staining was done by the Goodman Cancer Institute Histology Core.

Dr. William Muller and Dr. Alain Nepveu reviewed this thesis.

# LIST OF FIGURES AND TABLES

Figure 1-1: Schematic of KI ESR1 Y541S and Cre mediated excision of floxed Neo cassette and mutant exon 9 to generate mutant ER
Figure 2-1: Schematic of the AIC, FIC, and MTB constructs, and the AIC/MTB and FIC/MTB crosses.44
Figure 2-2: Simplified Schematic of the AIC and FIC Transgenic Founder Animal Production46
Figure 2-3: Image of genotyping PCR of AIC and FIC transgenic founder animals
Figure 2-4: Schematic of early AIC and FIC founder line characterization
Figure 2-5: Exploring transgene expression in different founder lines of AIC in mouse mammary epithelium following 1-week and 2-week Dox induction
Figure 2-6: 8-week induced pregnant and virgin AIC/MTB express AIC transgene in mammary glands
Figure 2-7: Exploring transgene expression in mouse mammary epithelium following 1-week Dox induction of different founder lines of the FIC model
Figure 2-8: 8-week induced pregnant and virgin FIC/MTB mice express the FIC transgene in mammary glands
Figure 2-9: 8-week induced virgin FIC-2/MTB mice express FIC transgene in mammary glands69
Figure 2-10: 10-week Dox-induced organoids grown from FIC-1/MTB and FIC-3/MTB mammary epithelia
Figure 2-11: Schematic of AIC/MTB and FIC/MTB cross into ER mutant model ESR1Y537S75
Figure 2-12: Employment of inducible CRISPR/Cas9 system to explore genes relevant to AIB1 and FOXA1 tumorigenesis
Table 3-1: 1X PCR master mix
Table 3-2: Genotyping primer sequences and PCR thermal cycling conditions
Table 3-3: Primary antibody summary used for varying protein analysis
Table 3-4: RT-qPCR primer sequences85

### LIST OF ABBREVIATIONS

ACTR Activator of thyroid hormone and retinoid receptor

AD1 Activation domain 1

AD2 Activation domain 2

ADH Atypical ductal hyperplasia

AF-1 Ligand-independent AF-1 transactivation domain

AF-2 Ligand-dependent AF-2 transactivation domain

AIs Aromatase inhibitors

AIB1 Amplified in breast cancer 1

ALH Atypical lobular hyperplasia

aPKC Atypical protein kinase C

BHLH/PAS Basic helix-loop-helix/Per-ARNT-Sim

bp Base pair

BRCA1 Breast Cancer gene 1

BRCA2 Breast Cancer gene 2

CBP Cyclic AMP response element-binding protein

CCAC Canadian Council on Animal Care

Cdk2 Cyclin-dependent kinase 2

DBD DNA binding domain

DCIS Ductal carcinoma in situ

diH20 Deionized water

DNA Deoxyribonucleic acid

E2F1 E2F transcription factor 1

EGFR Epidermal growth factor receptor

ERα Estrogen Receptors Alpha

ERβ Estrogen Receptors Beta

FACS Fluorescence-activated cell sorting

FISH Fluorescence in situ hybridization

FNDR Founder

FOXA1 Forkhead box protein A1

FVB Friend leukemia virus B

GATA3 GATA binding protein 3

GCI Goodman Cancer Institute

GEMM Genetically engineered mouse models

GRB7 Growth factor receptor bound protein 7

GREB1 Growth regulation by estrogen in breast cancer 1

HAT Histone acetyltransferase domain

HER2 Human epidermal growth factor receptor 2

H&E Hematoxylin and Eosin

HNF $3\alpha$  Hepatocyte nuclear factor  $3\alpha$ 

HR Hormone receptor

Hsp90 Heat shock protein 90

iCas9 Inducible Cas9 system

IF Immunofluorescence

IGF-1 Insulin-like growth factor 1

IHC Immunohistochemistry

IRES Internal ribosome entry site

KI Knock-in

KO Knock out

L Leucine

LA Lobulo-alveolar

LBD Ligand binding domain

LCIS Lobular carcinoma in situ

LoxP Locus of Crossover P1

LSD1 Lysine-specific demethylase 1

LTR Long terminal repeat

MAPK Mitogen-activated protein kinase

MG Mammary glands

MMTV-PyMT Mammary specific polyomavirus middle T antigen overexpression mouse model

NCOA Nuclear receptor co-activators

NCoA-3 Nuclear receptor coactivator-3

NCOR Nuclear receptor co-repressors

NID NR Interaction domain

NLS Nuclear localization signal

NMuMG Nontransformed mouse mammary gland epithelial cell line

NR Nuclear receptors

NS No significance

OVX Ovariectomies

PBS Phosphate buffered saline

PR Progesterone receptor

PTMs Posttranslational modifications

PyMT Murine polyomavirus

Q Glutamine

RAC-3 Receptor associated coactivator 3

rcf Relative centrifugal force

RIPA Radioimmunoprecipitation assay

RNA Ribonucleic acid

RT Room temperature

S Serine

SAg Superantigen

SERDs Selective ER degraders

SERMs Selective ER modulators

Serpinal  $\alpha$ 1-Antitrypsin

sgRNAs Single guide RNA

shRNA Short hairpin RNA

siRNA Small interfering RNA

SRC Steroid receptor coactivator

TADs Transactivation domains

TEB Terminal end buds

TDLU Terminal ductal lobular unit

Tet-O Tetracycline dependent operator

Ttr Transthyretin

WHO World health organization

WT Wild type

X Any amino acid

Y Tyrosine

#### 1 INTRODUCTION

## 1.1 Breast Cancer

#### 1.1.1 Breast Cancer Prevalence

Worldwide, breast cancer is the leading malignancy diagnosed in women [5] accounting for roughly 23% of all cancer cases [11]. Within Canada, 1 in 8 women are diagnosed every year with breast cancer, and of this population, 1 in 33 will pass away from the disease making it the second leading cause of cancer related deaths [13]. While there is no single-one cause of breast cancer, many factors may contribute to the development of the disease, including age, obesity, and mutations in BRCA1 and BRCA2 genes [13]. While statistics of breast cancer induced mortality are gradually declining on account of early detection and advancement in treatment, there is still a significant discrepancy in the understanding of treatment evasion, early breast cancer development, recurrence, and new molecular players [13][14]. It is therefore critical to continue the investigation of breast cancer development, treatment, and evasion to efficiently diagnose, treat, and prevent breast cancer development in human patients.

## 1.1.2 Mammary Gland Structure and Development

The mammary gland is a unique and dynamic organ within mammals which primarily functions to produce and secrete milk for offspring nourishment [18]. While the mammary gland begins development during puberty, it does not reach full developmental maturity until pregnancy in which hormonal regulation drives the milk synthesis and secretion within the organ [18]. The mammary gland is unique in its plasticity whereby the organ cycles through this functional and nonfunctional state through tight hormonal regulation [18]. Throughout the various stages of development including puberty, pregnancy, lactation, and involution, the mammary gland undergoes significant changes in gene expression leading to morphological, functional, and physiological changes [18].

Within the female mammary gland, exists several structures necessary for the functional capacity of the organ. The mammary gland glandular tissue, a secretory tissue lining organs, plays a key role in the secretory function of the mammary gland and is composed of both branching ducts and terminal secretory lobules [19]. Alveoli composes the mammary ducts, and structurally form milk-producing cavities lined by myoepithelial cells [95]. Clusters of alveoli are termed lobules and are connected to the nipple by lactiferous ducts responsible to carrying and releasing milk to the suckling infant [95]. A single mammary gland is composed of 10-20 lobules [95]. While the mammary gland is composed of many cell types, including adipose and lymphocytes, the functional glandular tissue is predominantly composed of epithelial cells [20]. Mammary epithelium composes the branching ducts which stem from the nipple and branch into the surrounding adipose tissue [20]. The branching ducts grow from branching terminal end buds that are composed of progenitor stem cells to form discrete triangular lobes that have separate ductal systems [20]. The terminal end buds also have the potential to mature as lobules and ultimately provide the matured function of the mammary gland which is to produce and secrete milk [20]. Majority of breast cancers arise within the mammary epithelium on account of the organ's high sensitivity to hormonal regulation and the high proliferative stem cell population [20].

The development, structure, and function of the human mammary gland shares comparable properties with that of mice [20]. The mouse mammary gland has thereby become a useful tool for understanding human breast cancer functioning as an animal model [20]. While the mammary gland is comparable within the two species, mouse mammary has unique structures different to that of the human organ. While the human female has two mammary glands located on the anterior chest wall, mice have 5 bilateral pairs situated at various locations between the neck and inguinal regions [20]. The first pair, typically denoted as pair 1, is located in the neck region, pairs 2 and 3 on the anterior chest wall, pair 4 on the abdominal wall, and finally pair 5 at the inguinal region [20]. Both human and mouse mammary epithelium contain progenitor stem cells that function to grow branching terminals and are responsible for the secretory properties of the organ, however, the functional portion of the mouse mammary is termed

the lobulo-alveolar (LA) while in humans it is termed the terminal ductal lobular unit (TDLU) [20]. Both the TDLU and LA are sensitive to hormones and primary locations for breast cancer disease development [20].

## 1.1.3 Histological Subtypes of Breast Cancer

Breast cancer is a heterogeneous disease that can begin in many different areas of the breast, including the ducts and lobules, and has distinct features and characteristics throughout disease progression [15]. Distinct histological features have been identified within these diverse types, and various stages which have led to the classification of breast cancer into histological subtypes by WHO [17]. The diverse types of breast cancer are denoted based on their histological grade and level of invasiveness, and it is important to distinguish between these subtypes because they have different prognoses and treatment implications [16]. According to these histological classifications, breast cancer can be broadly categorized into two main subtypes: carcinomas and sarcomas [16]. Carcinomas are the most common breast cancers arising from epithelial cells which are cells that line the lobules and terminal ducts responsible for producing milk [96]. Sarcomas originate from stromal cells which are connective tissue cells and are much more rare accounting for less than 1% of breast cancers [96]. Within the large group of carcinomas, breast cancers can be further divided into three major groups: non-invasive (or in situ), invasive, and metastatic breast cancers [96]. The disease begins as atypical ductal hyperplasia (ADH) and atypical lobular hyperplasia (ALH) in which atypical cell growth occurs within ducts or lobules [22]. The disease progresses into in-situ carcinomas which are further categorized into ductal and lobular subclasses; ductal carcinomas the most common at roughly 80% [24] originating within breast ducts, and lobular carcinomas accounting for approximately 15% [24] and originating in mammary lobules [21]. Non-invasive carcinomas are premalignant lesions that have the malignant property of uncontrolled cell growth; however, they are considered premalignant due to their lack of invasive properties [22]. During initial stages of the disease, cancer cells remain confined within the basement membrane, upon the breaking of this membrane, they are classified as invasive breast carcinomas (IBC)

in which the cancerous cells invade surrounding breast tissue [22]. IBC is the most common subtype in which over 90% of all breast cancers are categorized into invasive subtypes [96]. The final stage of disease progression is metastatic carcinomas in which cancer cells invade and spread from the primary site to other sites of the body [22], including lungs (11%), bones (40%0, liver (7%), and brain (2%) [23].

# 1.1.4 Molecular Subtypes of Breast Cancer

To address the therapeutic predictivity limitations of histological classifications of breast cancer, the disease has been further studied to identify molecular markers defining the various stages of breast cancer [21]. Through the use of microarray- based gene expression profiling, breast cancer has been characterized into five major intrinsic molecular subtypes, including Luminal A, luminal B, Her-2 overexpression, normal-like, and Basal-like breast cancer [8]. Through gene expression profiling specific gene expression patterns were identified within the different molecular subtypes, providing rational to the fundamental differences between tumors at the molecular level [15]. The molecular subtypes of breast cancer are denoted by the expression of specific biomarkers, which control how the cells behave and their treatment implications [8]. Furthermore, overall survival and disease-free survival of patients varies significantly between the varying molecular subtypes [21]. The identification of these biomarkers has been critical in clinical practice to determine how to accurately and successfully treat patients diagnosed with varying subtypes of breast cancer [21].

Luminal breast cancers are hormone receptor (HR) positive accounting for roughly 70% of all breast cancers; hormone receptors including estrogen receptor (ER) and progesterone receptors (PR) [27]. Luminal breast cancers are further subclassed into Luminal A and Luminal B breast cancers [15], Luminal A being the most common at about 30% of all breast cancers, Luminal B accounting for approximately 20% [26]. Luminal A breast cancers like Luminal B, are HR positive, meaning they express ER or PR, however, are human epidermal growth factor receptor 2 (HER2) negative [15]. Compared to Luminal B, Luminal A breast cancers are generally lower grade on account of decreased expression of proliferation related genes including Ki-67, a cell cycle antigen that is a key marker of

proliferation [15]. Luminal A cancers tend to grow more slowly than other cancers, are of lower grade, therefore, have a better clinical prognosis [15]. Luminal B breast cancers are HR-positive and HER2-positive with higher expression levels of Ki-67 than luminal A [15]. Luminal B cancers consequentially tend to grow faster than luminal A cancers and have a worse prognosis [15]. Clinal treatment of Luminal classified breast cancers typically consist of HR targeted drug therapy to reduce HR associated growth signaling [15]. While Luminal B has a worse prognosis than Luminal A, Luminal cancers overall have better clinical prognosis than all other molecular subtypes [26].

Normal-like breast cancer is ER-positive, HER2-positive, any level of Ki-67 expression, and may be progesterone receptor (PR)-positive or PR-negative [15]. This subtype tends to grow faster than luminal A cancers and has a slightly worse prognosis [15].

HER 2 overexpression breast cancers are the molecular subtypes with an HR-negative and HER2-positive gene expression profile and represent approximately 20% of all breast cancers [26]. Her2 overexpression classified tumors over express genes within the HER2 amplicon, including the growth factor receptor bound protein 7 (GRB7) gene associated with cell growth [15, 29]. While HER2 overexpression tumor development has not been associated with specific risk factors [28], the subtype grows faster than the Luminal subtype resulting in poorer worse prognosis [15].

Breast tumors classified as basal (triple-negative) are both HR-negative, and HER2-negative, representing roughly 15% of all breast cancers [26]. The gene expression profile of basal tumors is similar to that of basal epithelial cells which have low expression of HR and HER and high expression of proliferation markers such as Ki-67 [15]. Unlike other molecular subtypes, Basal breast cancers are most commonly diagnosed in young, pre-menopausal women, and more frequently in African American populations [30]. The basal molecular subtype characteristically is aggressive in nature, with no standard therapy available to patients in clinic [15]. As a result, basal tumors are high grade and carry the most severe prognosis of all other molecular subtypes [15].

#### 1.2 ER in Luminal Breast Cancers

#### 1.2.1 ER Structure and Function

In Luminal molecular subtypes of breast cancer, the estrogen receptor (ER) is over expressed in roughly 70% of tumors [31]. The ER has subsequently become a critical target of investigation to better understand the development and progression of HR positive Luminal breast cancers. The ER is a member of the broad nuclear receptor [NR] superfamily; one of the largest transcription factor groups with over 40 identified members [32]. Nuclear receptors (NR) function to regulate numerous physiological processes including cell proliferation and metabolism, thereby acting as integral players in cancer development and progression [33]. The NR family is unique from other transcription factors in their binding of lipophilic ligands, like steroids, which induce conformational changes affecting downstream activity [33]. Members of the NR superfamily share several distinct structural characteristics including highly conserved ligandindependent AF-1 transactivation domain (AF-1), ligand-dependent AF-2 transactivation domain (AF-2), and DNA binding domain (DBD) [32]. The DNA binding property of NRs is possible through the highly conserved DNA binding domains which consists of two zinc fingers responsible for the recognition and binding of specific DNA sequences within the genome [32]. The ligand binding domain (LBD) of NR is functionally the most important domain owing to the LBD housing of AF-2, the ligand binding site, and interaction sites for coactivators and corepressors [34]. The AF-2 domain was determined to be critical for ligand dependent activation of NR when initially discovered in mouse ER $\alpha$  where the deletion of a portion of the LBD's C terminus, now known as AF-2, halted ligand dependent activation of ER [35]. Located within the N-terminus of NR is the activation domain AF-1 which is the least conserved domain among all NR [35]. While the structure of AF-1 varies among members of NR superfamily, AF-1 functions to activate transcription of target genes through the recruitment of coactivators [35].

The ligand-dependent activity of the steroid nuclear receptor ER is driven by the sex hormone estrogen, which drives the development and physiological function of the human reproductive system [36]. The ER thus plays a critical role in regulating the growth and development of the human

reproductive system including the development and growth of breast epithelial cells [12]. Specifically, ER regulates the transcription of target genes by binding to estrogen response elements (EREs) in the DNA sequence via its DBD [12]. This binding activity causes the DNA to bend allowing for interaction of transcription machinery and coactivators [12].

### 1.2.2 Isoforms of ER

There are two identified subtypes of ER: ER $\alpha$  and ER $\beta$  [10]. Estrogen signaling is dependent on the levels of both subtypes, where it can be inhibited or stimulated depending on the expression levels between ER $\alpha$  and ER $\beta$  [36]. Both subtypes are expressed in breast tissue, and both are necessary for ER function [10], however, knockout studies in mouse models have identified distinct biological functions of ER $\alpha$  and ER $\beta$  [36]. The different subtypes are encoded by different genes on different chromosomes; ER $\alpha$  is encoded by ESR1 gene on chromosome 6, while ER $\beta$  is encoded by the ESR2 gene on chromosome 14 [37]. The different subtypes are both expressed in breast tissue, however, ER $\alpha$  expression is limited to luminal cells while ER $\beta$  is expressed in many different cells including luminal cells and adipose [10]. Another crucial difference comparing the isoforms lies within the AF-1 domain which plays a critical role in ER signaling activity and is necessary for interacting with coactivators of ER [26]. The AF-1 domain has only a 30% conserved identity between ER $\alpha$  and ER $\beta$ , with ER $\beta$  having the lowest AF-1 activity [36]. Finally, ER $\alpha$  and ER $\beta$  have distinct biological functions with divergent downstream signaling pathways and transcriptional activity [36]. The ER $\alpha$  is the principal receptor for estrogen function in the breast [10] and henceforth will be referred to as ER.

## 1.2.3 ER Signaling

To prevent degradation of unbound ERs, heat shock protein 90 (Hsp90) binds and stabilizes ER in the absence of estrogen [38]. In the presence of estrogen, the ER undergoes estrogen dependent

signaling in which estrogen binds the ligand binding site within the LBD, driving dimerization of the ER following the phosphorylation of serine (S) within AF-1 domain [36]. The ER is then transported to the nucleus where it acts as a transcription factor [36]. ER regulates the transcription of target genes by binding to estrogen response elements (EREs), a "GGTCAnnnTGACC" palindrome [40] in target DNA via its DBD [36, 39]. This binding activity causes the DNA to bend allowing for interaction of coregulators including coactivators and corepressors, and transcription machinery [36]. High throughput sequencing technologies have identified many ER target genes, including JUN gene that encodes the transcription factor Jun, and growth regulation by estrogen in breast cancer 1 gene GREB1 [41].

A non-classical signaling mechanism of ER exists in which ER drives transcription of target genes in the absence of estrogen, this mechanism is referred to as estrogen independent signaling [40]. The estrogen-independent signaling mechanism is activated by secondary messengers of growth factor signaling pathways, including epidermal growth factor receptor (EGFR) [40]. The second messengers induce altered intracellular kinase activity leading to the phosphorylation of ER at alternative phosphorylation sites [40]. The altered phosphorylation of ER drives alternative activation mechanisms of downstream transcription where ER engages in protein-protein interactions with other transcription factors to activate transcription [40]. This alternative signaling mechanism leads to altered gene expression providing escape mechanisms for breast cancers to continue growth and progression [40].

# 1.2.4 ER Targeted Therapies

Currently, many treatment plans exist for breast cancer patients, however, endocrine therapy has become a popular method of treatment for patients diagnosed with luminal breast cancers [12]. Luminal breast cancers are HR positive, and roughly 70% of breast cancers over express the ER [31]. Endocrine therapy has become a successful approach to treating ER positive breast cancers by targeting the ER activity through ER inhibition using selective ER modulators (SERMs) or selective ER degraders (SERDs), and estrogen degradation using aromatase inhibitors (AIs) [12]. Of the three endocrine therapy

mechanisms, the most common drugs prescribed in clinic are Tamoxifen; a SERM, Fulvestrant; a SERD, and letrozole; an AI [42].

Tamoxifen is a SERM, specifically the trans-tamoxifen (a citrate salt) which has a greater affinity for ER, that has both antagonist and agonist properties against estrogen [43]. Tamoxifen was initially synthesized in ICI laboratories (now AstraZeneca) as a method of contraception; however, it was quickly discovered that in utero, tamoxifen stimulated, rather than suppressed, ovulation thereby acting as an estrogen agonist [43]. A brief time after, tamoxifen was discovered to successfully inhibit breast cancer development and progression in at risk women during in clinical trials thereby acting as an estrogen antagonist in the breast [43]. Today, tamoxifen is the largest hormonal drug targeting ER positive breast cancers [43], successfully improving survival benefit of patients by 20% over 5 years [44].

Fulvestrant is an ER antagonist (SERD) typically administered intramuscularly to treat ER positive breast cancer [45]. Unlike tamoxifen. Fulvestrant has no estrogen agonist ramifications [45]. Fulvestrant prevents endogenous estrogen binding of ER thereby inhibiting the proliferative signaling of ER [45]. Additionally, Fulvestrant prevents nuclear translocation of ER by inhibiting dimerization and further, the Fulvestrant-bound ER is unstable thereby becoming more susceptible to degradation [45]. Clinically, Fulvestrant is used primarily as a second-line therapy to treat HR positive cancer in postmenopausal women that have become resistant to initial endocrine therapies [45].

Letrozole is a third generation reversible AI designed by Novartis [46]. Letrozole targets estrogen specifically by binding to cytochrome p-450 of aromatase enzyme to stimulate degradation, thereby reducing estrogen production [46]. In clinic, Letrozole is used as both a first-line therapy and second-line therapy to treat breast cancer in postmenopausal women [46]. First-line treatment of letrozole is used in hormone sensitive and metastatic breast cancers and used as a second-line therapy in women who have developed a resistance to initial drug therapies [46].

# 1.2.5 Drug Resistance and ER Positive Tumor Relapse

Current endocrine therapies are largely successful methods of treatment for ER driven carcinomas, however, roughly half of these patients relapse and develop resistance to hormonal therapies after prolonged exposure [12]. Several methods of endocrine therapy resistance have been identified, including crosstalk of ER with other growth factor receptors (estrogen-independent signaling), alterations in transcriptional programming, and increased rates of ESR1 mutations in tumors from patients who had relapsed while on hormonal therapy [7].

# 1.2.5.1 Alteration of Regulatory Elements

A method of endocrine resistance has been proposed through alterations in the activity of coregulators, including nuclear receptor co-activators (NCOA) and co-repressors (NCOR) [40]. Co regulators play a critical role in regulating the transcriptional activity of ERs, interacting with the AF domains to either drive or inhibit transcription of target genes [34]. An important coactivator identified in ER positive breast cancers is the NOCA amplified in breast cancer 1 (AIB1), which plays a key role in regulating ER transcriptional activity [1]. Specifically, AIB1 NCOA drives transcriptional activity of ER through the recruitment of histone acetyltransferases CBP/p300 [1]. AIB1 is amplified in over 10% and overexpressed in 64% of luminal breast cancers therefore has been proposed as a method of endocrine therapy resistance in ER positive breast cancer [1]. An alternative method of hormone therapy evasion is through ER interaction with other transcription factors [7]. Forkhead box protein A1 (FOXA1), a transcription factor, has been identified as a critical regulator of ER signaling whereby over 95% of all estrogen-regulated genes require FOXA1 for estrogen regulation [6]. Recent studies have shown FOXA1 is highly expressed in luminal subtypes of breast cancer, thereby altering the estrogen regulated gene expression profile [6].

### 1.2.5.2 Mutations in ER

Treatment is effective in many cases, however, resistance to therapeutics often emerges after prolonged exposure whereby over 50% of metastatic tumors harbored mutations in ER [12]. Within

luminal subtypes of breast cancer, circulating tumor DNA studies have detected ESR1 mutations at a frequency of 72% in luminal A, and 25% in luminal B breast cancer subtypes [94]. Furthermore, it has been found that higher rates of ESR1 mutations occur in tumors from patients who had relapsed while on hormonal therapy [12]. These mutations were found to cluster in a small region that encodes the LBD of ESR1; the most common being a missense mutation that altered the amino acid 537 tyrosine into serine (Y537S) and 538 aspartic acid into glycine (D538G) [7]. Identified mutations were found to increase ER activation and transcriptional functions leading to increased cell proliferation and tumor development and were resistant to ER targeted therapies [7].

Molecular dynamics and crystallography studies have shown ER mutants adopt a similar structure to estrogen bound ER [12]. Structural changes within Y537S and D538G mutations introduced hydrogen bonds between the co-factor recruiter helix 12 and helix 3, stabilizing the agonist confirmation and possibly supporting the increase activation levels of the mutants [12]. Additionally, in-vitro co-transfection assays showed constitutive activation of mutant ERs [47]. Specifically, HEK293T cells were co-transfected with ERE-firefly luciferase reporter plasmids carrying Y537S and D538G ESR1 mutants and starved of estrogen [47]. It was found that even in the absence of estrogen, HEK-293T cells carrying ESR1 mutations had constitutive activation of ERE reporter, with the ESR1 Y537S mutant being the most active, while wildtype (WT) HEK293T cells required estrogen for ER transcriptional activity [47]. ER mutants have been found to bind chromatin independently of estrogen through ChIP-seq analysis, a hypothesized mechanism of therapeutic resistance in ER positive tumors bearing ER mutations [93]. Differential gene expression studies have identified a specific ERBB2 gene set to be upregulated by ER mutants through the estrogen-independent binding mechanism employed by ER mutants [93].

#### 1.3 AIB1 in Breast Cancer

#### 1.3.1. AIB1 Structure and Function

An important player in ER signaling is the steroid receptor coactivator AIB1, which stands for amplified in breast cancer 1 [1]. It has been found that the AIB1 gene is amplified in about 10% of human breast cancers, and highly expressed in about 64% of estrogen receptor positive cancers [1]. Furthermore, AIB1 is associated with tumor size, histological grade, and overall survival in which patients with high AIB1 expression have significantly lower overall, and disease-specific survival [3]. Consequentially, AIB1 has become a target of investigation to better understand breast cancer development and progression.

AIB1, a member of the larger steroid receptor coactivator (SRC) family, functions to regulate the transcriptional activity of NRs, including the ER [48]. Functionally, the SRC family plays key roles in regulating both NR and non-NR signaling thereby playing key roles in many physiological pathways [49]. Three pleiotropic coregulators make up the SRC family; SRC-1, SRC-2, SRC-3, SRC-3 being AIB1 [49]. AIB1 goes by many names including SRC-3, nuclear receptor coactivator-3 (NCoA-3), receptor associated coactivator-3 (RAC-3), activator of thyroid hormone and retinoid receptor (ACTR), and more [48]. First identified in breast cancer, the AIB1 gene is found chromosome 20q12-12 and is 160 kDa in size [48]. AIB1 shares a 40% conserved sequence identity with the SRC family [54]. Structurally, AIB1 is composed of several conserved domains including an NR interaction domain (NID), activation domains AD1 and AD2, a basic helix-loop-helix/Per-ARNT-Sim domain (bHLH/PAS), histone acetyltransferase domain (HAT), and a glutamine (Q)-rich domain [48].

Centrally localized is the NIC domain which allows for the NR binding activity of AIB1, specifically through the conserved LXXLL motif, L representing Leucine and X representing any amino acid [48, 51]. Specifically, withing the secondary structure of AIB1, the LXXLL motif creates an amphipathic  $\alpha$ - helix whereby the non-polar leucine creates the hydrophobic surface that interacts with

the LBD of NR like ER [48, 50]. Similarly, the AD1 domain contains three LXXLL motifs necessary for the transcriptional co-factors p300/CBP interaction function of AIB1 [48, 52]. The AD1 domain is also termed CBP-interaction domain (CID) after its primary function of recruiting cyclic AMP response element-binding protein (CBP) and p300, which are transcription co-factors and histone acetyltransferases that open chromatin [48]. Comparably, the AD2 domain recruits coactivator-associated arginine methyltransferase-1 (CARM1) and other methyl transferases [48, 53]. Both AD1 and AD2 are located in the C-terminus of AIB1 [54]. Also, within the C-terminus is the HAT domain which possesses histone acetyltransferase activity, however, the level of necessity of the domain for gene activation remains unclear as CBP/p300, recruited by AD1, has greater activity than SRC HAT [54]. Within the N-terminus is the most highly conserved bHLH/PAS region with a conserved sequence identity of 60% [48]. Originally discovered in Drosophila, the bHLH/PAS domain activity was determined to play a critical role in DNA binding and protein heterodimerization [54]. Within the SRC family, the highly conserved bHLH/PAS is responsible for mediating protein-protein interactions between SRC and recruited coregulators and cofactors [48]. A serine/threonine rich domain has also been identified within the N-terminus of the AIB1 structure which is an important site of regulation by phosphorylation [48].

# 1.3.2 Posttranslational Modifications of AIB1

SRCs are modulated by numerous posttranslational modifications (PTMs) including phosphorylation and ubiquitination [49]. As aforementioned, the serine/threonine rich region of the N-terminus is a prime location for PTM phosphorylation [48]. In-vitro studies have shown the phosphorylation of the tyrosine residue Y1357 in the AD2 domain by an Abl kinase to be critical for the transcriptional activator activity of AIB1 in cancer cells [48, 55]. Recent studies have also found that phosphorylation of AIB1 by atypical protein kinase C (aPKC) allowed for evasion of ubiquitin-dependent degradation by stabilizing AIB1 in an ER-dependent fashion [48, 56]. Another regulator of AIB1 is mitogen-activated protein kinase (MAPK), whose phosphorylation of AIB1 was found to increase ER-dependent transcription by enhancing the AD1 activity of p300/CBP recruitment [54, 57]. Furthermore,

tyrosine kinases receptors like insulin receptor, are thought to regulate the localization of AIB1 when it was found that insulin treated cells in serum-free culture had restored the localization of AIB1 from the cytoplasm to the nucleus, its prime location under normal conditions [54].

## 1.3.3 AIB1 and ER Transcriptional Activity

AIB1 interacts with estrogen receptors in a ligand-dependent fashion and enhances estrogen-dependent transcription [1]. Specifically, AIB1 regulates ER transcriptional activity through recruitment of the histone acetyltransferases CBP/p300 [1]. As acetyltransferases, CBP/p300 add an acetyl group to lysine residues on histones leading to modified chromatin structure and allowing ER to bind promoters of target genes [1]. Recruitment of CBP/p300 by AIB1 coactivator induces increased ER binding of target genes thereby increasing gene expression, including oncogenes genes, including GREB1 and JUN, which contribute to the development of steroid-dependent cancers [1]. Exploring strong AIB1 binding sites through ChIP sequencing and mapping assays, 18 AIB1 target genes were identified, each with proven ER binding [48, 58].

### 1.3.4 AIB1 in Luminal Breast Cancer

### 1.3.4.1 AIB1 Overexpression

Fluorescence in situ hybridization (FISH) and immunohistochemistry (IHC) has identified AIB1 amplification in 11% and overexpression in 60% of 2000 human breast carcinomas [3]. Furthermore, AIB1 is associated with tumor size, histological grade, and overall survival in which patients with high AIB1 expression have significantly lower overall, and disease-specific survival [3]. In a transfection study, BT474 breast cancer cells were transfected with an RNA interference expression vector that targeted AIB1 mRNA [59]. It was found that AIB1 knockdown resulted in decreased cell proliferation compared to the parental and shControl cells [59].

## 1.3.4.1.1 Hormone-Independent AIB1 Signaling

While AIB1 overexpression leads to increased rates of estrogen-dependent ER signaling, recent investigations have discovered that AIB1 also functions to promote estrogen-independent cell proliferation in breast cancer [48, 60]. Specifically, AIB1 promotes expression of G1/S phase transition proteins like cyclin-dependent kinase 2 (Cdk2) by acting as a coactivator of transcription factor 1 (E2F1) and enhancing transcription of E2F target genes [48, 60]. Overexpression of AIB1 strongly stimulated proliferation in quiescent cells whereby AIB1 allowed complete negation of cell cycle arrest in cells, even in the presence of antiestrogens like tamoxifen, through the stimulation of E2F target genes [60]. AIB1 was also found to promote self-transcription through its coregulation E2F1 transcription thereby creating a positive feedback loop increasing its influence on cell growth [48, 60].

AIB1 has also been found to regulate insulin-like growth factor 1 (IGF-1) in human breast cancer where AIB1 knockout in MCF-7 led to decreased IGF-1 mRNA levels and consequently downregulated protein expression while overexpression increased IGF-1 mRNA and protein levels [48, 61]. The known cancer agent IGF-1 is a growth hormone that promotes breast cancer growth through several mechanisms including stimulation of cell growth and downregulation of apoptosis [62]. Looking at gene expression through cDNA array analysis, AIB1 knockdown was found to downregulate expression of genes controlling apoptosis and cell cycle progression [61]. Similarly, a study exploring AIB1 overexpression in transgenic mice found that AIB1 knockdown through small interfering RNA led to downregulated IGF-1 mRNA and increased apoptosis in AIB1-tg mouse mammary tumors cells [63]

## 1.3.4.1.2 AIB1 and Tamoxifen Resistance

At present, endocrine therapy, including tamoxifen, is the most effective treatment for patients with ER-positive breast cancers [43]. Tamoxifen, however, is not ideal as roughly 40% of breast cancer cases are resistant to tamoxifen and many patients who initially respond to tamoxifen eventually acquire resistance [59]. It has been proposed that AIB1, as a critical coactivator of ER, may play a role in patients

acquired resistance to tamoxifen treatment [59]. In a transfection study exploring the role of AIB1 in tamoxifen resistance, BT474 breast cancer cells were transfected with an RNA interference expression vector that targeted AIB1 mRNA and subsequently treated with varying concentrations of tamoxifen [59]. Within the tamoxifen treated populations, the inhibitory effects of tamoxifen on cell proliferation was restored in cells with AIB1 knockdown [59]. The subsequent conclusion is that tamoxifen behaves like an estrogen agonist in ER-positive breast cancer cells that express elevated levels of AIB1 resulting in tamoxifen resistance, and furthermore, knockdown of AIB1 can restore the antitumor effects of tamoxifen [59].

### 1.3.5 Mouse Models of AIB1

Today, transgenic mouse models are widely used to understand cancer pathogenesis. The homolog of AIB1 endogenous to mice is p/CIP, and when knocked out through null mutations, mice were dwarfed with impaired mammary gland development, specifically, with stunted duct formation suggesting a critical role of AIB1 in mammary morphogenesis [63, 65]. To further understand the role of AIB1 overexpression in human breast cancer, some transgenic mouse models overexpressing AIB1 have been generated [63]. One model of AIB1 overexpression (AIB1-tg) discovered increased levels of hyperplasia, hypertrophy, and abnormal involution in mice overexpressing AIB1 [63]. Specifically, AIB1-tg mice had mammary glands 30-40% larger than those of wild type (WT) controls, in which both epithelial cell size and count were greater [63]. Exploring mammary morphogenesis following postweaning involution, AIB1-tg mice had disorganized epithelium and delayed involution whereby AIB1 overexpression glands had much fewer apoptotic bodies resulting in delayed alveoli collapse and unsuccessful remodeling of the gland 21 days postpartum [63]. Furthermore, after roughly 9 months, 70% of AIB1-tg mice developed mammary adenocarcinomas, with increased metastasis to the uterus and pituitary [63]. Additionally, AIB1 knockdown using siRNA for AIB1 in mammary tumor cell lines led to significant downregulation of IGF-1, a known cancer agent, and increased apoptosis [63].

Exploring the relationship between AIB1 overexpression and ER function, AIB1-tg mice underwent ovariectomies (ovx) to abolish gonadal estrogen production and signaling [64]. Analyzing mammary gland development through whole mount analysis, no difference was observed between AIB1-tg and WT ovariectomized mice where both had a reduction in ductal elongation and branching, suggesting AIB1 overexpression is not sufficient to drive mammary gland development in the absence of estrogen [64]. It was observed, however, that despite impaired mammary gland development, OVX AIB1-tg mice had developed hyperplasia and DCIS, supporting evidence of AIB1 involvement in hormone-independent cancer growth [64].

#### 1.4 FOXA1 in Breast Cancer

### 1.4.1. FOXA1 Structure and Function

Another important player in ER signaling is the transcription factor FOXA1 which stands for forkhead box protein A1, effectively, FOXA1 is largely involved in luminal breast cancer [2]. FOXA1 was originally identified in hepatocytes as a transcription factor necessary for the transcriptional regulation of transthyretin (Ttr) and  $\alpha$ 1-antitrypsin (Serpina1) and was initially coined hepatocyte nuclear factor  $3\alpha$  (HNF3 $\alpha$ ) [66, 67]. It was later discovered that HNF proteins were homologs of forkhead proteins in Drosophila and effectively renamed FOXA1 [66, 68].

FOXA1 is a transcription factor and a member of the larger FOX family [66]. Several functionally critical domains have been identified through X-ray crystallography, including the DBD and two transactivation domains (TADs), all necessary for rudimentary transcriptional activity [69]. The DBD at approximately110 amino acids long, is the mostly highly conserved (>92%) domain within the FOXA family [2]. The DBD is a highly conserved helix-turn-helix motif located within the central region of the protein, that binds the consensus sequence A(A/T)TRTT(G/T)RYTY [2]. Flanking the DBD are two winged helices, a comparable structure to linker histones [70], that bind the minor groove of DNA aptly modulating the strength and stability of binding [66, 71]. Effectively, the flanking winged helices bind

high affinity sites more tightly, however the distribution of these sites within the genome remains unknown [66, 71]. Additionally, FOXA1 contains both N-terminus and C-terminus TADs which are responsible for recruiting coactivators leading to increased activation of target genes [66]. Finally, FOXA1 also contains a nuclear localization signal (NLS) allowing the protein to be transported into the nucleus and bind target DNA [66]. FOXA transcription factors have also been dubbed 'pioneer factors' on account of their unique chromatin remodeling function [2,66]. Specifically, following the binding of FOXA1 monomers to consensus element A(A/T)TRTT(G/T)RYTY, the C-terminus region interacts with histones H3 and H4 to induce an open configuration in chromatin [72, 73].

### 1.4.1.1 FOXA1 Function in Mammary Glands

FOXA1 expression has been identified in many organs, including the liver, lungs, prostate, and breast, and more than 100 FOXA1 associated genes have been revealed that control signaling pathways and the cell cycle [76, 79]. By nature of association with ER and GATA3, transcription factors necessary for mammary epithelial cell growth and differentiation, FOXA1 is subsequently involved in mammary gland development [66]. It has been observed that ablation of FOXA1 in mammary glands had no effect on lobulo-alveolar maturation, nor milk production [2]. A proposed explanation for this unexpected phenotype is that FOXA1 may actively repress alveolar lineage maturation and the downregulation within epithelia allows for premature ER-independent alveologenesis [2]. The regulation of mammary morphogenesis is a unique characteristic of FOXA1 as the sole FOXA member expressed in mature mammary gland [2].

# 1.4.2 Regulation of FOXA1

FOXA1 undergoes many levels of regulation, both transcriptional and posttranslational, through PTM, soluble factors, protein-proteins interactions, and chromatin modification to enhance or inhibit target gene expression [66]. Several proteins modulating the TAD of FOXA1 have been identified, including nuclear receptors apolipoprotein regulatory protein 1 (ARP-1) and small heterodimer partner

(SHP) which inhibit FOXA1 transactivation function [66]. In contrast, nuclear receptor androgen receptor (AR), has been discovered to enhance FOXA1 binding of target genes through DBD interactions [66]. The DBD is also heavily regulated through PTM, particularly through acetylation to inhibit chromatin binding, in which 11 acetylation sites within the DBD of FOXA1 have been disclosed by silico analysis [74].

Another point of FOXA1 regulation is through the activity of TFs, specifically the ER and GATA binding protein 3 (GATA3) which plays a vital role in mammary epithelial differentiation [66, 75]. FOXA1 is positively regulated by both GATA3 and ER estrogen-dependent signaling [66]. It has been predicted that luminal epithelial cells expressing high levels of both GATA3 and ER consequently have greater levels of FOXA1 [66].

Through genome wide analysis, it was discovered that FOXA1 recruitment was highly correlated with the methylation status of histone H3 lysine 4 (H3K4), by which majority of FOXA-1 binding sites harbored H3K4 mono- or di-methylations [66, 78]. Furthermore, overexpression studies of histone demethylase lysine-specific demethylase 1 (LSD1) demonstrated a reduction in recruitment of FOXA1 to chromatin in cells overexpressing LSD1 suggesting FOXA1 activity is regulated by histone methylation [66, 78]. The binding activity of FOXA1 to target DNA within chromatin is thereby regulated by the expression of demethylases and methyltransferases which control the methylation of H3K4 [66].

## 1.4.3 FOXA1 in Luminal Breast Cancer

FOXA1 has become recognized as an important player in ER+ luminal breast cancers [2].

FOXA1 expression has been found to be highly expressed in luminal breast cancers compared to ERsubtypes and downregulation of FOXA1 inhibits cell proliferation [6]. Knockdown of FOXA1 in MCF-7
cancer cells lead to significant growth arrest and decreased estrogen-dependent gene expression,
demonstrating the necessity of FOXA1 for estrogen response in luminal breast cancer cells [6, 72]. As a

pivotal regulator of ER hormone dependent signaling, FOXA1 is associated with ER+ breast cancer and has been identified as a prognostic factor in luminal subtypes [72].

# 1.4.3.1 FOXA1 and ER signaling

FOXA1 plays a key role in the development and differentiation of mammary glands specifically by modulating the ER [2]. Particularly, FOXA1 regulates ER signaling through its ability to bind chromatin [2]. FOXA1 is recruited to di-methylated lysine binding sites in histone H3, and upon binding, chromatin adopts an open configuration allowing the ER to bind promotors in target genes [2, 72]. As a key regulator of ER signaling, FOXA1 has become recognized as an important player in luminal breast cancers [2]. Furthermore, FOXA1 has been deemed essential for ER binding of chromatin and ergo the transcriptional function of ER [6]. Exploring the role of FOXA1 in ER transcriptional activity, MCF-7 cells treated with siRNA against FOXA1, in which FOXA1 silencing of lead to a significant decrease in ER binding chromatin [6]. Through ChIP-seq analysis, estrogen induced ER binding events were measured and found to be decreased by minimally 50% in 90% of all ER binding events (over 13000 estrogen induced ER binding events identified) following FOXA1 downregulation [6]. When FOXA1 was re-expressed within cells, ER binding was restored to original levels, effectively demonstrating the dependence of ER transcriptional activity on FOXA1 expression [6]. Additionally, FOXA1 regulates ER mRNA expression in luminal breast cancer cells through its binding of the ESR1 promotor to drive transcription of ER, in which loss of FOXA1 expression is concomitant with the loss of ER expression in mammary glands [66]. In conclusion, FOXA1 is critical for both the expression and activity of the ER in breast epithelium [66].

Different studies have shown FOXA1 activity to either drive or inhibit cell growth in metastatic breast cancers [76]. The growth promoting role is characterized through classical FOXA1 chromatin remodeling activity, and corresponding transcription of ER target genes, however, studies have shown FOXA1 overexpression to inhibit cell growth by inhibiting cell cycle progression [76, 80] Specifically, overexpression of FOXA1 increased expression of p27, a BRCA1 associated cell cycle inhibitor [76, 80].

It has been suggested that FOXA1 might be a favorable prognostic factor in breast cancer as FOXA1 depletion may shift ER signaling from estrogen-dependent to estrogen-independent pathways in neoplastic mammary epithelium resulting in hormonal therapy resistance [72, 76]. In contrast, a study exploring the role of FOXA1 in tamoxifen resistance found that silencing FOXA1 in tamoxifen resistant breast cancer cells significantly reduced ER binding and proliferation suggesting FOXA1 is necessary for hormone independent growth in tamoxifen resistant cancers [6].

#### 1.4.3.2 FOXA1 and Breast Cancer Patient Survival

FOXA1 was found to be a significant predictor of patient survival, effectively defining FOXA1 as a potentially useful prognostic biomarker in luminal breast cancer [81]. In over 400 breast tumor samples, 74% expressed FOXA1, and were further significantly correlated with ER and luminal subtypes [81]. Patients with loss of FOXA1 expression had tumors of lower grade [81]. Moreover, FOXA1 was predictive of patient survival by which higher cancer survival was associated with FOXA1 expression [81]. Patient survival was better predicted by FOXA1 expression than expression progesterone receptor in luminal breast cancers [81].

## 1.4.4 Mouse Models of FOXA1

Several transgenic mouse models of FOXA1 have been generated to explore the role of FOXA1 in metastatic cancers [82]. In the Krt14-Cre model, FOXA1 was fully ablated in mammary epithelium leading to complete abolishment of ductal formation in the mammary gland [82]. Other models, like MMTV-Cre have been used to partially delete FOXA1 in the mouse mammary consequently impairing duct mammary duct formation [82]. Knockdown and ablation models have demonstrated the necessity of FOXA1 in mouse mammary development and tumorigenesis [82].

Full body knockout of FOXA1 was postnatally lethal in FOXA1 null mice in which global loss of FOXA1 lead to severe hypoglycemia and dehydration [2].

#### 1.5 Mouse Models of Breast Cancer

#### 1.5.1 MMTV

Transgenic animal models have become an invaluable tool in researching pathogenesis of countless human diseases, including breast cancer. The high degree of similarity, in both structure and function, between human and mouse mammary has made mice a primary model and allowed for marked advances in breast cancer research [20]. In the early 19th century, it was discovered that mice infected by the mouse mammary tumor virus (MMTV), a murine retrovirus, developed spontaneous tumors that have a high degree of morphological and cytochemical similarity to human carcinomas [20]. The virus was initially found in mouse mammary whereby gene expression by the MMTV promoter was specific to mammary glands [83]. While the viral promoter was originally identified as a milk agent, the life cycle of the virus typically begins within dendritic, and gut associated cells [83]. The exogenous promoter then infects B cells which express the long terminal repeat (LTR)-encoded superantigen (SAg) to induce B-cell proliferation through the T-cell release of lymphokines [83]. The amplified infected B lymphocytes then transport the MMTV promoter to the mammary gland where it further replicates and is transmitted to nursing offspring through breast milk [83]. The LTR was then identified as the specific promotor of MMTV as mammary growth and viral amplification are favored by enhancers within this LTR region [83]. Today, MMTV is the most commonly used promoter to control oncogene expression within mammary tissue [20, 83].

While MMTV promoter successfully drives gene expression in 70% of mammary epithelium, several caveats exist using exogenous promoter systems, including leakiness, uncontrolled integration, and inherent model limitations [85]. Expression of reporter genes have been observed within different organs of mice suggesting the MMTV promotor displays a certain degree of leakiness [85]. Additionally, integration of transgenes cannot be regulated thereby prompting the random insertion of the transgene within the genome [65]. Finally, while many aspects of human and mouse mammary are comparable, the

MMTV promotor system activates different cellular transcriptional machinery than that controlling human endogenous ERBB2 locus effectively limiting the comparability to human disease [85].

## 1.5.1.1 MMTV-PyMT

The murine polyomavirus (PyMT), when expressed in mice, drives high frequency epithelial tumors [98, 99]. Specifically, the PyMT DNA encodes three proteins responsible for driving tumorigenesis in the mouse host: small, middle, and large T antigen acting as scaffolding proteins to drive downstream signaling of Ras/MAPK and PI3K/Akt pathways [76]. Today, PyMT is widely used in transgenic models of breast cancer for their high resemblance to human luminal cancers [100]. Tumors driven in mammary epithelium by MMTV-PyMT are multifocal, have a short latency (40 days), and progress through the histological stages in a comparable fashion to human patients [100]. Additionally, MMTV-PyMT tumors have a loss of ER activity, mimicking endocrine resistant human breast carcinomas [101].

## 1.5.2 Cre Recombinase/loxP System

Transgenic models have become an indispensable instrument for medical advances, specifically through genetic modification using gene targeting technologies like the recombinase system [84]. The recombinase system allows for conditional DNA knockout to induce or inhibit gene expression within a specific tissue [84]. A common recombinase system is the Cre recombinase/loxP system that mediates site-specific recombination of two loxP sites [84]. LoxP sites are 34 base pair (bp) sequences containing a central nonpalindromic sequence that regulates loxP orientation [84]. Cre recombinase recognizes loxP sites within the genome and excises DNA intervening identically oriented loxP sites [84]. The Cre recombinase/loxP system has subsequently become a widely employed gene targeting technology in oncogenic mice (oncomice) with many functions including silencing, mutating, and inducing gene expression [84].

## 1.5.3 rtTA/TetO System

The reverse tetracycline (rtTA)/ Tet-operon (TetO) system is used in transgenic mouse models to regulate transgene expression both temporally and spatially [86]. The system is characterized by the tetracycline-induced activation of rtTA, whereby tetracycline binds and activates rtTA [86]. The active rtTA binds the TetO to induce transcription of downstream genes [70]. Mouse transgenomics has integrated the rtTA/TetO system with MMTV, placing rtTA downstream of the MMTV promoter driving constitutive expression of rtTA in mouse mammary epithelia [86]. Upon addition of doxycycline (dox), a stable derivative of tetracycline, to transgenic mice through drinking water, rtTA activates transcription downstream of TetO exclusively within mammary epithelium [86]. The combined MMTV and rtTA/TetO, denoted MTB, is largely implemented in breast cancer models to control gene expression in mammary epithelium [86].

#### 1.5.4 Mouse Models of ER

#### 1.5.4.1 TetO-ER

At present, there is a lack of transgenic mouse models investigating the role of ER in mammary tumorigenesis [87]. Several models have been engineered; however, many are unable to recapitulate human ER-positive tumors accurately [87]. The TetO-ER model, a recent model of ER in luminal breast cancer, exhibits reasonable resemblance to human ER positive breast cancer [87]. The model design allows for conditional overexpression of ER within mouse mammary epithelium through the rtTA/TetO system [87]. A long tumor latency of over 12 months, with a penetrance of 3-5%, was observed within the model [87]. Currently there is a significant disparity in existing ER mouse models adequate for in vivo studies [87].

#### 1.5.4.2 KI ESR1 Y541S

A new mouse model of ER, the knock in (KI) ESR1Y541S, explores the role of the analogous Y537S mutant ER in luminal breast cancer [88]. The model utilizes the MTB and Cre recombinase/loxP

systems to excise exon 9 containing the WT Y541 bringing the mutant exon 9 in frame, thereby introducing the Y541S mutant in mammary epithelium of transgenic mice upon dox induction [88]. A Neo cassette has also been introduced to the construct placed before the mutant exon 9 to allow for expression of WT ER in uninduced mice [88]. The Neo cassette functions to silence expression of the mutant exon 9 in the absence of dox, and effectively Cre [88]. A full body KI of the ER Y541S mutant, achieved through a cross with Cre recombinase controlling beta-actin promoter, lead to runted mice with lower overall survival, as well as observed abnormal mammary morphogenesis in virgin females [88]. Additionally, full body ER mutant KI males displayed nipple development and smaller anogenital regions that WT males [88]. KI ER mutant in the mammary gland, however, was insufficient to drive tumorigenesis after 2 years of induction in virgin female mice [89].

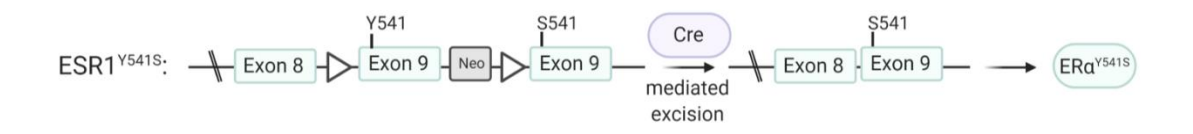


Figure 1-1: Schematic of KI ESR1 Y541S and Cre mediated excision of floxed Neo cassette and mutant exon 9 to generate mutant ER.

Created with BioRender.com

#### 1.6 Experimental Rationale

As a critical coactivator of ER, AIB1 is an obvious candidate for functional studies. The AIB1 gene is amplified in about 10% of human breast cancers, and highly expressed in about 64% of estrogen receptor positive cancers [1]. In mouse models, AIB1 overexpressing is sufficient to drive tumorigenesis, whereby over 70% of mice overexpressing AIB1 develop adenocarcinomas [63]. Another important player in ER signaling is the transcription factor FOXA1, acting as a pioneer factor that modifies chromatin structure allowing for ER binding [2]. FOXA1 is a pivotal regulator of ER, in which ER transcriptional activity is

dependent on FOXA1 binding of chromatin [2]. Effectively, FOXA1 is recognized as an important contestant in luminal breast cancers development [2]. While there is sufficient evidence of AIB1 and FOXA1 involvement in luminal breast cancer development and progression, the underlying mechanisms of this process are poorly understood. Additionally, there is a substantial need for in vivo models to investigate molecular mechanisms of early neoplasia, endocrine resistance, recurrence, and patient risk in ER-positive breast cancers [97]. Ergo, using our research groups specialized transgenic engineering expertise, we seek to elucidate the role of oncoproteins AIB1 and FOXA1 in mammary tumorigenesis, and provide further investigation into the ESR1 Y537S mutant through the KI Y541S mouse analogue model. As fundamental players in the development of ER+ tumors we hypothesize that AIB1 and FOXA1 overexpression may be sufficient to drive tumorigenesis in ER+ luminal breast cancer mouse models. We aim to create (1) Create novel inducible ER+ luminal breast cancer mouse models of AIB1 and FOXA1 overexpression. (2) Characterize these new mouse models, exploring tumor latency and progression in an aging cohort to determine if overexpression of these oncoproteins alone is sufficient to drive tumorigenesis. (3) Explore overexpression of oncoproteins AIB1 and FOXA1 in the context of a mutated ER by crossing AIC and FIC constructs in ESR1YS model. These novel inducible models of ER will further illuminate the role of AIB1 and FOXA1 in early neoplasia and provide valuable tools to explore ER mediated tumorigenesis. Furthermore, these transgenic models overexpress members of the ERmediated transcriptome will more accurately model ESR1, which is significantly underrepresented in current animal models.

#### 2. RESULTS AND DISCUSSION

# 2.1 Characterizing novel AIB1 and FOXA1 overexpression mouse models AIC and FIC

## 2.1.1 Experimental Rational and Generation of AIC and FIC Constructs.

The ER coactivator AIB1 has been identified as a critical player in luminal breast cancer development whereby the AIB1 gene is amplified in roughly 10% of human breast cancers, and highly expressed in 64% of estrogen receptor positive cancers [1]. Additionally, AIB1 is associated with tumor size, histological grade, and overall survival in which patients with high AIB1 expression have significantly lower overall, and disease-specific survival [3]. Endocrine therapy is a widely practiced method of ER-positive breast cancer treatment, however, AIB1 overexpression in luminal cancers plays a key role in tamoxifen resistance [59]. In AIB1 overexpression breast cancers, Tamoxifen has been found to behave like an estrogen agonist resulting in tamoxifen resistance, and furthermore, knockdown of AIB1 can restore the antitumor effects of tamoxifen [59]. Consequentially, AIB1 has become a critical target of investigation to better understand breast cancer development and progression.

The transcription factor FOXA1 has been highly correlated with ER-positive breast cancers, whereby over 70% of breast tumors express FOXA1 [81]. Furthermore, FOXA1 was identified as a critical player in ER activity and expression, controlling over 95% of all estrogen regulated genes. FOXA1 has thus become a significant target in ER-positive breast cancer, as a potential biomarker and target for endocrine therapy.

To better understand the roles of AIB1 and FOXA1 in cancer development and progression, we generated two Doxycycline (Dox) inducible mouse models; AIC and FIC, which overexpress oncoproteins AIB1 and FOXA1 (Fig. 2-1). Models express the AIB1 or FOXA1 proteins by the tetracycline dependent operator (TetO) linked to Cre recombinase via an internal ribosome entry site (IRES). The TetO-AIB1-IRES-Cre and TetO-FOXA1-IRES-Cre constructs are called the AIC and FIC constructs respectfully. Additionally, within the AIC and FIC constructs are Flag-Tags which have been added for experimentation further characterizing the transgenic AIB1 and FOXA1, and validation of

transgene through immunoprecipitation and IHC staining. The AIC and FIC constructs are crossed into the MTB construct to generate AIC/MTB and FIC/MTB mice. The MTB construct contains a mouse mammary tumor virus promotor (MMTV) which activates downstream genes in mammary epithelium. The reverse tetracycline transactivator (rtTA) is downstream of MMTV, restricting translation of our transgenes specifically to the mammary epithelium. Following Doxycycline administration, Dox binds and activates rtTA, active rtTA subsequently binds the TetOperon of the AIC and FIC construct to activate transcription of downstream AIB1, FOXA1 and Cre. IRES, RNA elements that allow for capindependent translation, allows for translation of the AIB1-Cre and FOXA1-Cre mRNA to generate AIB1, FOXA1, and Cre recombinase proteins.

The inducible feature of these models allows for control of spatial and temporal expression of the AIC and FIC transgenes. Temporally, we can control the time at which mice express the transgene and consequentially develop tumors. Spatially, transgene expression is localized to mammary epithelial cells. AIC and FIC models are additionally unique from other models expressing AIB1 and FOXA1 through the employment of Cre recombinase. Coupling transgene expression with Cre allows for functional experimentation through knockout crosses which is important for determining molecular events that are critical for FOXA1 and for AIB1-mediated mammary tumorigenesis. Cre specifically recognizes loxP sites and excises DNA between them, thereby introducing an array of different gene manipulations. Another benefit of these models is that Dox is reversible; the removal of Dox stops transgene expression, de-induces tumors, and allows for tumor reoccurrence which better models human breast cancer where greatest death risk arises from recurrent tumors [1].

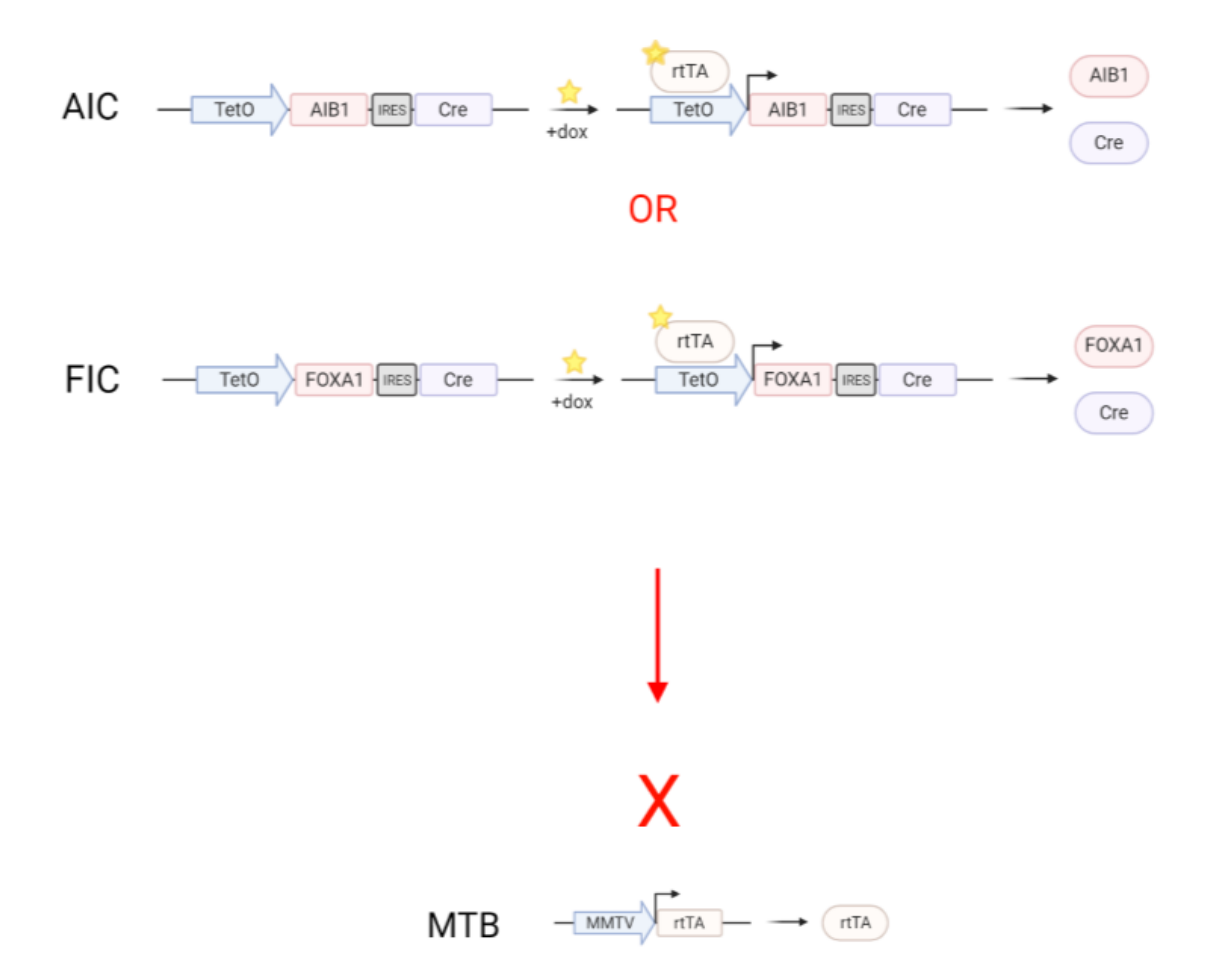


**Figure 2-1:** Schematic of the AIC, FIC, and MTB constructs, and the AIC/MTB and FIC/MTB crosses. AIC and FIC constructs are expressed through the TetO/MTB system. AIC and FIC constructs implement the Cre recombinase system whereby AIB1 and FOXA1 genes are attached to Cre recombinase through IRES, allowing for future functional experimentation. AIC/MTB experimental mice were generated by crossing AIC with the MTB strain. The FIC/MTB strain was generated by crossing the MTB strain with FIC strain. AIC, FIC, and MTB were all heterozygous in experimental mice. Schematic created with BioRender.com.

## 2.1.2 Generating Transgenic AIC and FIC Founder Animals

Founder animals from the AIC and FIC cohorts were generated through the process of microinjections. FVB embryos were injected with our TetO-AIB1-IRES-Cre (AIC) or TetO-FOXA1-IRES-Cre (FIC) transgene constructs. Microinjections were completed by the McGill Animal Core Facility. From the AIC injection, 5 transgenic offspring were generated, and 4 from the FIC injection (Fig. 2-3). The offspring were subsequently screened for the AIC and FIC transgene by polymerase chain

reaction (PCR) targeting AIB1, and CRE genes, respectively. With the lack of an appropriate FOXA1 primer at the time of experimentation, a CRE primer was used to detect the presence of the FIC transgene. The CRE gene is attached to FOXA1 by IRES, therefore we could be confident of the presence of FOXA1. Transgenic animal DNA was extracted from earpieces received from McGill transgenic core. From the AIC subset of transgenic offspring, 4 of the 5 were positive for the AIB1, and of the FIC subset, 3 of the 4 were positive for CRE (Fig. 2-3). Progeny positive for the AIC or FIC transgene were kept as founder animals to generate and propagate the AIC and FIC cohorts. The founders were labelled as founders 1 through 4 in the AIC cohort, and 1 through 3 in the FIC cohort. At about 3 months of age, founder 4 of the AIC cohort had passed due to natural causes, leaving three remaining AIC founders; AIC-1, 2, and 3.

To allow for dox-inducible transgene expression, the transgenic founder animals were crossed into the MTB construct at approximately 8 weeks of age, to generate AIC/MTB and FIC/MTB progeny. The heritability of the AIC and FIC transgenes was screened within the offspring of the AIC/MTB and FIC/MTB crosses by PCR targeting AIB1, FOXA1, MTB, and CRE genes. Animals positive for AIB1 or FOXA1, CRE, and MTB (AIC/MTB or FIC/MTB) were kept for early characterization of the models. The presence of the transgene in AIC/MTB and FIC/MTB progeny demonstrates the heritability of the FIC and AIC transgenes. The presence of MTB allows for the capacity to activate expression of the AIC and FIC transgenes in mammary epithelium of the AIC/MTB and FIC/MTB models through Dox administration to activate transgene transcription.

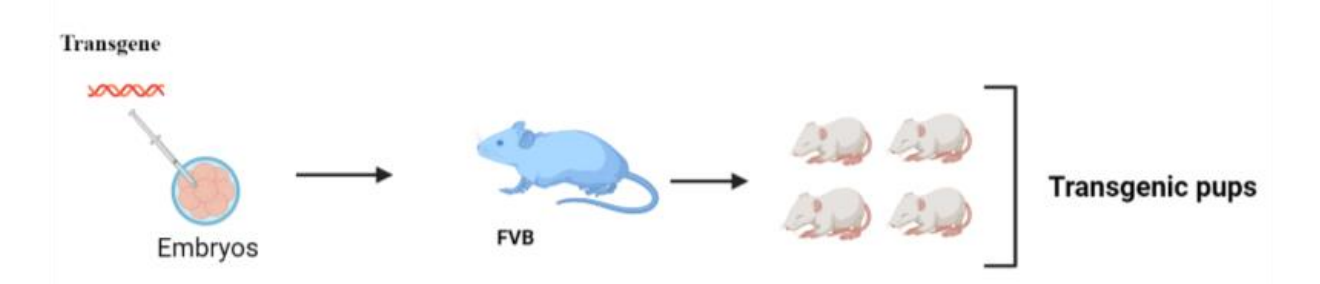


**Figure 2-2: Simplified schematic of the AIC and FIC transgenic founder animal production.**AIC and FIC founder animals were generated by injecting FVB embryos with our AIC or FIC transgene constructs. Microinjections were completed by the McGill Animal Core Facility. Transgenic pups were screened for the transgene by PCR targeting AIB1, FOXA1, MTB, and CRE. Offspring carrying the AIC or FIC transgene were kept as founder animals. Figure created with BioRender.com.

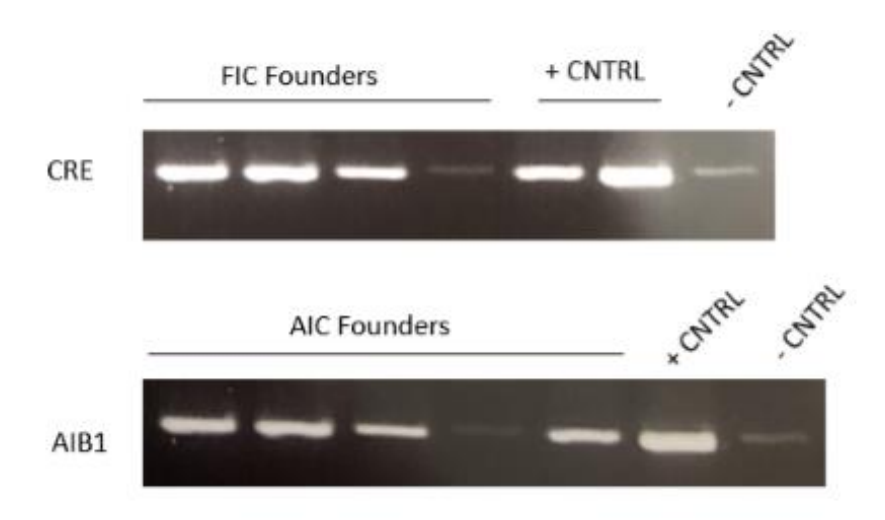


Figure 2-3: Image of genotyping PCR of AIC and FIC transgenic founder animals.

Initial selection of potential AIC and FIC founder animals was determined through PCR. Ear clippings were received from the McGill transgenic core. DNA was extracted from earpieces and the presence of AIC or FIC transgenes within sample genomes was determined by PCR. AIB1 and CRE primers targeting and amplifying the AIB1 and CRE gene sequences within the transgene constructs were used in AIC PCRs. Within the FIC transgenic animals, only CRE primers were used to identify the transgene within samples due to lack of appropriate FOXA1 primer. The original TetO-AIB1-IRES-Cre (AIC) and TetO-FOXA1-IRES-Cre (FIC) transcripts were used as positive controls for the AIC and FIC genotyping PCRs, respectively. Negative controls in both AIC and FIC PCRs were PCR reaction mixtures with no nucleic content. Animals positive for both AIB1 and CRE in the AIC sample subset, and positive for CRE in the FIC subset, were confirmed as positive for the transgene and kept as founder animals for further characterization.

## 2.1.3 Early Characterization of Novel AIC Founder Lines

To confirm our transgene is expressed within mouse mammary epithelium, a small cohort (approximately 3 mice per cohort) of AIC/MTB founder lines 1-3 were induced with doxycycline (Dox) through drinking water for one week to turn on the transgene through the activation of rtTA. Additionally, MTB/TetO-Cre animals were also induced for one week with Dox to act as controls. The MTB/TetO-Cre animals carry the TetO-IRES-Cre transgene, lacking the experimental AIB1 transgene. Following the 1-week induction, experimental and control animals were sacrificed and the mammary glands R2/3, L2/3, R4, and L4 were collected for histology, RNA, and protein collection. Mammary glands R2/3 and L2/3 were dissociated in tissue culture and epithelial cells were isolated to enhance epithelial RNA and protein signals of AIB1 and CRE. From the isolated epithelial pellets, RNA was extracted. AIB1 and CRE mRNA levels were measured by real time qPCR (RT-qPCR).

Within the AIC/MTB experimental subset, progeny from founders 1 (AIC-1) and 2 (AIC-2) had significantly greater levels of AIB1 mRNA expression than the MTB/Tet-O Cre controls (Fig. 2-5A). Cre mRNA levels were not measured due to the lack of a functional Cre qPCR primer at the time of the experiment. The AIB1 mRNA expression is significantly greater within our founder 1 (AIC-1/MTB) and founder 3 (AIC-3/MTB) transgenic AIC models, suggesting founder lines 1 and 3 successfully express the transgene within mammary epithelium and Dox-induced expression of the transgene increases levels of AIB1 transcription within mammary epithelium (Fig. 2-5A.). AIB1 mRNA levels within the AIC-2/MTB animals are comparable to that of the MTB/CRE controls, suggesting the AIC-2 line does not express our transgene (Fig. 2-5A). Without the confirmation of Cre mRNA expression within the mammary epithelium, it cannot be confirmed that the higher levels of AIB1 translation are a direct result of our transgene, nor that the transgene has been turned on following Dox induction, however, the trend is consistent with what we expect from a functioning AIC transgene. With AIB1 mRNA levels being the highest of all the founder lines, AIC-3 has been deemed the greatest expressor of our AIC transgene. Both AIC-1/MTB and AIC-3/MTB express greater levels of AIB1 within mammary epithelium than the control

and thus were selected for further characterization. IHC staining was performed on mammary gland L4 of AIC-1/MTB, staining for AIB1 (Fig. 2-5B). AIB1 protein is expressed within the AIC-1/MTB mammary gland, however, expression is largely cytoplasmic. Cytoplasmic AIB1 expression is atypical, whereby AIB1 functions to regulate the transcriptional activity of NRs within the nucleus [48]. Cytoplasmic AIB1 has been observed within cells that had downregulated insulin receptor activity, whereby insulin treated cells in serum-free culture had restored the localization of AIB1 from the cytoplasm to the nucleus [54]. An explanation for cytoplasmic AIB1 may be that AIB1 overexpression effects insulin signaling, thereby decreasing insulin receptor regulation of AIB1. The protein level of AIB1 expression across the different AIC founder lines cannot be confirmed due to lack of AIC-3/MTB sample and appropriate MTB/TetO-Cre. Due to the small sample size of AIC-3/MTB and AIC-2/MTB, too few glands were available for histological analysis. Furthermore, at the time of staining, we lacked a functioning Cre antibody, therefore it is difficult to decipher the nature of AIB1 as transgenic as opposed to endogenous. Staining will be repeated using proper MTB/TetO-Cre control and both AIC-1/MTB and AIC-3/MTB mammary glands, staining for both AIB1 and Cre to confirm the expression of the AIC transgene at a protein level.

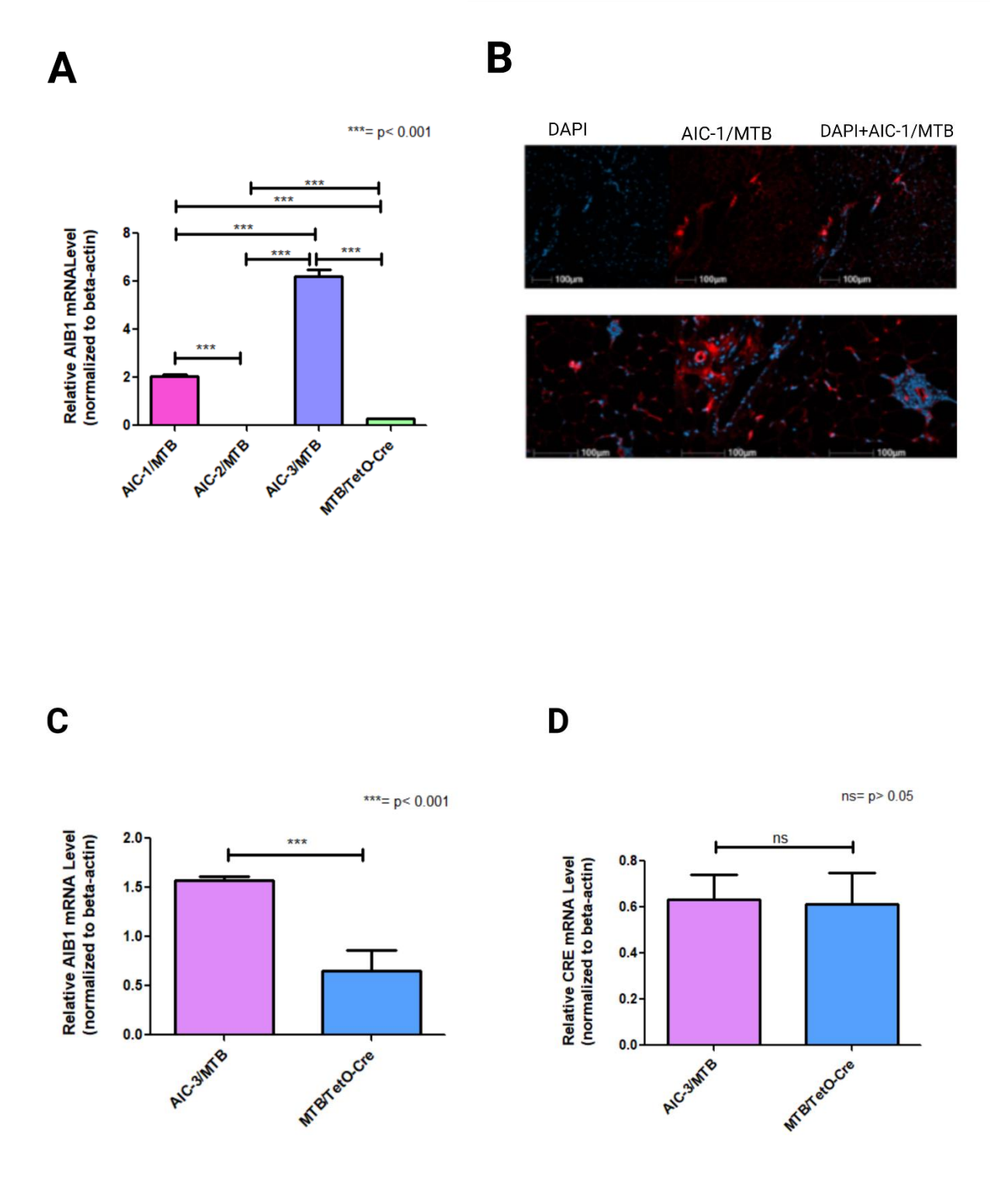


Figure 2-4: Schematic of early AIC and FIC founder line characterization.

Original AIC and FIC founder animals are crossed with the MTB strain to generate AIC/MTB and FIC/MTB progeny. AIC/MTB and FIC/MTB positive animals are induced with Dox through drinking water for 1 or more weeks to induce transgene expression in mammary epithelium. MGs are extracted and analyzed by IHC, RT-qPCR, WB, and wholemounts to confirm AIB1 and FOXA1 overexpression and explore differences in histopathology within our AIC and FIC models. Figure created with BioRender.com.

AIC/MTB founder line 3 (AIC-3/MTB) and MTB/TetO-Cre control mice were induced with Dox for 2 weeks. Mammary glands R2/3 and L2/3 were combined, and epithelial cells isolated. Mammary gland L4 was used for histology, and R4 for wholemounts. The mRNA levels of AIB1 and Cre from AIC-3/MTB and MTB/TetO-Cre mammary epithelium was measured by RT-qPCR targeting AIB1, Cre, and β-Actin (Fig. 2-5 C-D.). AIC-3/MTB mice had significantly higher levels of AIB1 mRNA than the MTB/TetO-Cre controls (Fig. 2-5C). Differences in Cre mRNA levels were non-significant between founder line 3 and the control (Fig. 2-5D). Cre mRNA expression within the mammary epithelium suggests the transgene is successfully expressed within the mammary epithelium and turned-on following 2-weeks Dox induction. With equivalent levels of mammary Cre expression between AIC-3/MTB and MTB/TetO-Cre, greater levels of AIB1 mRNA in the AIC model can be credited to AIC transgene expression. The AIC founder line 3 strain is thus an expressor of the AIC transgene, and the transgene successfully increases AIB1 transcription within the AIC model. Finally, a 2-week Dox induction is sufficient to turn on transgene expression in mammary epithelium.

Mammary glands R4 from AIC experimentals and Cre controls were stained in hematoxylin and fixed in Xylene for wholemounts (Fig 2-5E). No apparent difference in mammary gland morphology is observed between the AIC/MTB and MTB/TetO-Cre control MGs after a 2-week Dox induction. What may be abnormalities within the AIC experimentals, indicated with a white arrow, are large buds not seen within the control MGs (Fig 2-5D). Overall, a 2-week expression of the AIC transgene is insufficient to drive morphological differences in MG development within the AIC model. While morphological differences in mammary gland development are anticipated in the AIC model, these phenotypes are expected following longer inductions and in older virgin glands which allow for sufficient time for gland development and AIB1 protein overexpression.



E

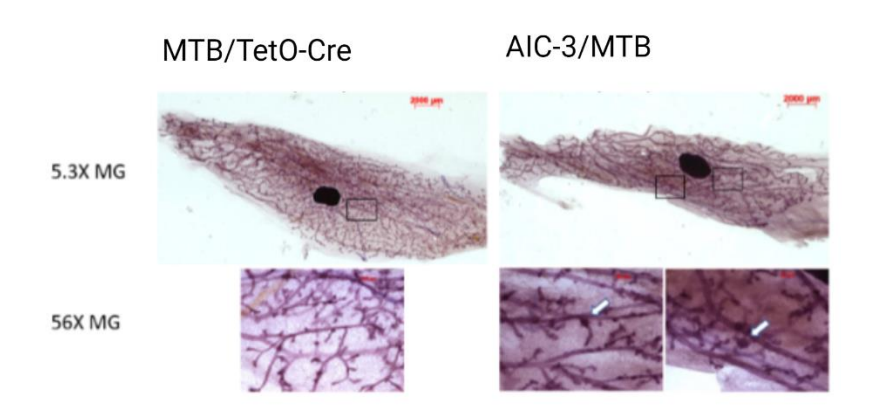


Figure 2-5: Exploring transgene expression in different founder lines of AIC in mouse mammary epithelium following 1-week and 2-week Dox induction. A-B) Mice (AIC-1/MTB: n= 2, age=12-16 weeks; AIC-2/MTB: n= 3, age=7 weeks; AIC-3/MTB: n= 2, age=6-8 weeks; MTB/TetO-Cre: n= 3, age=16 weeks) were induced with Dox through drinking water for 1 week. A) RNA was extracted from epithelial cells isolated from R2/3 and L2/3 and AIB1 mRNA levels were measured by RT-qPCR. AIB1 mRNA levels were normalized to β-Actin. B) AIB1 protein levels were measured in 1-week induced AIC-1/MTB L4 mammary gland by IHC, staining for AIB1. L4 mammary glands were embedded in paraffin and sectioned for H&E staining by McGill histology core. Nuclei were stained using blue DAPI stain, AIB1 protein was stained in red fluorescence. Top section of image displays AIB1 and AIB1/DAPI merged fluorescent signals. Bottom section of image displays DAPI/AIB1 merged fluorescent signals in screenshots of different areas within the gland. Image generated with Halo. C-D) mRNA levels of AIB1 (C) and Cre (D) were measured in the 2-week induced AIC/MTB founder 3 (AIC-3/MTB) and MTB/TetO-Cre R2/3 and L2/3 mammary gland epithelial cells by RT-qPCR and normalized to β-Actin. AIC-3/MTB and MTB/TetO-Cre control animals, were induced for 2-weeks with Dox through drinking water (AIC-3/MTB: n= 2 aged 6-7weeks; MTB/TetO-Cre: n= 3 aged 12-16 weeks). E) Mammary glands R4 were collected from AIC-3/MTB, and CNT 2-week Dox induced mice and stained in hematoxylin. Images were taken using AXIO-Zoom at 5.3X (top) and 56X (bottom) magnification. Black boxes represent areas of 56X magnification, white arrows highlight areas of abnormality. Figure images were generated using BioRender.com, figure graph and statistics were generated using GraphPad Prism.

## 2.1.3.1 Exploring longer Dox inductions in different AIC founder lines

The AIC model was further characterized, exploring mammary histopathology after longer Dox induction times. Mice aged 6-10 weeks from founder lines 1 and 3 of the AIC/MTB cross, and MTB/TetO-Cre mice were induced with Dox for 8 weeks. Following the 8-week induction, virgin mammary glands were extracted; R2/3 and L2/3 for protein and RNA extraction; R4 for histology; and L4 for wholemounts. To better explore our transgene in mammary epithelium at a protein and nucleic level, another group of the same design was induced for 8 weeks and made pregnant to expand mammary epithelium. Following the 8-week induction of pregnant AIC/MTB and MTB/TetO-Cre mice, pregnant mammary glands were collected identically to the virgin 8-week induced group.

Following the 8-week induction, pregnant mice of founder lines 1 and 3 (AIC-1 and AIC-3) had significantly greater levels of AIB1 mRNA in mammary epithelium compared to the MTB/TetO-Cre and MTB controls, with AIC-3 expressing significantly higher levels than AIC-1 (Fig 2-6 A). The Cre mRNA expression is significantly greater in AIC-1, AIC-3, and MTB/Teto-Cre than the MTB Cre negative control (Fig. 2-6 B). Cre expression is significantly lower in AIC-1/MTB than both AIC-3/MTB and the MTB/TetO-Cre control. The expression of Cre in AIC-1/MTB and AIC-3/MTB demonstrates that the AIC transgene is turned on and transcribed. Furthermore, with the expression of Cre within the MTB/TetO-Cre being significantly greater than that of AIC-1, it can be concluded that elevated AIB1 mRNA levels are not a result of greater Cre expression, and ultimately AIC transgene expression increases AIB1 mRNA expression in the AIC-1 and AIC-3 mice. Significantly greater levels of AIB1 mRNA expression are measured within AIC/MTB experimental mice originating from founder line 3 in comparison to experimental progeny of founder line 1. In conclusion, founder line 3 is the strongest expressor of our transgene and will be further characterized.

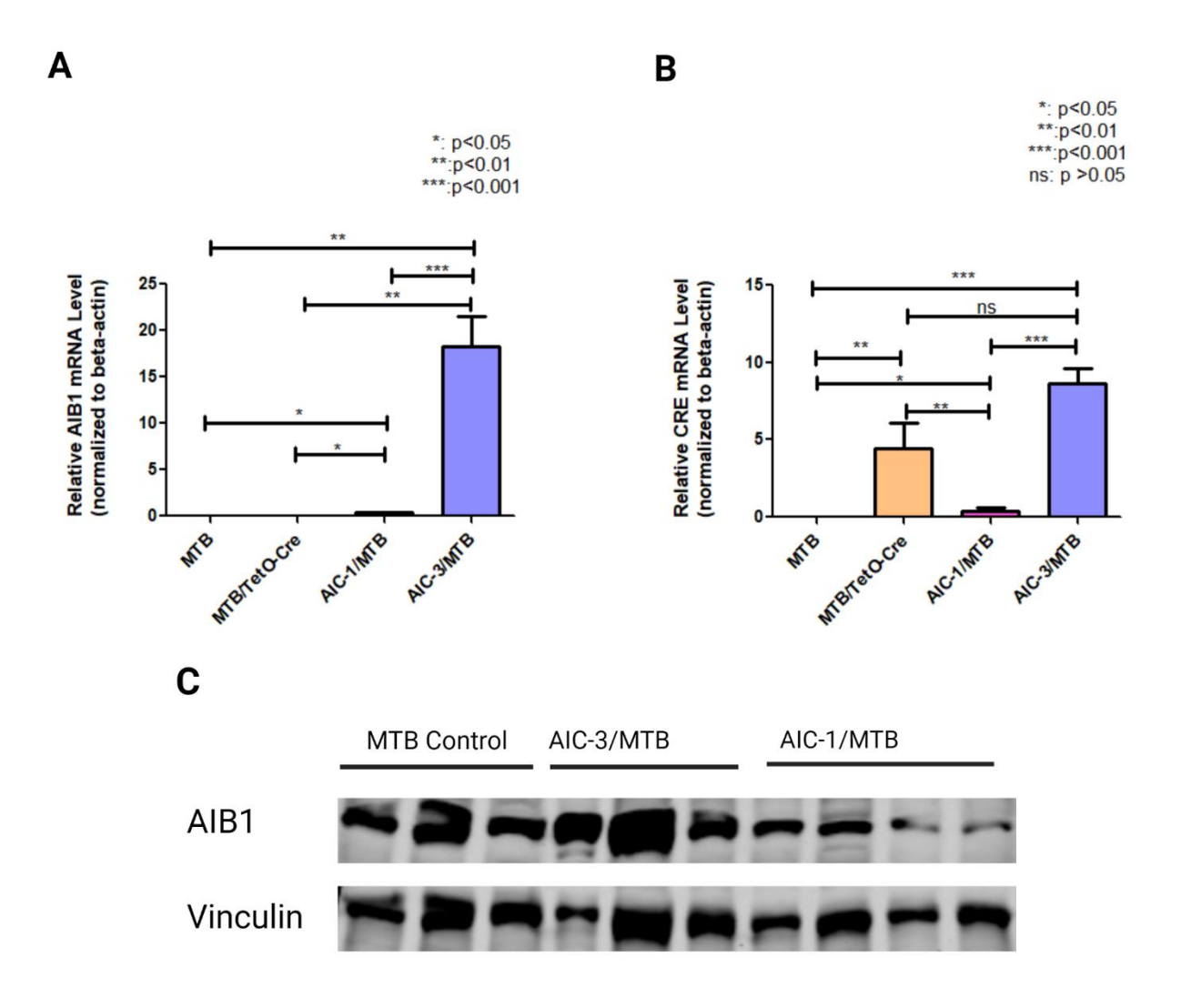
Protein was extracted from whole R2/3 and L2/3, crushed, pregnant mammary glands and analyzed by western blot, blotting for AIB1 and Vinculin (Fig. 2-6 C). AIB1 protein signal is measured within every sample, with stronger signals within AIC experimentals (Fig. 2-6 D). To determine the level

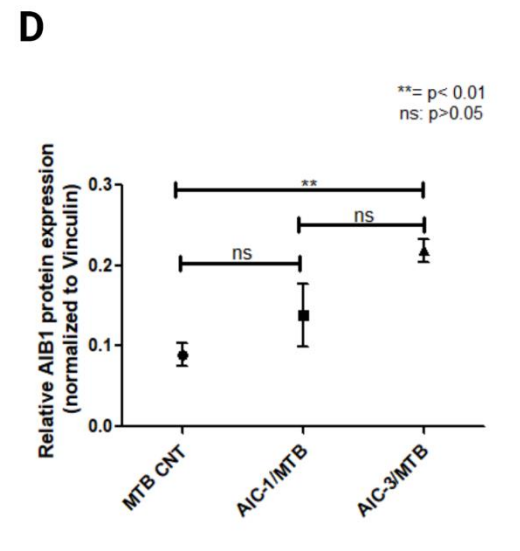
of AIB1 protein signal within each sample, AIB1 protein expression was quantified by normalizing AIB1 signal intensity to the Vinculin loading control intensity (Fig. 2-6 D). The AIB1 protein signal in AIC-3/MTB was significantly greater than both AIC-1/MTB and MTB/TetO-Cre mice. AIC-1/MTB AIB1 signal was not significantly greater than MTB/TetO-Cre, however, AIB1 protein signal trend in the AIC-1/MTB cohort is greater than the control. No significant difference in AIB1 signal within founder lines 1 and 3 of the AIC/MTB mice was measured, however, founder line 3 AIB1 expression trend is greater than founder line 1. Signal intensity corresponding to protein expression level, the significantly greater intensity of AIC-3/MTB than MTB/TetO-Cre can be interpreted as significantly higher AIB1 expression within the AIC founder line 3mice. In conclusion, AIC founder line 3 successfully overexpresses AIB1 at a protein level. Additionally, AIC-1/MTB AIB1 expression trend is greater than the control, suggesting founder line 1 is expressing higher levels of AIB1 at a protein level, further implying AIB1 overexpression in mammary glands. The trend of higher AIB1 expression within AIC founder line 3 than founder line 1, and the significantly higher AIB1 protein expression than the control, suggests AIC founder line 3 is the strongest expressor of the AIC transgene in comparison to founder line 1. Fitting with the relative mRNA expression levels of AIB1, the greater protein AIB1 levels were largely anticipated. With AIB1 mRNA expression levels being significantly greater within the AIC-3/MTB, greater AIB1 protein levels than both the MTB control and AIC-1/MTB were predicted. Being a greater expressor of the AIC transgene, founder line 3 has been selected for further characterization through long term expression studies.

Mammary glands L4, from both virgin and pregnant mice, were stained in hematoxylin, fixed in xylene, and mounted for wholemounts (Fig. 2-6 E-G). Within the virgin condition, both AIC-1/MTB and AIC-3/MTB have abnormal mammary gland development. Visually, AIC/MTB mice have greater branching compared to the MTB/TetO-Cre controls. To quantify, the number of alveolar buds within the MG was counted within the 37X magnification imaged sections of the MG (Fig. 2-6 F). Within the AIC-1/MTB experimentals a mean of 135 alveolar buds were counted, AIC-3/MTB 128 buds, and MTB/TetO-

Cre a mean of 67. AIC models overexpressing AIB1 have significantly greater number of alveolar buds, approximately 2X more than the MTB/TetO-Cre controls. The overexpression of AIB1 within the AIC models drives increased ductal branching and alveolar bud development within virgin mammary glands. Increased budding suggests elevated mammary gland development and may be reflective of early mammary transformation. Subsequently, AIB1 overexpression within AIC-3 mammary glands may drive ductal hyperplasia, an initial stage of breast cancer, after 8-weeks of induction. AIB1 overexpression, however, is sufficient to drive increased ductal branching and consequentially mammary growth.

Within the pregnancy condition, 8-week induced pregnant AIC experimental MGs appeared to be visually larger in overall size compared to the MTB/TetO-Cre controls, however, there was notable variation in MG size and branching between glands, therefore, there is no conclusive evidence of morphological difference in development during pregnancy (Fig. 2-6 G). To further explore pregnant gland development, 8-week induced AIB1/MTB mice will be sacrificed at different time points postpartum to explore how AIB1 overexpression in mammary epithelium effects involution. Previous studies have demonstrated delayed alveoli collapse and unsuccessful remodeling of the mammary gland 21 days postpartum in AIB1-tg mice overexpressing AIB1 [63]. We thereby predict similar phenotypes within our AIB1 over expression AIC model. To clarify the role of AIB1 in mammary gland development, we will continue exploring the role of AIB1 overexpression in early mammary gland development, involution, and tumorigenesis using our AIB1 overexpression model.





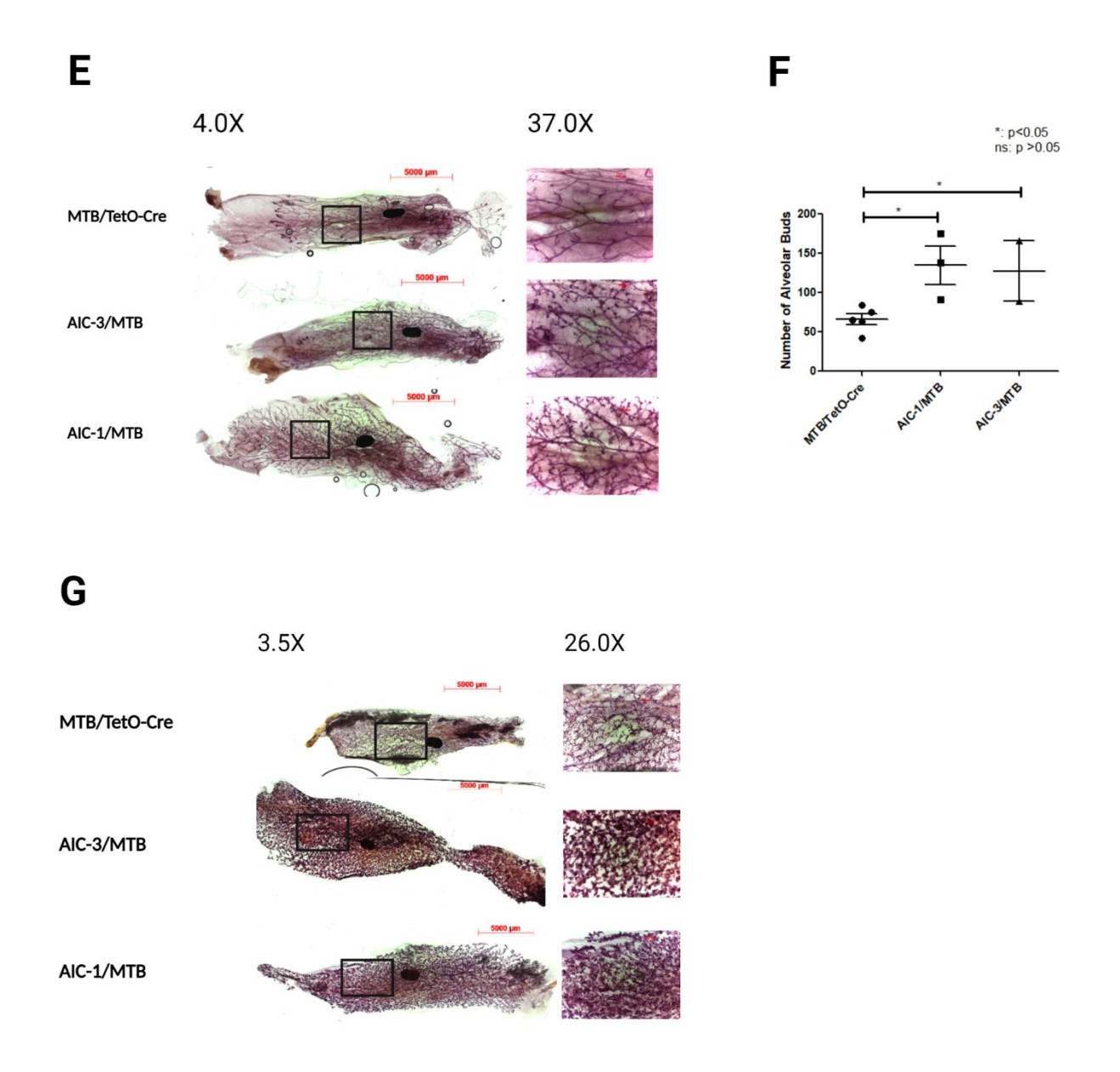


**Figure 2-6: 8-week induced pregnant and virgin AIC/MTB express AIC transgene in mammary glands.** Mice were induced for 8-weeks with Dox water and MG R2/3, L2/3, R4, and L4 were collected for RNA analysis by qPCR (A-B), protein analysis by western blotting (C-D), and wholemounts (E-G). AIC-1/MTB: virgin n= 3, pregnant n= 2 age 11-15 weeks; AIC-3/MTB: virgin n= 2, pregnant n= 5 age 12-15 weeks; MTB/TetO-Cre: virgin n= 5, pregnant n= 5 age 11-15 weeks. 8-week induction mice were separated into two conditions; virgin and pregnancy. Mice in virgin condition were sacrificed after 8-weeks of Dox induction, pregnancy condition mice were bred with FVB males after 6-weeks of induction and sacrificed at the 8-week dox induction time point (in late pregnancy). A-B) RNA expression of AIB1 (A) and Cre (B) in AIC/MTB founder lines 1 and 3, MTB/TetO-Cre, and Cre negative MTB control mice from the pregnancy condition was measured by RT-qPCR and relative mRNA expressions graphed using GraphPad Prism [ns= p-value >0.05, \*= p-value <0.05, \*\*= p-value <0.01, \*\*\*= p-value <0.001]. C-D) Western blot analysis of crushed whole R2/3, L2/3 pregnant mammary gland lysates. Blots were probed for AIB1 (150kDa) and Vinculin (124kDa) (C). Blot images were generated using Image Studio Lite and

BioRender.com. AIB1 protein expression was quantified by normalizing band intensity to loading controls Vinculin using Image Studio Lite and GraphPad Prism (D) [MTB Control: mean= 0.08933, SD= 0.02563, SE= 0.01480, n=3; AIC-1/MTB mean= 0.1379, SD= 0.06753, SE= 0.03899, n=4; AIC-3/MTB mean= 0.2188, SD= 0.02861, SE= 0.01430, n=3]. E-G) Virgin (E) and pregnant (G) MG wholemounts were stained with hematoxylin and imaged at 3.5X, 4.0X, 26X, and 37X magnification using AXIO-Zoom microscope. Black boxes on whole gland images represent areas of magnification taken for 26X and 37X magnification images. Wholemount figures were created with BioRender.com. F) Changes in virgin mammary gland development were quantified by counting the number of alveolar buds within 37X magnification images of virgin mammary glands [AIC-1/MTB: mean= 134.7, SD= 42.10, SE= 24.31, n= 3; AIC-3/MTB: mean= 127.5, SD= 54.45, SE= 38.50, n= 2; MTB/TetO-Cre: mean= 65.80, SD= 15.74, SE= 7.038, n= 5].

## 2.1.4 Early Characterization of Novel FIC Founder Lines

Similar to the AIC model characterization, we confirmed our transgene expression within mouse mammary epithelium, through a 1-week Dox induction. A small cohort (approximately 3 mice per cohort) of FIC/MTB mice from founder lines 1-3 and MTB/TetO-Cre control mice were induced with doxycycline (Dox) through drinking water for one week to turn on the transgene through the activation of rtTA. The MTB/TetO-Cre animals carry the TetO-IRES-Cre transgene, lacking the experimental FOXA1 transgene, therefore, should express basal levels of FOXA1 within the mammary gland. Following the 1-week induction, experimental and control animals were sacrificed and the mammary glands R2/3, L2/3, R4, and L4 were collected for histology, RNA, and protein collection. Mammary glands R2/3 and L2/3 were dissociated in tissue culture and epithelial cells were isolated to enhance epithelial RNA and protein signals of FOXA1 and CRE. From the isolated epithelial pellets, RNA was extracted. FOXA1 and CRE mRNA levels were measured by real time qPCR (RT-qPCR).

The FIC transgene expression was measured within the 3 FIC founder lines by qPCR (Figure 2-7. A-B). Between the three founder lines, founder line 1 (FIC-1/MTB) showed the greatest expression of FOXA1 mRNA, with FOXA1 mRNA levels significantly greater than the MTB/TetO-Cre control (Fig. 2-7 A). Founders 2 (FIC-2/MTB) and 3 (FIC-3/MTB) had no FOXA1 or CRE signals, suggesting these founders may not be expressors of our FIC transgene. Both FIC-1/MTB and the MTB/TetO-Cre controls have Cre mRNA expression, however, the Cre signal is significantly greater within FIC-1/MTB

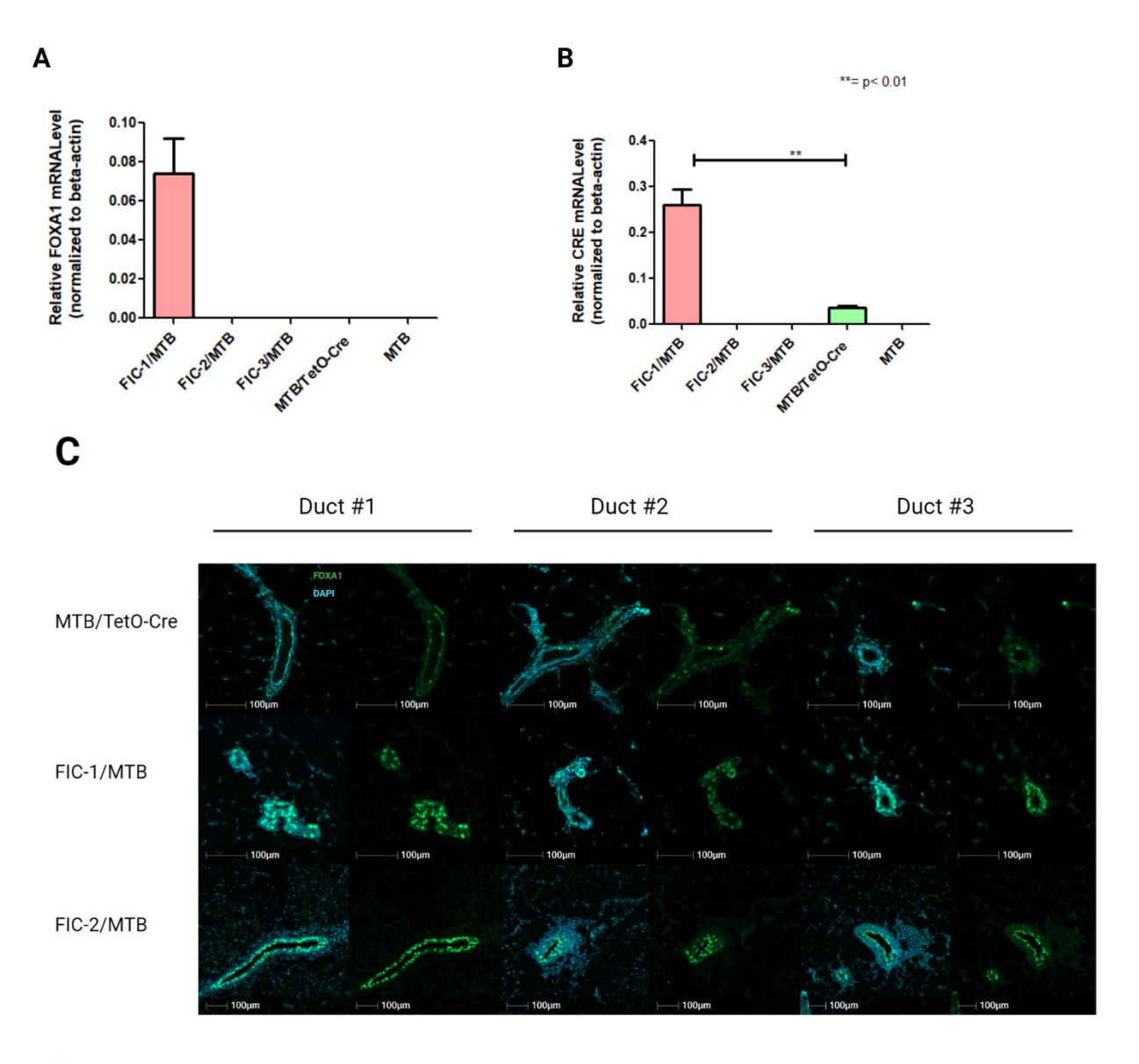
mammary (Fig. 2-7 B). The greater Cre expression is an unexpected phenotype, however, an explanation for this may be that the mice of the FIC founder 1 cohort have greater expression of the TetO system leading to increased levels of Cre mRNA expression. The expression of Cre mRNA is exclusive to mammary epithelial cells through the MMTV system, therefore Cre expression within the FIC-1/MTB demonstrates that the FIC transgene is turned on within mammary epithelium. The greater FOXA1 mRNA levels within the FIC-1/MTB are subsequently a result of transgene expression within mammary epithelium, and suggest the model overexpresses FOXA1 at an RNA level. Cre mRNA and greater levels of FOXA1 mRNA expression within the FIC-1/MTB demonstrate the founder line 1 as an expressor of our transgene and has been selected for further characterization.

Mammary glands (MG) L4 from MTB/TetO-Cre, and FIC/MTB founder lines 1 and 2 were sectioned and stained by IHF for the FOXA1 protein in 1-week induced mammary epithelium of FIC/MTB cohorts. In figure 2-7 C, staining of FOXA1 in EGFP green (right panel), and nuclear staining in DAPI blue (left panel) was done in the L4 mammary glands of MTB/TetO-Cre control, and FIC/MTB founders 1 and 2. Positive DAPI blue signal shows nuclei within the mammary epithelium; the expected spatial localization of FOXA1 protein (Fig. 2-5iii). Cells expressing green fluorescence EGFP signal are positive for FOXA1 protein. The overlay image of DAPI and FOXA1 (merge) shows FOXA1 is nuclear. As a nuclear transcription factor, nuclear localization of FOXA1 was anticipated. To quantify the level of FOXA1 expression in mammary epithelium, nuclei expressing the green, fluorescent FOXA1 signal were counted within the total epithelial nuclei populations of multiple mammary structures (ducts, TEB, and alveolar buds) within the gland, and graphed as %FOXA1 positive nuclei (Fig. 2-7 D). No significant difference in nuclear FOXA1 protein expression was measured between the FIC/MTB founders 1 and 2. However, mammary epithelium within both FIC founders had significantly higher levels of nuclear FOXA1 protein expression than the MTB/TetO-Cre (30%). FIC founder 1 had a mean of 72%, founder 2 62% and the MTB/TetO-Cre control 30% of epithelial nuclei positive for FOXA1. A positive fluorescent signal of FOXA1 within mammary epithelium demonstrates that FOXA1 is being expressed at a protein

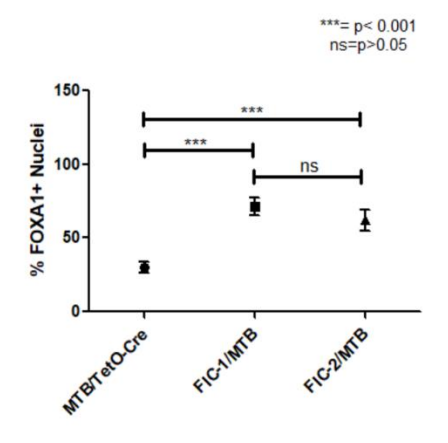
level within the FIC model. Furthermore, the significantly greater levels of FOXA1, a 2-fold increase, within the FIC model demonstrates the capacity of the model to successfully overexpress FOXA1 at a protein level within mammary epithelium. No significant differences in FOXA1 protein expression were measured within founders 1 and 2, it is concluded that both founders 1 and 2 are equal expressors of the FIC transgene. In contrast to the mRNA quantification (Fig 2-7 A), FIC-2/MTB expresses the FIC transgene at the protein level. An explanation for these contrasting results may lie within the RNA content within the FIC-2/MTB and FIC-3/MTB samples. The beta-Actin signal was low within both FIC-2/MTB and FIC-3/MTB compared to FIC-1/MTB and MTB/TetO-Cre control, suggesting the epithelial RNA content was low within the crushed mammary glands of these founder samples. To clarify the mRNA expression levels of the FIC transgene in FIC founders 2 and 3, future RNA extractions will be optimized by increasing mammary gland content, and transgenic FOXA1 and CRE mRNA levels will be measured by RT-qPCR.

Mammary glands (MG) L4 from MTB/TetO-Cre, and FIC/MTB founder lines 1 and 2 were stained with hematoxylin and eosin by McGill histology core (Fig. 2-7 E). A small sample size of FIC-3/MTB limited glands available for histological analysis, therefore, H&E was not performed on MGs from founder line 3. To confirm founder line 3 expression of our FIC transgene, and consequential impacts on mammary gland development, the experiment will be repeated with a larger sample size. When imaged and analyzed by Halo, abnormal mammary gland development was observed within the MGs of both FIC/MTB founder lines. FIC/MTB glands had delayed development with very few ducts, ductal branching, and terminal end buds (TEBs). The number of mammary structures, structures being ducts, alveolar buds, and TEB, were fewer within the FIC/MTBs with MTB/TetO-Cre having 4X the amount of counted structures (Fig. 2-7 F). Due to small sample size, differences cannot be confirmed statistically, however, FOXA1 overexpression trends with decreased mammary gland structure formation. Studies have shown FOXA1 ablation in mammary glands had no effect on lobulo-alveolar maturation, nor milk production [2]. It was further proposed that FOXA1 may actively repress alveolar lineage

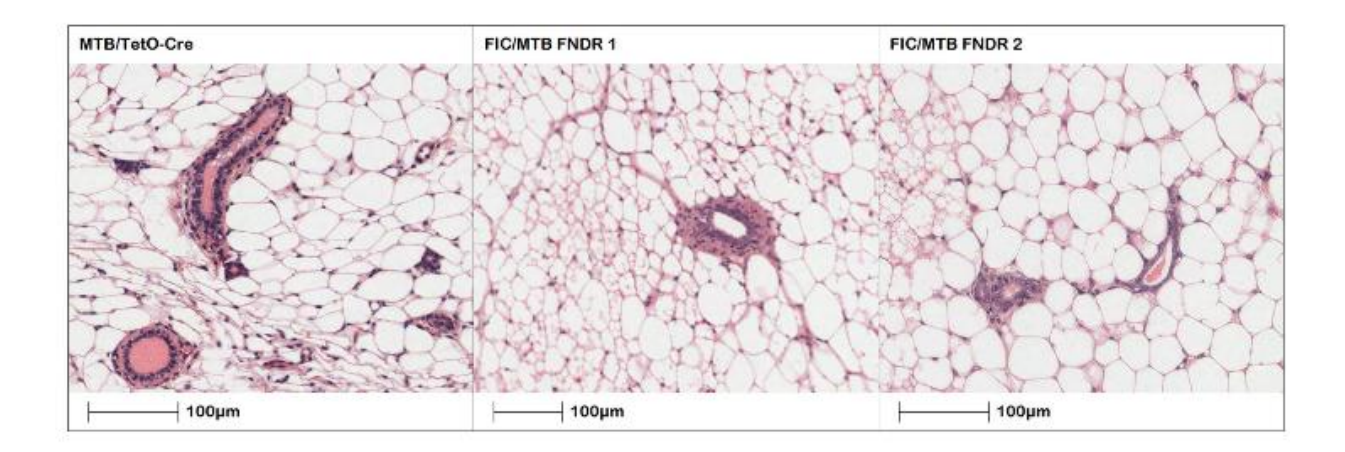
maturation and alveologenesis [2]. The observed trend within our H&E-stained mammary glands supports this proposed function of FOXA1 in early mammary gland development, whereby MGs overexpressing FOXA1 are underdeveloped with fewer ducts, TEBs and alveolar buds.



# D



E



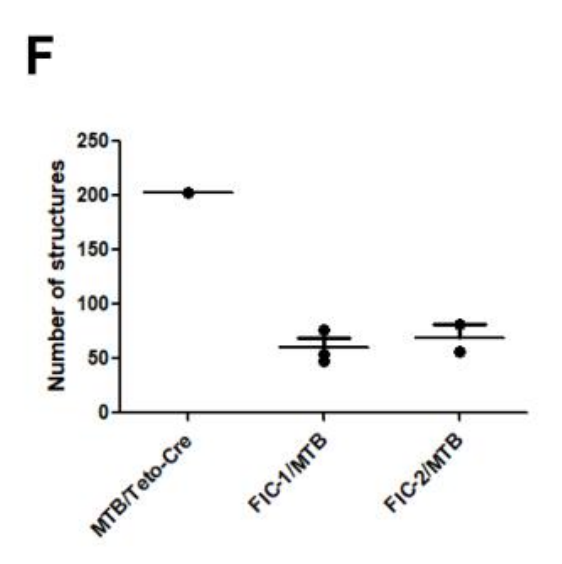


Figure 2-7: Exploring transgene expression in mouse mammary epithelium following 1-week Dox induction of different founder lines of the FIC model. Mice (FIC-1/MTB: n=3, age=8 weeks; FIC-2/MTB: n=2, age=6-12 weeks; FIC-3/MTB: n=2, age=16 weeks; MTB/TetO-Cre: n=3, age=16 weeks) were induced with Dox through drinking water for 1 week. A-B) RNA was extracted from epithelial cells isolated from R2/3 and L2/3 and FOXA1 and Cre mRNA levels were measured by RT-qPCR. FOXA1 and Cre mRNA levels were normalized to β-Actin. Mammary epithelial Cre (B) and FOXA1 (A) mRNA levels were measured within FIC founder lines 1, 2, and 3. No FOXA1 signal was detected in FIC-3/MTB, FIC-2/MTB, or controls (MTB and MTB/Teto-Cre), and no Cre signal in FIC-3/MTB, FIC-2/MTB, and Cre-negative MTB control. C) IHF staining of FOXA1 in EGFP green (right panel), and nuclear staining in DAPI blue (left panel) was done in the L4 mammary glands of MTB/TetO-Cre control, and FIC/MTB founders 1 and 2. Multiple representative images of stained ducts and TEBs were taken (Duct #1-#3). D) Nuclei with the green FOXA1 signal were counted within the total epithelial nuclei populations of multiple mammary structures using HALO (ducts, TEB, and alveolar buds) and graphed as %FOXA1 positive nuclei (\*\*\*= p<0.001, ns= p>0.05). MTB/TetO-Cre: mean=30.04% ± 3.822% n=19, IC-1/MTB: mean=71.66 %± 6.000% n=14, FIC-2/MTB: mean=62.28% ± 7.180% n=12. E)

H&E staining of FIC-1/MTB and FIC-2/MTB L4 mammary glands. L4 mammary glands were embedded in paraffin, sectioned, and stained (H&E) by McGill histology core. Magnified images of H&E staining were taken using Halo. Number of structures, structures being ducts, terminal end buds (TEB), and alveolar buds, were counted in the entire gland and values graphed. Number of structures measured; FIC-1/MTB: 48 (n= 3, SD=, 15.31 SE= 8.838), FIC-2/MTB: 57 (n= 2, SD= 16.97, SE= 12.00), MTB/TetO-Cre: 203 (n= 1, SD= 0.0 SE= 0.0). Figure images were generated using Halo, figure graphs and statistics were generated using GraphPad Prism.

#### 2.1.4.1 Exploring longer Dox inductions in FIC model

Like the AIC model, the FIC model was further characterized through longer Dox induction, and the mammary histopathology explored. Mice aged 6-10 weeks from FIC founder lines 1, 2, and 3 of the and MTB/TetO-Cre control were induced with Dox for 8 weeks. Following the 8-week induction, virgin mammary glands were extracted; R2/3 and L2/3 for protein and RNA extraction; R4 for histology; and L4 for wholemounts. To better explore our transgene in mammary epithelium at a protein and nucleic level, another group of the same design was induced for 8 weeks and made pregnant to expand mammary epithelium. Following the 8-week induction of pregnant FIC/MTB, and MTB/TetO-Cre mice, pregnant mammary glands were collected identically to the virgin 8-week induced group.

8 week induced pregnant glands from both FIC-1/MTB and FIC-3/MTB had significantly greater levels of FOXA1 mRNA in mammary epithelium than the MTB/TetO-Cre and MTB controls (Fig, 2-8, A). Furthermore, both FIC-1/MTB and FIC-3/MTB had significant levels of Cre mRNA expression showing that the FIC transgene is expressed within both founder lines, and FIC transgene expression induces greater levels of FOXA1 mRNA in mammary epithelium (Fig. 2-8 B). The FIC founder line 3 had significantly greater levels of both Cre and FOXA1 mRNA than founder line 1. It is concluded that FIC founder line 3 is a higher expressor of the FIC transgene and has greater FOXA1 expression at an RNA level. To mention the discrepancy between the 1-week and 8-week induction; following the 1-week induction, there was no FOXA1 mRNA signal in the FIC-3/MTB experimentals, however, following the 8-week induction, the FOXA1 mRNA levels are significantly greater than FIC-1/MTB. Several factors may have contributed to this discrepancy. One such factor may be on account of RNA quality, leading to

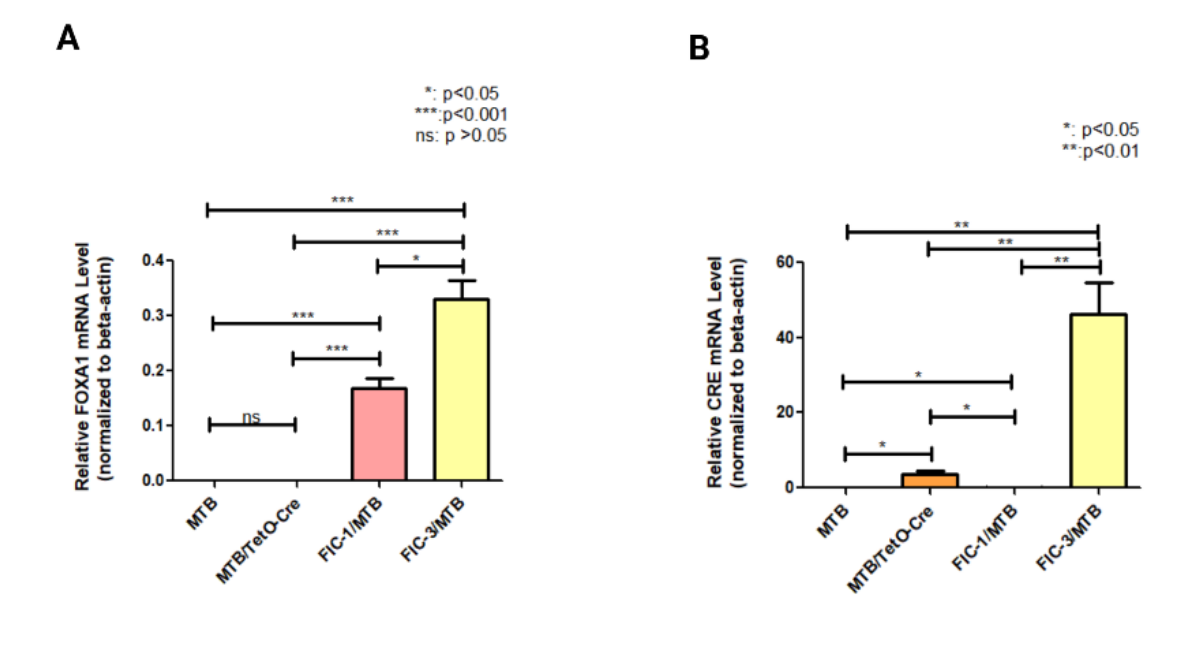
no signal detection within the set qPCR cycle range. Another factor may be that 1-week induction was insufficient time to turn on the transgene within the FIC-3/MTB experimental mice.

Protein was extracted from whole R2/3 and L2/3, crushed, pregnant mammary glands and analyzed by western blot, blotting for FOXA1 and Vinculin (Fig. 2-8 C). FOXA1 protein signal was measured within both FIC-1/MTB and FIC-3/MTB at a stronger intensity than the MTB controls. To determine FOXA1 expression levels, the FOXA1 signal intensity was normalized to the loading control Vinculin (Fig. 2-8 D). The FOXA1 protein signal was significantly greater within both FIC founder lines than the MTB control, with the strongest signal of FOXA1 in the FIC-3/MTB mammary. FOXA1 protein expression signals show the FIC models as significantly greater expressors of FOXA1 suggesting FOXA1 is being overexpressed at a protein level within the FIC model. FOXA1 overexpression within the FIC founder lines demonstrates the capacity of the dox-inducible transgene to overexpress FOXA1 at a protein level within mouse mammary glands. Furthermore, FIC-3/MTB has the strongest FOXA1 signal suggesting founder line 3 to be the strongest expressor of the FIC transgene. Following the FOXA1 mRNA expression trend, greater expression of FOXA1 protein in the mammary glands of FIC mice was anticipated, and furthermore founder line 3 with greater FOXA1 protein expression than founder line 1.

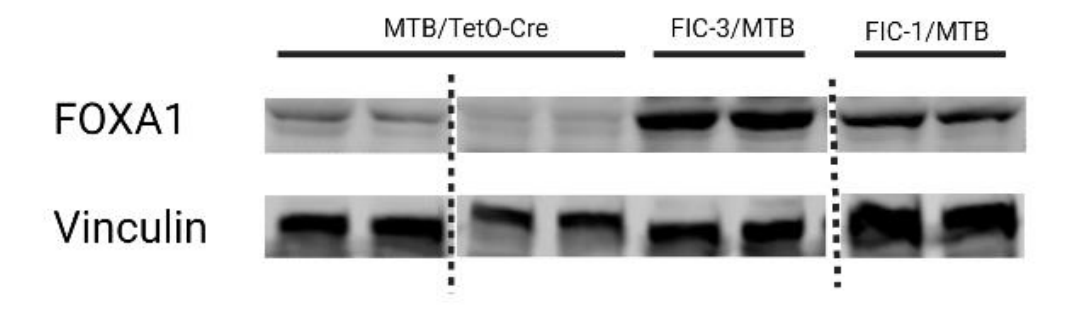
Mammary glands L4, from both virgin and pregnant mice, were stained in hematoxylin, fixed in xylene, and mounted for wholemounts (Fig. 2-8 E-G). FIC/MTB 8-week induced virgin MGs, visually resembles the MTB/TetO-Cre control MGs, with FIC-3/MTB having slightly greater branching and alveolar bud formation than FIC-1/MTB and the control (Fig. 2-8 E). FIC-3/MTB had a significantly greater count of alveolar buds (mean= 104) than FIC-1/MTB (mean=37) and the control (mean=67) (Fig. 2-8 F). In reference to mRNA expression levels of FOXA1, greater levels of FOXA1 mRNA trends with increased alveolar budding. Contrarily, FOXA1 overexpression trends with delayed mammary gland development following 1-week induction while FOXA1 overexpression following an 8-week induction increased alveolar bud formation in founder line 3 (Fig. 2-7 F, Fig. 2-8 F). An explanation for this trend may be that FOXA1 overexpression stimulates an immune response targeting epithelial cells

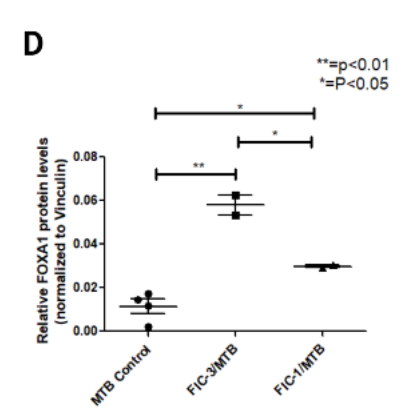
overexpressing FOXA1, resulting in delayed mammary gland development. However, after an extended period of FOXA1 overexpression, the cells are able to escape immune cell targeting resulting in increased mammary gland development and hyper alveolar budding in longer inductions.

Within the pregnancy condition, 8-week induced pregnant FIC experimental MGs had no notable variation in MG size and branching compared to the MTB controls. Ultimately, there is no conclusive evidence of FOXA1 driven morphological changes in development during pregnancy (Fig. 2-8 G). As mentioned above, consequences of FOXA1 overexpression in pregnant and virgin MG development will be further explored, investigating mammary gland morphology following various induction time points. FOXA1 plays a key role in the development and differentiation of mammary glands specifically by modulating the ER, however, the specific role of FOXA1 in mammary gland development is yet to be defined [2]. To elucidate the function of FOXA1 in mammary gland development, we will continue investigate FOXA1 overexpression in early mammary gland development and tumorigenesis using our FIC overexpression model. Finally, founder line 2 was not analyzed in the 8-week induction experiment due to an insufficient number of FIC-2/MTB experimental animals at the time of analysis. When sufficient FIC-2/MTB animals are generated, the experiment will be repeated to explore mammary gland histopathology and investigate FOXA1 overexpression within mammary glands of this founder line.



С





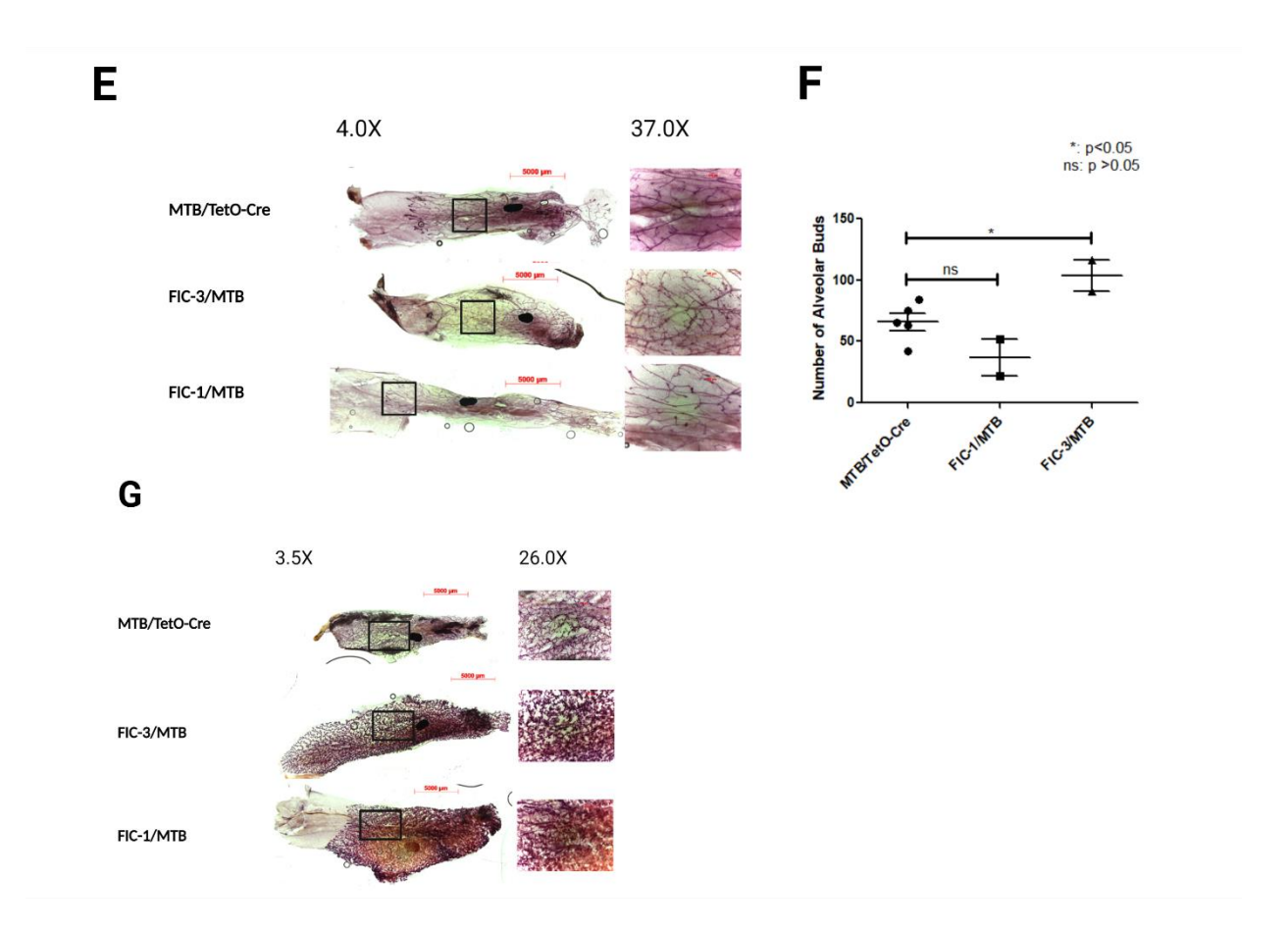


Figure 2-8: 8-week induced pregnant and virgin FIC/MTB mice express the FIC transgene in mammary glands. Mice were induced for 8-weeks with Dox water and MG R2/3, L2/3, R4, and L4 were collected for RNA analysis by qPCR (A-B), protein analysis by western blotting (C-D), and wholemounts (E-G). FIC-1/MTB: virgin n= 2, pregnant n= 2 age 10-15 weeks; FIC-3/MTB: virgin n= 2, pregnant n= 2 age 15-20 weeks, MTB/TetO-Cre: virgin n= 5, pregnant n= 5 age 11-15 weeks. 8-week induction mice were separated into two conditions; virgin and pregnancy. Mice in virgin condition were sacrificed after 8-weeks of Dox induction, pregnancy condition mice were bred with FVB males after 6-weeks of induction and sacrificed at the 8-week dox induction time point during late pregnancy. A-B) RNA expression of FOXA1 (A) and Cre (B) in FIC-1/MTB, FIC-3/MTB, MTB/TetO-Cre, and Cre negative MTB control mice from the pregnancy condition was measured by RT-qPCR and relative mRNA expressions graphed using GraphPad Prism [ns= p-value <0.05, \*= p-value <0.05, \*\*= p-value <0.01, \*\*\*= p-value <0.001]. C-D) Western blot analysis of crushed whole R2/3, L2/3 pregnant mammary gland lysates. Blots were probed for Vinculin (124kD) and FOXA1 (50kDa) (C). Blot images were generated using Image Studio Lite and BioRender.com. FOXA1 protein expression was quantified by normalizing band intensity to loading control Vinculin using Image Studio Lite and GraphPad Prism (D) [D: MTB Control: mean= 0.01137, SD= 0.006683, SE= 0.003342, n=4; FIC-1/MTB mean= 0.02976, SD= 0.0008786, SE= 0.0006212, n=2; FIC-3/MTB mean= 0.05800, SD= 0.006425, SE= 0.004543, n=2]. Dotted lines in figure C represent cropped lanes from the same blot. E-G) Virgin (E) and pregnant (G) MG wholemounts were stained with hematoxylin and imaged at 3.5X, 4.0X, 26X, and 37X magnification using AXIO-Zoom microscope. Black boxes on whole gland images represent areas of magnification taken for 26X and 37X magnification images. Wholemount figures were created with BioRender.com. F) Changes in virgin mammary gland development were quantified by counting the number of alveolar buds

within 37X magnification images of virgin mammary glands [FIC-1/MTB: mean= 37.00, SD= 21.21, SE= 15.00, n= 2; FIC-3/MTB: mean= 103.5, SD= 17.68, SE= 12.50, n= 2; MTB/TetO-Cre: mean= 65.80, SD= 15.74, SE= 7.038, n= 5].

Founder line 2 was analyzed later than the FIC-1/MTB and FIC-3/MTB 8-week induced mice due to an insufficient number of FIC-2/MTB experimental animals at the time of analysis. Furthermore, due to an insufficient number of FIC-2/MTB experimental mice, protein and RNA analysis was done in only virgin, and not pregnant, 8-week induced mammary glands of FIC-2/MTB mice. Similar to FIC-1/MTB and FIC-3/MTB, virgin mammary glands R2/3 and L2/3 were extracted for protein and RNA analysis following the 8-week induction of a small cohort of FIC-2/MTB, MTB/TetO-Cre and MTB controls (Fig. 2-9). Measuring RNA expression by RT-qPCR, FOXA1 mRNA expression is significantly higher in FIC-2/MTB than both the MTB/TetO-Cre and MTB controls (Fig 2-9 A). Cre expression is significantly higher in both the FIC-2/MTB and MTB/TetO-Cre than the Cre negative MTB control (Fig. 2-9 B). The negative Cre signal in the MTB Cre negative controls demonstrates that Cre is positively expressed within the Cre is positively expressed within FIC founder line 2 and the MTB/TetO-Cre mammary glands.

Consequentially, Cre expression signifies the transgene is turned on within mammary epithelium, and FOXA1 mRNA overexpression within the FIC-2/MTB is a result of transgene expression. In conclusion, FIC founder line 2 is a positive expressor of the FIC transgene.

FOXA1 protein expression was measured in founder line 2 by western blot (Fig. 2-9 C). A strong FOXA1 protein signal was detected in the FIC-2/MTB experimentals, and very weak signals were detected in the MTB controls. When quantified, FOXA1 protein expression was significantly greater within the FIC-2/MTB than the controls (Fig. 2-9 D). A significant greater FOXA1 protein expression within the FIC-2/MTB demonstrates that FOXA1 is overexpressed at a protein level within FIC founder line 2. Consequentially, founder line 2 expresses the FIC transgene, and FIC transgene expression drives FOXA1 overexpression within the mammary gland. In conclusion, FIC founder line 2 is a positive expressor of the FIC transgene. Following the FOXA1 mRNA expression trend, greater expression of

FOXA1 protein in the mammary glands of FIC founder line 2 mice was anticipated. As FOXA1 is expressed within normal mammary gland, the weak signals from the MTB controls can be interpreted as basal FOXA1 expression in normal mammary glands.

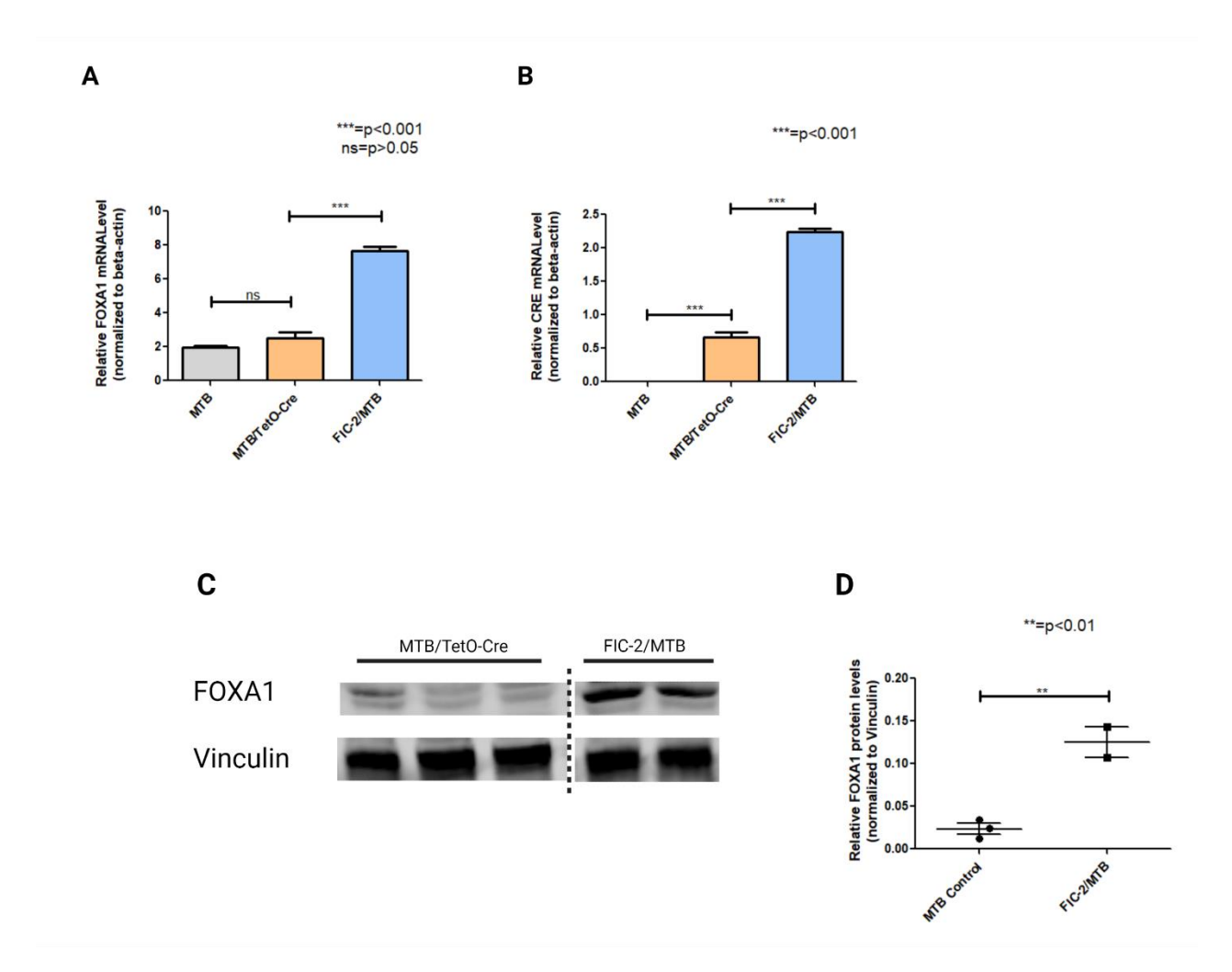


**Figure 2-9: 8-week induced virgin FIC-2/MTB mice express FIC transgene in mammary glands.** Mice were induced for 8-weeks with Dox water and MG R2/3, L2/3, R4, and L4 were collected for RNA analysis by qPCR (A-B) and protein analysis by western blotting (C-D). FIC-2/MTB: n= 2, age 11-16 weeks; MTB/TetO-Cre: n= 2 age 11-16 weeks. A-B) RNA expression of FOXA1 (A) and Cre (B) in FIC-2/MTB, MTB/TetO-Cre, and Cre negative MTB control mice was measured by RT-qPCR and relative mRNA expressions graphed using GraphPad Prism [ns= p-value >0.05, \*= p-value <0.05, \*\*= p-value <0.01]. C-D) Western blot analysis of crushed whole R2/3, L2/3 virgin mammary gland lysates. Blots were probed for Vinculin (124kDa) and FOXA1 (50kDa). Blot images were

generated using Image Studio Lite and BioRender.com. FOXA1 protein expression was quantified by normalizing band intensity to loading controls Vinculin and Actin, respectively, using Image Studio Lite and GraphPad Prism (D) [MTB Control: mean= 0.02381, SD= 0.3325. SE= 0.1920, n=3; FIC-2/MTB mean= 0.1251, SD= 0.02535, SE= 0.01793, n=2]. Dotted lines in figure C represent cropped lanes from the same blot.

# 2.1.4.2 Exploring FOXA1 overexpression in organoid culture

To explore FOXA1 overexpression in vitro, we generated organoid systems from mammary epithelium of 8-week Dox-induced MTB/TetO-Cre and FIC/MTB founder lines 1 and 3 mice (Fig. 2-10). FOXA1 and Cre staining was performed on organoid culture (Fig. 2-10 A-B). Greater FOXA1 staining is seen in both FIC founder line 1 and 3 compared to the MTB/TetO-Cre control, with FIC founder line 3 having the strongest FOXA1 expression. Cre staining was unsuccessful showing non-specific staining in all the organoid systems, including the Cre-positive MTB/TetO-Cre control. Cre staining will be performed again using a new sensitive Cre antibody. Organoid size (µm) was measured and quantified (Fig. 2-10 B) to explore how FOXA1 overexpression affects organoid growth. Organoids from FIC mice were significantly larger than the MTB/TetO-Cre control (33.9 ±9.6µm). FIC-3/MTB organoids were largest in diameter ( $106.3 \pm 41.5 \mu m$ ), and significantly greater in size than FIC-1/MTB ( $48.2 \pm 11.7 \mu m$ ). The significant increase in organoid diameter upon FOXA1 overexpression indicates FOXA1 overexpression induces a hyper-proliferative state which is a hallmark of cancer. FOXA1 staining within organoids of the FIC founders demonstrates the FIC transgene is turned on within the FIC models, and FIC transgene expression drives FOXA1 overexpression. Furthermore, FOXA1 expression levels trend with organoid size, whereby FIC founder line 3 organoids expressing the highest levels of FOXA1 are also largest in diameter. FOXA1 overexpression is sufficient to drive hyper proliferation within mammary-derived organoids, suggesting that FOXA1 overexpression is sufficient to drive breast tumor growth. FIC founder line 3 had the strongest expression of FOXA1, indicating that founder line 3 is the strongest expressor of the FIC transgene.

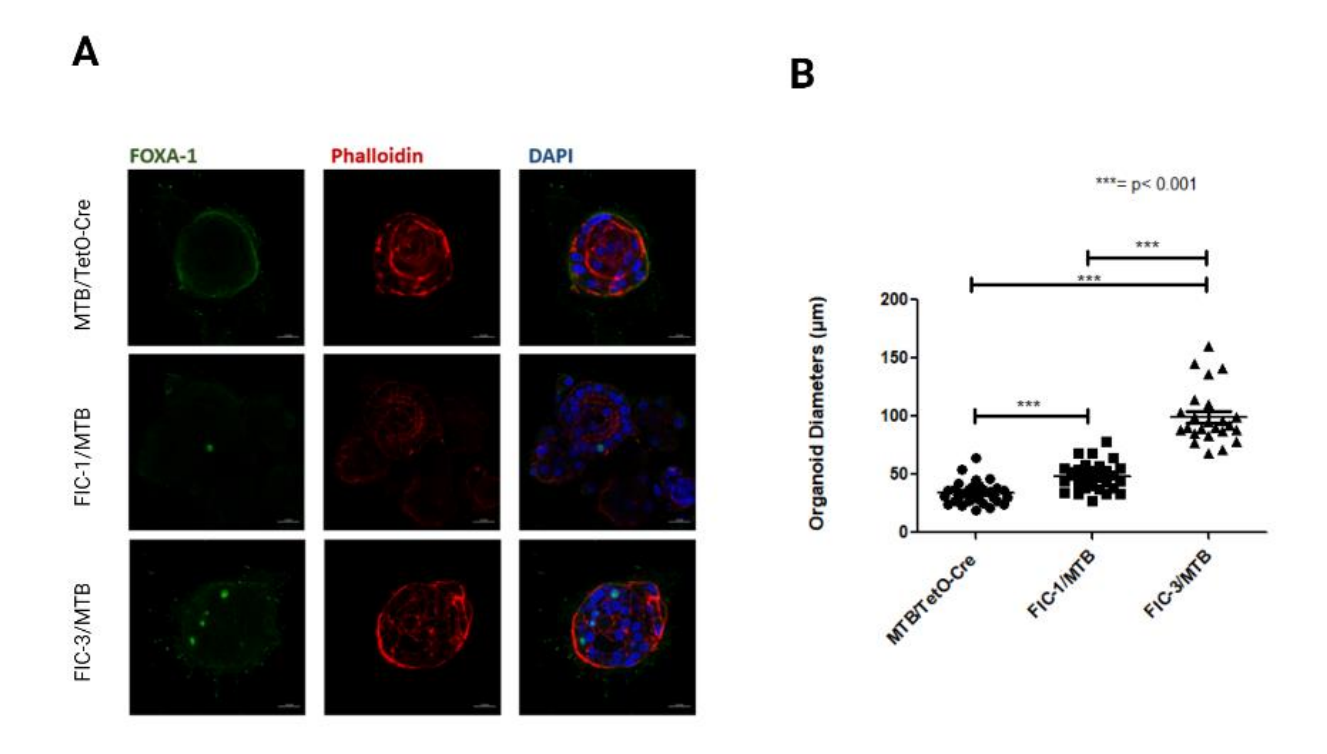


**Figure 2-10: 10-week Dox-induced organoids grown from FIC-1/MTB and FIC-3/MTB mammary epithelia.** Organoids were grown from 8-week induced mammary glands of MTB/TetO-Cre and FIC/MTB founder lines 1 and 3. Organoids were induced in culture with doxycycline for another 2 weeks. Organoids were stained for FOXA1 (green), Phalloidin (red), and DAPI nuclear staining (blue). Organoid images were taken using EVOS XL Core microscope and figure created with BioRender.com. Organoid diameter was measured in μm using ZEN and graphed using GraphPad Prism. Organoid diameter (μm): MTB/TetO-Cre: mean= 33.87, SD= 9.619, SE= 1.728, n= 31; FIC-1/MTB: mean= 48.22, SD= 11.67, SE= 2.096, n= 31; FIC-2/MTB: mean= 106.3, SD= 41.51, SE= 8.302, n= 25.

#### 2.2 Future Directions

#### 2.2.1 Further characterization of AIC and FIC mouse models

At present, AIC and FIC founder lines 3 have been identified as strong expressors of the AIC and FIC transgenes and will be further characterized in long term induction studies. Additionally, expression of the AIC and FIC transgene drives AIB1 and FOXA1 overexpression within mammary epithelium. AIB1 overexpression has been shown to increase alveolar bud formation and mammary gland development in AIC/MTB mice following 8-week Dox induction (Fig. 2-8, iii.). In the FIC/MTB model, FOXA1 overexpression trends with delayed mammary gland development following 1-week induction and increased alveolar bud formation in founder line 3 following an 8-week induction (Fig. 2-5, ii., Fig. 2-8 iii.). Furthermore, FOXA1 overexpression within organoid culture drove hyper-proliferation, suggesting FOXA1 as a sufficient driver of mouse mammary tumorigenesis (Fig. 2-9). While this project has accomplished early characterization of AIC and FIC founder lines 1 and 3, much remains to be done characterizing the novel AIC and FIC mouse models overexpressing AIB1 and FOXA1. Firstly, the lack of a sensitive Flag-tag, and Cre antibody for western blotting and IHC limited our ability to confirm transgene expression at a protein level. Antibodies will be tested with appropriate controls to find functioning antibodies that successfully identify transgenic proteins. In the event that poor transgenic protein detection is a result of low transgenic protein concentration within MG protein lysates, the AIC and FIC models have been crossed into the MIC strain which have shown increased MG transformation, consequentially expanding mammary epithelium and the population of cells expressing the AIC and FIC transgene [85]. To further explore mammary histopathology, H&E and IHC analysis and quantification will be performed on 8-week induced mammary glands of both AIC and FIC models. Finally, AIB1 overexpression will be explored in AIC mammary organoid systems to elucidate the role of AIB1 in epithelium growth and tumorigenesis.

A small cohort of AIC-3/MTB, FIC-3/MTB, FIC-2/MTB and MTB/TetO-Cre mice have been induced (at 8-12 weeks of age) with Dox for a long-term induction study to determine tumor onset and penetrance, exploring the tumorigenic capacity of the AIC and FIC models. Mice will be induced until

clinical endpoint or until they reach 2 years of age and palpated weekly to determine tumor onset. Long term induction will provide insight to whether AIB1 and FOXA1 overexpression is sufficient to drive tumorigenesis within the AIC and FIC models. These experimental and control cohorts are currently being expanded to increase the sample size for improved statistical significance. Differences in histopathology and biochemical signaling will be studied in the breast tumours of mice sacrificed at tumour endpoint. An AIB1-tg mouse model overexpressing AIB1 found that mice overexpressing AIB1 developed mammary adenocarcinomas after roughly 9 months [63]. Having shown AIB1 to be sufficient to drive tumorigenesis, and through the TetO system which allows for high expression, we predict the AIC model to develop tumors within the same time frame. The FIC model being a novel transgenic model of FOXA1 overexpression, tumor onset has yet to be identified within mouse models of breast cancer overexpressing FOXA1. However, FOXA1 has been shown to play a role in proliferation whereby knockdown of FOXA1 in MCF-7 cancer cells resulted in significant growth arrest demonstrating the requirement of FOXA1 for estrogen response in luminal breast cancer cells [6, 72]. Furthermore, FOXA1 overexpression within organoid systems of our FIC models drove organoid hypertrophy, a distinctive feature of cancer. Acting as a strong regulator of the ER, and being sufficient to drive organoid hyperproliferation, we anticipate FOXA1 overexpression to be sufficient to drive tumorigenesis in the FIC model.

2.2.2 Exploring the role of overexpressed AIB1 and FOXA1 in mammary gland development.

The role of AIB1 and FOXA1 in mammary gland development is not fully defined. As key regulators and coactivators of ER, FOXA1 and AIB1 have been identified as important players in mammary gland development [63]. An AIB1-tg mouse model overexpressing AIB1 discovered increased levels of hyperplasia, hypertrophy, and abnormal involution in mouse mammary gland [63]. Following postweaning involution, AIB1-tg mice had disorganized epithelium and delayed involution and unsuccessful remodeling of the gland 21 days postpartum [63]. KO studies have shown FOXA1 ablation in mammary glands has no effect on lobulo-alveolar maturation, nor milk production, proposing that

FOXA1 may actively repress alveolar lineage maturation and alveologenesis [2]. Evidently, FOXA1 and AIB1 play key roles in mammary gland development. With the AIC and FIC models, the role of overexpressed AIB1 and FOXA1 in mouse mammary gland can be further explored, providing insight to the role of these oncoproteins in mammary gland development and initial stages of breast cancer. Mammary gland structure and histopathology can be studied following different points of induction, and furthermore, AIB1 and FOXA1 inhibition in overexpression mammary glands can provide insight into development restoration.

## 2.2.3 Exploring the role of overexpressed AIB1 and FOXA1 in the context of a mutant ER.

Oncoproteins AIB1 and FOXA1 are critical regulators of ER transcriptional activity; AIB1 acting as a coactivator to increased ER binding and FOXA1 a critical transcription factor regulating over 90% of all ER target transcription [1, 2, 6]. Both AIB1 and FOXA1 are overexpressed in ER-positive luminal breast cancers [1,2]. To explore methods of upregulating ER activity, the AIC and FIC models will be crossed into the ESR1Y537S mutation model. The ESR1Y537S model employs a Cre recombinase/loxP systems to excise exon 9 containing the WT Y541 bringing the mutant exon 9 in frame, thereby introducing the Y541S mutant in mammary epithelium of transgenic mice upon Dox induction [88]. Through this cross, the transcriptional regulators of ER; AIB1 and FOXA1, can be expressed in an inducible fashion (Fig. 2-9). The cross will be an extension of our lab's investigation of the ESR1Y537S mutation model of luminal B breast cancer, exploring how overexpressing ER regulators AIB1 and FOXA1, affect mutant ER activity and these consequences on breast cancer development and endocrine therapy resistance [88].

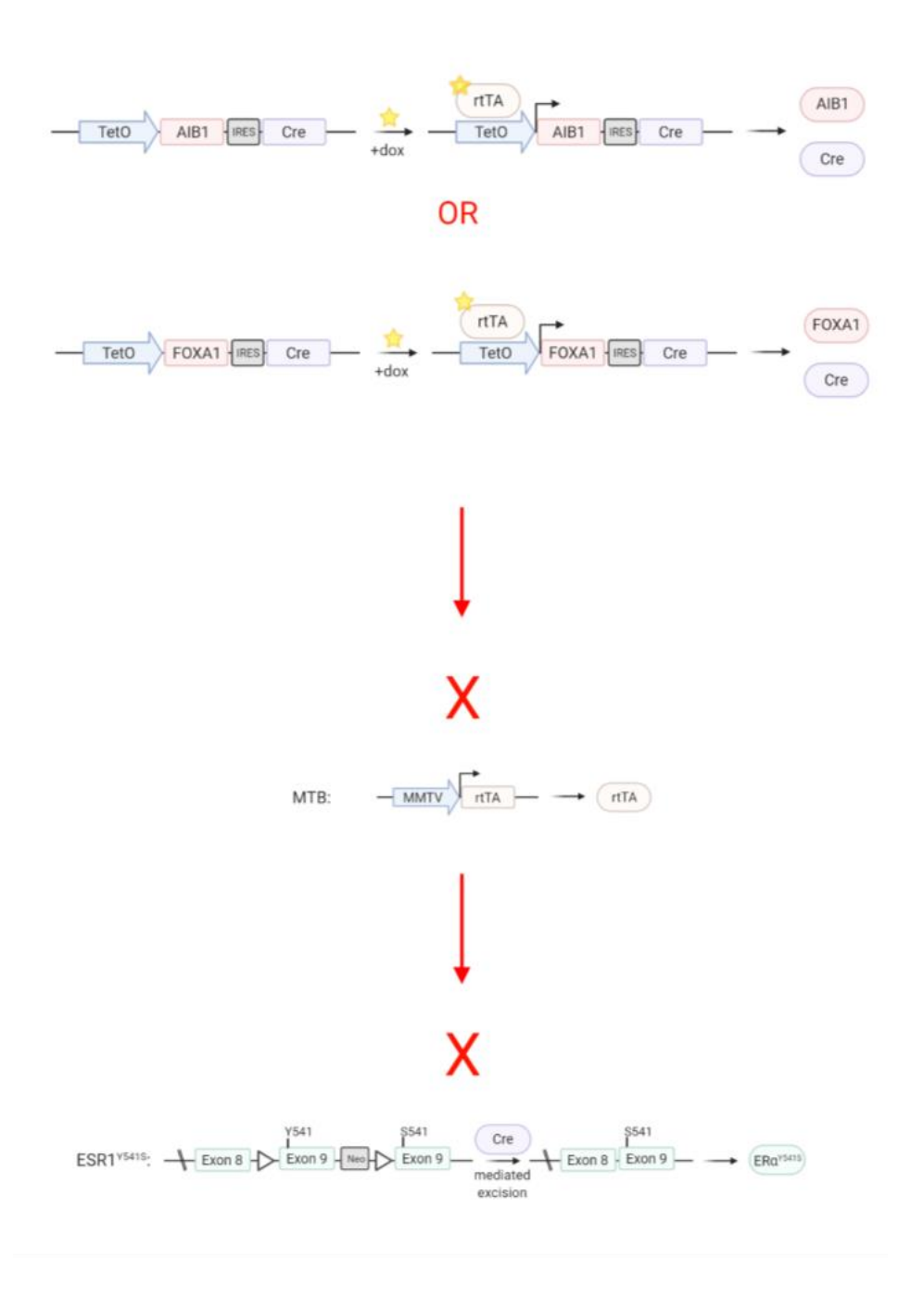


**Figure 2-11: Schematic of AIC/MTB and FIC/MTB cross into ER mutant model ESR1Y537S.**The ESR1Y541S construct carrying the ESR1Y541S mutation (analogous to the human Y537S mutation) will be crossed with the AIB1 and FOXA1 constructs. When these constructs are crossed with the ESR1 YS model, Cre will recognize the lox P sites and excise the DNA between them bringing the exon 9 with

S541 in frame thus introducing the YS mutation to ESR1. Schematic created with BioRender.com.

## 2.2.4 Exploring genes involved in AIB1 and FOXA1 driven tumorigenesis.

To further explore the role of AIB1 and FOXA1 in breast cancer, our lab will use the inducible CRISPR/Cas9 system to identify genes relevant to AIB1 and FOXA1 tumorigenesis. Specifically, cells from the nontransformed mouse mammary gland epithelial cell line (NMuMG) containing the inducible Cas9 system (iCas9) will be transfected with the pMSCV-AIB1 or pMSCV-FOXA1 retrovirus plasmid. The clones with the greatest expression of AIB1 and FOXA1 will be selected and transfected with single guide RNA (sgRNAs), which target and knockout genes throughout the entire mouse genome. The cells, each containing one specific sgRNA, will subsequently be injected into mammary fat pads of immune deficient mice. Tumors arising from these mice will be sequenced to identify genes that were knocked out by sgRNA barcodes. Ultimately, employment of the CRISPR/Cas9 system will provide insight into what players are involved in AIB1 and FOXA1 overexpression tumorigenesis and elucidate the role of oncoproteins AIB1 and FOXA1 in breast cancer development.

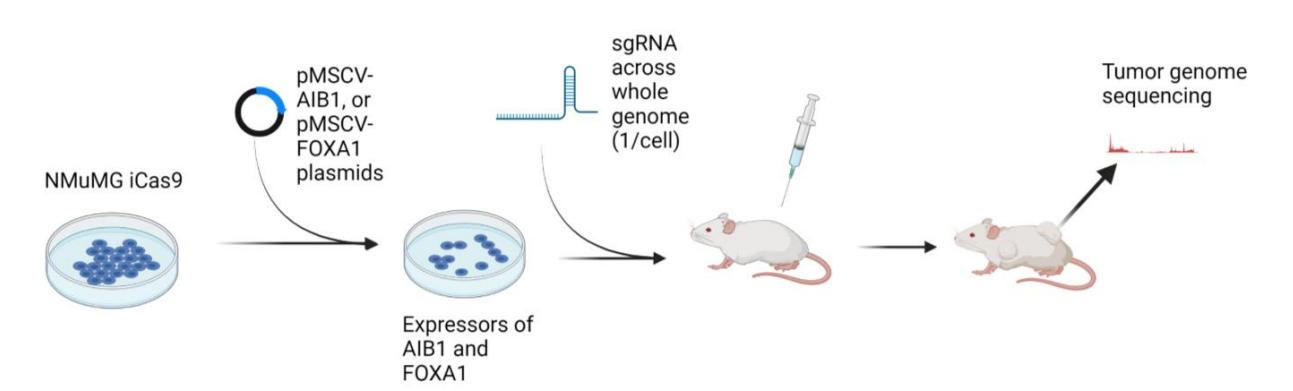


**Figure 2-12:** Employment of inducible CRISPR/Cas9 system to explore genes relevant to AIB1 and FOXA1 tumorigenesis. NMuMG iCas9 cells transfected with pMSCV-AIB1 and pMSCV-FOXA1 will be scanned for high expressors of AIB1 and FOXA1. High expressing cells will be transfected with sgRNA to knockout genes throughout the mouse genome. Cells containing a single sgRNA are injected into mammary fat pads of immune deficient mice. Resulting tumors will be sequenced to identify genes related to AIB1 and FOXA1 driven tumorigenesis. Schematic created with BioRender.com.

#### 3. MATERIALS & METHODS

#### 3.1 Transgenic Animals

# 3.1.1 Mouse Husbandry

Animal housing and experimentation followed guidelines and standards established by the McGill Facility Animal Care Committee and the Canadian Council on Animal Care (CCAC). Mice were housed within the Animal Facility of the Goodman Cancer Institute (GCI) at McGill University. The ESR1Y541S mouse strain was developed by Dr. Chen Ling and maintained through backcrossed breeding into the FVB background strain. Dr. Bin Xiao, with the assistance of Gabriella Johnson, generated the TetO-IRES-Cre-SV40 construct for the AIB1 and FOXA1 models. The McGill transgenic core injected the AIB1 and FOXA1 constructs into FVB mouse embryos and weaned original FIC and AIC founders. Dr. Lewis Chodosh provided the MTB strain for the AIC/MTB and FIC/MTB cross. Dr. Bin Xiao and Alice Nam assisted with the AIC and FIC cohort maintenance. Vasilios Papavasiliou performed sperm extractions for AIC and FIC expressing founders.

## 3.1.2 Doxycycline Induction

Experimental and control mice were induced with doxycycline water containing 200 mg/mL dox (Wisent). Dox water was replenished fresh every week, and dox bottles were cleaned every month. Mice were induced between the ages of 6-12 weeks and maintained on dox for 1-8 weeks in early characterization studies, or until sacrificed at tumor endpoint or sacrificed at 1-year post-induction with no tumor development in long-term induction cohorts.

## 3.1.3 Mammary Tumor Monitoring

In long-term induction cohorts, tumor onset and growth were assessed in experimental and control mice via weekly palpations of mammary glands (MG) and caliper measurements of tumors. Following CCAC guidelines, mice were sacrificed at ethical maximal tumor burden, defined as single tumor volume of 2.5 cm3 or multiple tumor total volume of 6.5 cm3 calculated using the formula V=(4/3)p(L/2)(W/2)2 (L and W representing the length and width respectively).

## 3.1.4 Tissue Sample Processing

Tissue samples, mammary gland, liver, and tail samples, were collected at necropsy, following CCAC guidelines. Collected tissue underwent several pre-processing handlings for epithelial cell extraction, long term storage processing, tissue fixation, viable storage, wholemounts, and DNA extraction. For epithelial cell extraction, harvested MG was kept in 1X phosphate buffered saline (PBS) (137mM NaCl, 2.7mM KCl, 10mM Na2PHO4, 1.8mM KH2PO4) on ice until further processing. Tissue used for RNA and protein extractions were flash frozen in liquid nitrogen and stored at -80°C until further use. Tissue used for Hematoxylin and Eosin (H&E), immunohistochemistry (IHC) or immunofluorescence (IF) were immediately fixed in 10% neutralized formalin for 24 hours, then stored in 70% ethanol at 4°C until further processing. Fixed tissue was paraffin-embedded and sectioned at a thickness of 4µm by the McGill GCI Histological core facility. H&E staining was additionally performed by the Histology Core Facility. Freshly extracted tissues for wholemount analysis were flattened on glass slides and kept in 100% acetone until further processing. Tail segments were collected for DNA extraction and stored at -20°C until further processing.

#### 3.1.4.1 Wholemounts

Following varying induction timepoints, mice were sacrificed according to CCAC guidelines and the left mammary gland 4 (L4) was excised and flattened on a glass slide. Slides were stored in 100% accetone for minimally 24hrs then stained in 100% Harris Modified Hematoxylin (Fisher) overnight. Stained MGs were washed in de-staining solution (70% ethanol, 1% concentrated HCl) overnight. MGs were then dehydrated in 70% ethanol for 30 minutes, again in 100% ethanol for 30 minutes, and then put in xylene for minimally 24hrs. Slides were mounted using glass coverslips and Permount mounting media (Fisher SP15-500) and dried for 48hrs in fume hood. Wholemounts were imaged at 5.3X and 56X magnification using an AxioZoom microscope equipped with a digital camera (Carl Zeiss, Inc.).

## 3.2 DNA Analysis

## 3.2.1 Tail DNA Extraction

Mouse tail segments were collected pre-weaning (2-3 weeks old) and at necropsy for genotyping. Collected tails were digested in 500μL tail buffer (10 mM Tris pH 7.4, 100 mM NaCl, 10 mM EDTA, 0.5% SDS) and 10μL Proteinase K (20 mg/mL) for minimally 24hrs at 55°C. Following digestion, DNA was extracted through a salt wash using 200μL of 5M NaCl. Samples were mixed via inverting tubes and centrifuged at 15 000 rpm for 8 minutes. Supernatant was transferred to a clean Eppendorf tube and the remaining volume filled with 100% ethanol. Mixture was mixed by inverting, DNA was then pelleted by 15 000 rpm centrifugation for 10 minutes at 4°C. Supernatant was aspirated, and pellet dried at room temperature (RT). DNA was resuspended in 200μL of deionized water (diH20) and stored at RT. For more pure DNA extractions, a phenol-chloroform DNA extraction method was used.

## 3.2.2 Genotyping

A polymerase chain reaction (PCR) method was used for identifying the transgene within mice for experimental or breeding purposes. Following tail DNA extractions,  $1\mu$ L of resuspended DNA was added to  $24\mu$ L of PCR master mix (Table 2-1) and run through varying PCR programs (Table 2-2). PCR products were run on 2.5% agarose gel (with 0.5  $\mu$ g/mL ethidium bromide) and imaged by UV light.

Table 3-1: 1X PCR master mix.

PCR Master Mix Component	1X Volume (μL)
ddH2O	19.4
10X EasyTaq Buffer (Civic Bioscience AP111)	2.5
5 mM dNTPs	1
Forward Primer (1/10 dilution)	0.5
Reverse Primer (1/10 dilution)	0.5
Easy Taq	0.1

Table 3-2: Genotyping primer sequences and PCR thermal cycling conditions.

Transgene	Primer Sequences	Thermal Cycling Conditions
AIB1	F1: CTCAGGTCCGCCSGTGAAGAATGT	1. 98°C – 2 mins
	R:GCGTTGCTGCTGTTGTTTG	2. 98°C – 20s
		$3.60^{\circ}\text{C} - 30\text{s}$
		4. 72°C – 1 min
		Repeat 2-4, 29x
		5. 72°C – 2 mins
		6. 4°C – pause
Cre Recombinase	F: GCTTCTGTCCGTTTGCCG	1. 94°C – 2 mins
	R: ACTGTGTCCAGACCAGGC	2. 94°C – 30s
ESR1	F: GCCTTTGCAGTTGCTCATCC	3. 58°C – 45s
	R: TTGTAGACATGCTCCATGCC	4. 72°C – 1 min
		Repeat 2-4, 29x
FOXA1	F: ATGAGAGCAACGACTGGAACA	5. 72°C – 2 mins
	R: TCATGGAGTTCATAGAGCCCA	6. 4°C − pause
GFP	F: AAGTTCATCTGCACCACCG	]
	R:TGCTCAGGTAGTGGTTGTCG	
MT	F: GGAAGCAAGTACTTCACAAGGG	]
	R: GGAAAGTCACTAGGAGCAGGG	
MTB	F: ACCGTACTCGTCAATTCCAAGGG	1
	R: TGCCGCCATTATTACGACAAGC	

## 3.3 Tissue Culture

## 3.3.1 General Cell Culture

All cells grown in culture were plated on Thermo Fisher Scientific NUNC plates in media composed of DMEM, 5  $\mu$ g/mL human insulin, 1  $\mu$ g/L hydrocortisone, 5 ng/mL epidermal growth factor, 35  $\mu$ g/mL bovine pituitary extract, 50  $\mu$ g/mL gentamycin, 1% penicillin streptomycin, 1% amphotericin and varying concentrations of FBS (0-5%). Cells were housed in incubators at 37°C with 5% carbon dioxide. Cells were passed after reaching 70% or greater confluency. To pass cells, cells were washed with 1X PBS, treated with trypsin (Wisent) and incubated for approximately 10 min at 37°C to detach

cells. DMEM was added to deactivate trypsin, and suspended cells were pelleted by centrifugation at 800 rcf (relative centrifugal force) for 3 min, plated on new NUNC plates and incubated at 37°C.

## 3.3.2 Tissue Dissociation and Epithelial Cell Isolation

Mouse mammary glands were dissociated in cell culture to isolate epithelial cells for Fluorescence-activated cell sorting (FACS), protein, and RNA analysis. First MG were finely chopped using a tissue chopper. Homogenized tissue was digested in a 10mL of digestion media (24 mg/tumor Collagenase B; Roche, 24 mg/tumor Dispase II; Roche, 1% penicillin streptomycin in 10 mL DMEM; sterile filtered prior to use) and incubated at 37°C for 2 hours in a hybridization oven. Digested MG solution was centrifuged at 1000 rcf for 1 min, cell pellet was then resuspended in 2 mL Ack lysis buffer (8.3 g NH4Cl, 1.0 g KHCO3, 200 μL 0.5 M EDTA; sterile filtered prior to use) for 2 mins at RT to eliminate red blood cells. 8mL FACS buffer was added to stop Ack lysis incubation, and solution was centrifuged for 1 min at 1000 rfc. Pellet was resuspended in 10 mL FACs buffer and centrifuged at 1000 rcf for 1 min. Pellet was washed in 10mL 1X PBS and cells were pelleted by centrifugation at 1000 rcf for 1min. Supernatant was aspirated, and isolated epithelial cell pellet was flash frozen in liquid nitrogen and stored at -80°C until further processing.

#### 3.3.3 FACS analysis

Isolated MG epithelial cells were used for FACs analysis. Cells were stained then fixed using IC Fixation Buffer (eBioscience). The following antibodies were used in an appropriate combination of fluorochromes: CD29 (clone M1/70, BioLegend), CD24 (clone N418, BioLegend), Cy7-A (clone 30-F11, BD). Samples were analyzed with a BD LSRFortessa flow cytometer (BD Biosciences) and FlowJo software (Tree Star).

## 3.3.4 Organoid Culture

Mammary gland pairs 2, 3, and 4 were collected from mice following mouse necropsy. Mammary glands were finely chopped using a tissue chopper, added to digestion media (DMEM/F12 supplied with

100μg/ml Pen/Strep, 50μg/ml Gentamicin, and 20mg of Collagenase), and incubated at 37°C with rotation, for 2hrs. Following incubation, epithelial cells were pelleted via centrifugation at 1000rpm for 5 minutes. Epithelial cell pellet was washed 5 times using PBS with 5% FBS. Epithelium-derived organoids were treated with trypsin/EDTA and frequent mixing. Trypsin digestion was neutralized with calf serum and the supernatant was passed through a 45μm strainer. Single cells were pelleted and re-suspended in Mammary Epithelial Cell growth medium and seeded on sterile coverslips layered with 15μl of Geltrex. Organoid images were taken with EVOS XL Core microscope (AMEX1000) and analyzed using ZEN software.

#### 3.4 Protein Analysis

#### 3.4.1 Protein extraction

Using either flash frozen and crushed MG or flash frozen MG epithelial cell pellets, tissue was digested with radioimmunoprecipitation assay (RIPA) lysis buffer (10 mM Tris pH 8.0, 1 mM EDTA, 0.5 mM EGTA, 1% Triton X-100, 0.1% sodium deoxycholate, 0.1% SDS, 140 mM NaCl) supplemented with protease inhibitors (1 µg/mL leupeptin, 1 µg/mL aprotinin and 1 mM sodium orthovanadate) on ice for 2hrs. Following the 2-hour digestion, mixture was homogenized. Homogenized lysate was pelleted at 15 000 rpm for 5 min and proteins within the supernatant were collected into new Eppendorf tube and stored at -80°C.

## 3.4.2 Immunoblotting

Protein concentration was determined by Bradford assay (BioRad) and made to equal 2μg/μL protein concentration with 6X SDS-PAGE loading buffer (375 mM Tris pH 6.8, 10% SDS, 60% glycerol, 0.6 M DTT, 0.06% bromophenol blue) and water. Samples were boiled for 5 min at 95°C on heating block and loaded onto acrylamide gels (6-10%) and separated via SDS-PAGE. Protein was transferred onto a polyvinylidene fluoride membrane (Immobilon-FL, Millipore) and blocked in Licor blocking buffer (BSA). Membranes were incubated in primary antibodies (50% Licor blocking buffer and 50% 1X

TBS-T (137 mM NaCl, 2.7 mM KCl, 19 mM Tris base, 0.1% Tween20)) either at RT for 2hrs or overnight at 4°C. Membranes were then incubated in secondary antibodies in (50% Licor blocking buffer, 50% 1X TBS-T, 1/1000 Tween 20) for 1hr at RT and imaged using the Odyssey Imaging System by LI-COR Biosciences. Blots were analyzed using the ImageStudioLite software.

# 3.4.3 Immunohistochemistry (IHC)

Parafin embedded sections processed by McGill's histology core were deparaffinized in xylene, then dehydrated in 100% EtOH. Slides were pressure cooked for 10 minutes in 10 mM sodium citrate solution (pH6) in the antigen retrieval step. Slides were cooled under cold water stream for 10 minutes and subsequently blocked with Power Block (Biogenex) for 5 min at RT. Slides were incubated in primary antibody solution (2% BSA) for either 1hr at RT or overnight at 4°C. Secondary incubation was fone for 1hr at RT, slides were then treated with DAB reagent (Cell Signaling Technologies) for exposure between 10 s and 2 min depending on the antibody. Slides were counterstained with 20% Harris Modified Hematoxylin (Thermo Fisher Scientific) for 30 s and dehydrated using EtOH and xylenes treatments. Stained slides were mounted using ClearMount Mounting Media (America Master Tech) and dried overnight.

#### 3.4.4 Immunofluorescence (IHF)

Immunofluorescence analysis followed identical procedure to IHC, only sections were incubated with fluorescently labeled secondary antibodies (Invitrogen) for 1hr at RT and stained with 0.5 ng/mL 4,6-Diamidino-2-phenylindole (DAPI) in PBS for 5 min at room temperature. Stained slides were washed with PBS and mounted with ImmunoMount (Thermo Scientific). Immunostained sections were imaged using a Zeiss LSM800 confocal microscope and analyzed using the ZEN software.

Table 3-3: Primary antibody summary used for varying protein analysis.

Antibody	Manufacturer	Catalogue	Application
		Number	
AIB1	abcam	ab2831	WB
AIB1	abcam	173287	IHC/IHF
Cre Recombinase	Cell Signalling	15036S	IHC
E-Cadherin	BD Transduction	610182	WB
Flag Tag	Cell Signalling	D6W5B	WB
FOXA1	abcam	ab23738	WB
FOXA1	BD Transduction	611104	IHC
FOXA1	abcam	ab173287	IHC organoid
Vinculin	Milipore	MAB3574	WB

# 3.5 RNA Analysis

## 3.5.1 RNA extraction and cDNA synthesis

RNA was extracted from both flash frozen and crushed MG, and flash frozen epithelial cell pellets using RNA mini kit (Favorgen) according to the manufacturer's instructions. All RNA extractions entailed a 30-minute DNase incubation at RT. NanoDrop Spectrophotometer ND-1000 (NanoDrop Technologies) was used to quantify total RNA. TransGen Biotech kit (AT341) was used to generate first strand cDNA from purified RNA samples.

## 3.5.2 RT-qPCR

Roche LC480 SYBR Green RT-PCR kit (Roche) was used to prepare samples for RT-qPCR analysis. Samples were loaded onto plates in triplicates and run using a LightCycler (Roche) under the GAPDH program (annealing: 56°C, extension: 8 seconds, detection: 75°C. p110a: annealing: 60°C, extension: 8 seconds, detection: 82°C. PTEN: annealing: 62°C, extension: 8 seconds, detection: 76°C. 35 cycles).

Table 3-4: RT-qPCR primer sequences.

Primer	Sequence
Beta-Actin	F: TCCATCATGAAGTGTGACGT
	R: GAGCAATGATCTTCAT
AIB1	F: AGTGGACTAGGCGAAAGCTCT
	R: GTTGTCGATGTCGCTGAGATTT
FOXA1	F: GGAGTTGAAGTCTCCAGCGTC
	R: GGGGTGATTAAAGGAGTAGTGGG
CRE	F: CGGGCTGCCACGACCAAGTGACAG
	R: GTTATAAGCAATCCCCAGAAATGCCAG

# •

# 3.6 Statistical Analysis

All statistical and graphical analysis were generated using Prism software (GraphPad, San Diego, CA). Statistical significance was measured using the two-tailed unpaired Student's t-test.

#### 4. REFERENCES

- [1] Anzick, S. L., Kononen, J., Walker, R. L., Azorsa, D. O., Tanner, M. M., Guan, X. Y., ... & Meltzer, P. S. (1997). AIB1, a steroid receptor coactivator amplified in breast and ovarian cancer. Science, 277(5328), 965-968.
- [2] Bernardo, G. M., & Keri, R. A. (2012). FOXA1: a transcription factor with parallel functions in development and cancer. Bioscience reports, 32(2), 113-130.
- [3] Burandt, E., Jens, G., Holst, F., Jänicke, F., Müller, V., Quaas, A., ... & Lebeau, A. (2013). Prognostic relevance of AIB1 (NCoA3) amplification and overexpression in breast cancer. Breast cancer research and treatment, 137(3), 745-753.
- [4] Foulds, L. (1958) The natural history of cancer, Journal of chronic diseases 8, 2-37.
- [5] Harbeck, N., Penault-Llorca, F., Cortes, J., Gnant, M., Houssami, N., Poortmans, P., ... & Cardoso, F. (2019). Breast cancer. Nature reviews Disease primers, 5(1), 1-31.
- [6] Hurtado, A., Holmes, K. A., Ross-Innes, C. S., Schmidt, D., & Carroll, J. S. (2011). FOXA1 is a key determinant of estrogen receptor function and endocrine response. Nature genetics, 43(1), 27-33.
- [7] Jeselsohn, R., Yelensky, R., Buchwalter, G., Frampton, G., Meric-Bernstam, F., Gonzalez-Angulo, A. M., ... & Miller, V. A. (2014). Emergence of constitutively active estrogen receptor-α mutations in pretreated advanced estrogen receptor–positive breast cancer. Clinical cancer research, 20(7), 1757-1767.
- [8] Makki, J. (2015). Diversity of breast carcinoma: histological subtypes and clinical relevance. Clinical medicine insights: Pathology, 8, CPath-S31563.
- [9] Özdemir, B. C., Sflomos, G., & Brisken, C. (2018). The challenges of modeling hormone receptor-positive breast cancer in mice. Endocrine-related cancer, 25(5), R319-R330.
- [10] Thomas C, Gustafsson JÅ. The different roles of ER subtypes in cancer biology and therapy. Nat Rev Cancer. 2011 Jul 22;11(8):597-608. doi: 10.1038/nrc3093. PMID: 21779010.
- [11] Torre, L. A., et al. (2015) Global cancer statistics, 2012, CA: a cancer journal for clinicians 65, 87-108
- [12] Toy, W., Shen, Y., Won, H., Green, B., Sakr, R. A., Will, M., ... & Chandarlapaty, S. (2013). ESR1 ligand-binding domain mutations in hormone-resistant breast cancer. Nature genetics, 45(12), 1439-1445.
- [13] Breast cancer statistics, <a href="http://www.cancer.ca/en/cancer-information/cancertype/breast/statistics/?region=on">http://www.cancer.ca/en/cancer-information/cancertype/breast/statistics/?region=on</a>
- [14] Riggio, A. I., Varley, K. E., & Welm, A. L. (2021). The lingering mysteries of metastatic recurrence in breast cancer. British journal of cancer, 124(1), 13-26.
- [15] Dai, X., Li, T., Bai, Z., Yang, Y., Liu, X., Zhan, J., & Shi, B. (2015). Breast cancer intrinsic subtype classification, clinical use and future trends. American journal of cancer research, 5(10), 2929–2943.
- [16] Malhotra, G. K., Zhao, X., Band, H., & Band, V. (2010). Histological, molecular and functional subtypes of breast cancers. Cancer biology & therapy, 10(10), 955-960.

- [17] Boisserie-Lacroix, M., Hurtevent-Labrot, G., Ferron, S., Lippa, N., Bonnefoi, H., & Mac Grogan, G. (2013). Correlation between imaging and molecular classification of breast cancers. Diagnostic and interventional imaging, 94(11), 1069-1080.
- [18] Hassiotou, F., & Geddes, D. (2013). Anatomy of the human mammary gland: Current status of knowledge. Clinical anatomy, 26(1), 29-48.
- [19] Khan, Y. S., & Sajjad, H. (2019). Anatomy, Thorax, Mammary Gland.
- [20] Cardiff, R. D., & Wellings, S. R. (1999). The comparative pathology of human and mouse mammary glands. Journal of mammary gland biology and neoplasia, 4(1), 105-122.
- [21] Malhotra, G. K., Zhao, X., Band, H., & Band, V. (2010). Histological, molecular and functional subtypes of breast cancers. Cancer biology & therapy, 10(10), 955-960.
- [22] Allred, D. C., Mohsin, S. K., & Fuqua, S. A. (2001). Histological and biological evolution of human premalignant breast disease. Endocrine-related cancer, 8(1), 47-61.
- [23] Wang, R., Zhu, Y., Liu, X., Liao, X., He, J., & Niu, L. (2019). The Clinicopathological features and survival outcomes of patients with different metastatic sites in stage IV breast cancer. BMC cancer, 19(1), 1-12.
- [24] Li, C. I., Anderson, B. O., Daling, J. R. & Moe, R. E. Trends in incidence rates of invasive lobular and ductal breast carcinoma. JAMA 289, 1421-1424, doi:10.1001/jama.289.11.1421 (2003).
- [25] Rivenbark, A. G., O'Connor, S. M., & Coleman, W. B. (2013). Molecular and cellular heterogeneity in breast cancer: challenges for personalized medicine. The American journal of pathology, 183(4), 1113-1124.
- [26] Parker, J. S., Mullins, M., Cheang, M. C., Leung, S., Voduc, D., Vickery, T., ... & Bernard, P. S. (2009). Supervised risk predictor of breast cancer based on intrinsic subtypes. Journal of clinical oncology, 27(8), 1160.
- [27] Lin, N. U., Vanderplas, A., Hughes, M. E., Theriault, R. L., Edge, S. B., Wong, Y. N., ... & Weeks, J. C. (2012). Clinicopathologic features, patterns of recurrence, and survival among women with triplenegative breast cancer in the National Comprehensive Cancer Network. Cancer, 118(22), 5463-5472.
- [28] Colditz, G. A., Rosner, B. A., Chen, W. Y., Holmes, M. D., & Hankinson, S. E. (2004). Risk factors for breast cancer according to estrogen and progesterone receptor status. Journal of the national cancer institute, 96(3), 218-228.
- [29] Dai, X., Chen, A., & Bai, Z. (2014). Integrative investigation on breast cancer in ER, PR and HER2-defined subgroups using mRNA and miRNA expression profiling. Scientific reports, 4(1), 1-10.
- [30] Carey, L. A., Perou, C. M., Livasy, C. A., Dressler, L. G., Cowan, D., Conway, K., ... & Millikan, R. C. (2006). Race, breast cancer subtypes, and survival in the Carolina Breast Cancer Study. Jama, 295(21), 2492-2502.
- [31] Dustin, D., Gu, G., & Fuqua, S. A. (2019). ESR1 mutations in breast cancer. Cancer, 125(21), 3714-3728.
- [32] Francis, G. A., Fayard, E., Picard, F., & Auwerx, J. (2003). Nuclear receptors and the control of metabolism. Annual review of physiology, 65(1), 261-311.

- [33] Dhiman, V. K., Bolt, M. J., & White, K. P. (2018). Nuclear receptors in cancer—uncovering new and evolving roles through genomic analysis. Nature Reviews Genetics, 19(3), 160-174.
- [34] Renaud, J. P. (2000). Structural studies on nuclear receptors. Cellular and Molecular Life Sciences CMLS, 57(12), 1748-1769.
- [35] Wärnmark, A., Treuter, E., Wright, A. P., & Gustafsson, J. A. (2003). Activation functions 1 and 2 of nuclear receptors: molecular strategies for transcriptional activation. Molecular endocrinology, 17(10), 1901-1909.
- [36] Lee, H. R., Kim, T. H., & Choi, K. C. (2012). Functions and physiological roles of two types of estrogen receptors,  $ER\alpha$  and  $ER\beta$ , identified by estrogen receptor knockout mouse. Laboratory animal research, 28(2), 71-76.
- [37] Kong EH, Pike AC, Hubbard RE. Structure and mechanism of the oestrogen receptor. Biochem Soc Trans. 2003. 31(Pt 1):56–59.
- [38] Beliakoff J, Whitesell L. Hsp90: an emerging target for breast cancer therapy. Anticancer Drugs. 2004. 15(7):651–662.
- [39] Park MA, Hwang KA, Choi KC. Diverse animal models to examine potential role(s) and mechanism of endocrine disrupting chemicals on the tumor progression and prevention: Do they have tumorigenic or anti-tumorigenic property? Lab Anim Res. 2011. 27(4):265–273.
- [40] Barone, I., Brusco, L., & Fuqua, S. A. (2010). Estrogen receptor mutations and changes in downstream gene expression and signaling. Clinical Cancer Research, 16(10), 2702-2708.
- [41] Ikeda, K., Horie-Inoue, K. & Inoue, S. Identification of estrogen-responsive genes based on the DNA binding properties of estrogen receptors using high-throughput sequencing technology. Acta Pharmacol Sin 36, 24-31, doi:10.1038/aps.2014.123 (2015).
- [42] Robinson, D. R. et al. Activating ESR1 mutations in hormone-resistant metastatic breast cancer. Nat Genet 45, 1446-1451, doi:10.1038/ng.2823 (2013).
- [43] Quirke, V. M. (2017). Tamoxifen from failed contraceptive pill to best-selling breast cancer medicine: a case-study in pharmaceutical innovation. Frontiers in pharmacology, 8, 620.
- [44] Buckley, M. M. T., & Goa, K. L. (1989). Tamoxifen. Drugs, 37(4), 451-490.
- [45] Croxtall, J. D., & McKeage, K. (2011). Fulvestrant. Drugs, 71(3), 363-380.
- [46] Geisler, J. (2011). Differences between the non-steroidal aromatase inhibitors anastrozole and letrozole–of clinical importance?. British journal of cancer, 104(7), 1059-1066.
- [47] Robinson, D. R., Wu, Y. M., Vats, P., Su, F., Lonigro, R. J., Cao, X., ... & Chinnaiyan, A. M. (2013). Activating ESR1 mutations in hormone-resistant metastatic breast cancer. Nature genetics, 45(12), 1446-1451.
- [48] Chang, A. K., & Wu, H. (2012). The role of AIB1 in breast cancer. Oncology Letters, 4(4), 588-594.
- [49] Szwarc, M. M., Kommagani, R., Lessey, B. A., & Lydon, J. P. (2014). The p160/steroid receptor coactivator family: potent arbiters of uterine physiology and dysfunction. Biology of reproduction, 91(5), 122-1.

- [50] Amazit, L., Pasini, L., Szafran, A. T., Berno, V., Wu, R. C., Mielke, M., ... & Mancini, M. A. (2007). Regulation of SRC-3 intercompartmental dynamics by estrogen receptor and phosphorylation. Molecular and cellular biology, 27(19), 6913-6932.
- [51] Savkur, R. S., & Burris, T. P. (2004). The coactivator LXXLL nuclear receptor recognition motif. The journal of peptide research, 63(3), 207-212.
- [52] Voegel, J. J., Heine, M. J., Tini, M., Vivat, V., Chambon, P., & Gronemeyer, H. (1998). The coactivator TIF2 contains three nuclear receptor-binding motifs and mediates transactivation through CBP binding-dependent and-independent pathways. The EMBO journal, 17(2), 507-519.
- [53] Qi, C., Chang, J., Zhu, Y., Yeldandi, A. V., Rao, S. M., & Zhu, Y. J. (2002). Identification of protein arginine methyltransferase 2 as a coactivator for estrogen receptor α. Journal of Biological Chemistry, 277(32), 28624-28630.
- [54] Liao, L., Kuang, S. Q., Yuan, Y., Gonzalez, S. M., O'Malley, B. W., & Xu, J. (2002). Molecular structure and biological function of the cancer-amplified nuclear receptor coactivator SRC-3/AIB1. The Journal of steroid biochemistry and molecular biology, 83(1-5), 3-14.
- [55] Oh, A. S., Lahusen, J. T., Chien, C. D., Fereshteh, M. P., Zhang, X., Dakshanamurthy, S., ... & Riegel, A. T. (2008). Tyrosine phosphorylation of the nuclear receptor coactivator AIB1/SRC-3 is enhanced by Abl kinase and is required for its activity in cancer cells. Molecular and cellular biology, 28(21), 6580-6593.
- [56] Yi, P., Feng, Q., Amazit, L., Lonard, D. M., Tsai, S. Y., Tsai, M. J., & O'Malley, B. W. (2008). Atypical protein kinase C regulates dual pathways for degradation of the oncogenic coactivator SRC-3/AIB1. Molecular cell, 29(4), 465-476.
- [57] Font de Mora, J., & Brown, M. (2000). AIB1 is a conduit for kinase-mediated growth factor signaling to the estrogen receptor. Molecular and cellular biology, 20(14), 5041-5047.
- [58] Labhart, P., Karmakar, S., Salicru, E. M., Egan, B. S., Alexiadis, V., O'Malley, B. W., & Smith, C. L. (2005). Identification of target genes in breast cancer cells directly regulated by the SRC-3/AIB1 coactivator. Proceedings of the National Academy of Sciences, 102(5), 1339-1344.
- [59] Su, Q., Hu, S., Gao, H., Ma, R., Yang, Q., Pan, Z., ... & Li, F. (2008). Role of AIB1 for tamoxifen resistance in estrogen receptor-positive breast cancer cells. Oncology, 75(3-4), 159-168.
- [60] Louie, M. C., Zou, J. X., Rabinovich, A., & Chen, H. W. (2004). ACTR/AIB1 functions as an E2F1 coactivator to promote breast cancer cell proliferation and antiestrogen resistance. Molecular and cellular biology, 24(12), 5157-5171.
- [61] Oh, A., List, H. J., Reiter, R., Mani, A., Zhang, Y., Gehan, E., ... & Riegel, A. T. (2004). The nuclear receptor coactivator AIB1 mediates insulin-like growth factor I-induced phenotypic changes in human breast cancer cells. Cancer research, 64(22), 8299-8308.
- [62] Shanmugalingam, T., Bosco, C., Ridley, A. J., & Van Hemelrijck, M. (2016). Is there a role for IGF-1 in the development of second primary cancers?. Cancer medicine, 5(11), 3353–3367.
- [63] Torres-Arzayus, M. I., de Mora, J. F., Yuan, J., Vazquez, F., Bronson, R., Rue, M., ... & Brown, M. (2004). High tumor incidence and activation of the PI3K/AKT pathway in transgenic mice define AIB1 as an oncogene. Cancer cell, 6(3), 263-274.

- [64] Torres-Arzayus, M. I., Zhao, J., Bronson, R., & Brown, M. (2010). Estrogen-dependent and estrogen-independent mechanisms contribute to AIB1-mediated tumor formation. Cancer research, 70(10), 4102-4111.
- [65] Xu, J., Qiu, Y., DeMayo, F. J., Tsai, S. Y., Tsai, M. J., & O'Malley, B. W. (1998). Partial hormone resistance in mice with disruption of the steroid receptor coactivator-1 (SRC-1) gene. Science, 279(5358), 1922-1925.
- [66] Nakshatri, H., & Badve, S. (2009). FOXA1 in breast cancer. Expert reviews in molecular medicine, 11.
- [67] Costa, R. H., Grayson, D. R., & Darnell Jr, J. E. (1989). Multiple hepatocyte-enriched nuclear factors function in the regulation of transthyretin and alpha 1-antitrypsin genes. Molecular and cellular biology, 9(4), 1415-1425.
- [68] Lai, E. S. E. N. G., Prezioso, V. R., Tao, W. F., Chen, W. S., & Darnell, J. E. (1991). Hepatocyte nuclear factor 3 alpha belongs to a gene family in mammals that is homologous to the Drosophila homeotic gene fork head. Genes & development, 5(3), 416-427.
- [69] Cirillo, L. A., & Zaret, K. S. (2007). Specific interactions of the wing domains of FOXA1 transcription factor with DNA. Journal of molecular biology, 366(3), 720-724.
- [70] Clark, K. L., Halay, E. D., Lai, E., & Burley, S. K. (1993). Co-crystal structure of the HNF-3/fork head DNA-recognition motif resembles histone H5. Nature, 364(6436), 412-420.
- [71] Qian, X., & Costa, R. H. (1995). Analysis of hepatocyte nuclear factor-3β protein domains required for transcriptional activation and nuclear targeting. Nucleic acids research, 23(7), 1184-1191.
- [72] Badve, S., Turbin, D., Thorat, M. A., Morimiya, A., Nielsen, T. O., Perou, C. M., ... & Nakshatri, H. (2007). FOXA1 expression in breast cancer—correlation with luminal subtype A and survival. Clinical cancer research, 13(15), 4415-4421.
- [73] Cirillo, L. A., Lin, F. R., Cuesta, I., Friedman, D., Jarnik, M., & Zaret, K. S. (2002). Opening of compacted chromatin by early developmental transcription factors HNF3 (FoxA) and GATA-4. Molecular cell, 9(2), 279-289.
- [74] Kohler, S., & Cirillo, L. A. (2010). Stable chromatin binding prevents FoxA acetylation, preserving FoxA chromatin remodeling. The Journal of biological chemistry, 285(1), 464–472.
- [75] Tong, Q., & Hotamisligil, G. S. (2007). Cell fate in the mammary gland. Nature, 445(7129), 724-726.
- [76] Albergaria, A., Paredes, J., Sousa, B., Milanezi, F., Carneiro, V., Bastos, J., ... & Schmitt, F. (2009). Expression of FOXA1 and GATA-3 in breast cancer: the prognostic significance in hormone receptornegative tumours. Breast cancer research, 11(3), 1-15.
- [77] Theodorou, V., Stark, R., Menon, S., & Carroll, J. S. (2013). GATA3 acts upstream of FOXA1 in mediating ESR1 binding by shaping enhancer accessibility. Genome research, 23(1), 12-22.
- [78] Lupien, M., Eeckhoute, J., Meyer, C. A., Wang, Q., Zhang, Y., Li, W., ... & Brown, M. (2008). FoxA1 translates epigenetic signatures into enhancer-driven lineage-specific transcription. Cell, 132(6), 958-970.

- [79] Carlsson, P., & Mahlapuu, M. (2002). Forkhead transcription factors: key players in development and metabolism. Developmental biology, 250(1), 1-23.
- [80] Williamson, E. A., Wolf, I., O'kelly, J., Bose, S., Tanosaki, S., & Koeffler, H. P. (2006). BRCA1 and FOXA1 proteins coregulate the expression of the cell cycle-dependent kinase inhibitor p27Kip1. Oncogene, 25(9), 1391-1399.
- [81] Badve, S., Turbin, D., Thorat, M. A., Morimiya, A., Nielsen, T. O., Perou, C. M., ... & Nakshatri, H. (2007). FOXA1 expression in breast cancer—correlation with luminal subtype A and survival. Clinical cancer research, 13(15), 4415-4421.
- [82] Liu, Y., Zhao, Y., Skerry, B., Wang, X., Colin-Cassin, C., Radisky, D. C., ... & Li, Z. (2016). Foxal is essential for mammary duct formation. Genesis, 54(5), 277-285.
- [83] Cardiff, R. D., & Kenney, N. (2007). Mouse mammary tumor biology: a short history. Advances in cancer research, 98, 53-116.
- [84] Bouabe, H., & Okkenhaug, K. (2013). Gene targeting in mice: a review. Virus-Host Interactions, 315-336.
- [85] Ursini-Siegel, J., Schade, B., Cardiff, R. D., & Muller, W. J. (2007). Insights from transgenic mouse models of ERBB2-induced breast cancer. Nature Reviews Cancer, 7(5), 389-397.
- [86] Gossen, M., Freundlieb, S., Bender, G., Müller, G., Hillen, W., & Bujard, H. (1995). Transcriptional activation by tetracyclines in mammalian cells. Science, 268(5218), 1766-1769.
- [87] Dabydeen, S. A., & Furth, P. A. (2014). Genetically engineered ERα-positive breast cancer mouse models. Endocrine-related cancer, 21(3), R195-R208.
- [88] Simond, A. M., Ling, C., Moore, M. J., Condotta, S. A., Richer, M. J., & Muller, W. J. (2020). Point-activated ESR1Y541S has a dramatic effect on the development of sexually dimorphic organs. Genes & development, 34(19-20), 1304-1309.
- [89] Moore, M. Investigating the role of the mutant estrogen receptor in mammary gland development and tumourigenesis Master of Science thesis, McGill University, (2020).
- [90] Hoffman, R. M. (2002). Green fluorescent protein imaging of tumour growth, metastasis, and angiogenesis in mouse models. The lancet oncology, 3(9), 546-556.
- [91] Mao, X., Fujiwara, Y., Chapdelaine, A., Yang, H., & Orkin, S. H. (2001). Activation of EGFP expression by Cre-mediated excision in a new ROSA26 reporter mouse strain. Blood, The Journal of the American Society of Hematology, 97(1), 324-326.
- [92] Chishima, T., Miyagi, Y., Wang, X., Yamaoka, H., Shimada, H., Moossa, A. R., & Hoffman, R. M. (1997). Cancer invasion and micrometastasis visualized in live tissue by green fluorescent protein expression. Cancer research, 57(10), 2042-2047.
- [93] Jeselsohn, R. et al. Allele-Specific Chromatin Recruitment and Therapeutic Vulnerabilities of ESR1 Activating Mutations. Cancer Cell 33, 173-186 e175, doi:10.1016/j.ccell.2018.01.004 (2018).
- [94] Spoerke, J. M., Gendreau, S., Walter, K., Qiu, J., Wilson, T. R., Savage, H., ... & Lackner, M. R. (2016). Heterogeneity and clinical significance of ESR1 mutations in ER-positive metastatic breast cancer patients receiving fulvestrant. Nature communications, 7(1), 1-10.

- [95] Team, the H. E. (2018, January 22). Mammary duct anatomy, Function & Diagram | Body Maps. Healthline. Retrieved May 16, 2022, from <a href="https://www.healthline.com/human-body-maps/mammary-duct#2">https://www.healthline.com/human-body-maps/mammary-duct#2</a>
- [96] Laronga, C. (2020, November 13). Patient education: Breast cancer guide to diagnosis and treatment (Beyond the Basics)Christine. UpToDate. Retrieved May 16, 2022, from <a href="https://www.uptodate.com/contents/breast-cancer-guide-to-diagnosis-and-treatment-beyond-the-basics/print">https://www.uptodate.com/contents/breast-cancer-guide-to-diagnosis-and-treatment-beyond-the-basics/print</a>
- [97] Bertucci, F., Borie, N., Ginestier, C., Groulet, A., Charafe-Jauffret, E., Adelaide, J., ... & Birnbaum, D. (2004). Identification and validation of an ERBB2 gene expression signature in breast cancers. Oncogene, 23(14), 2564-2575.
- [98] Fluck, M. M. & Schaffhausen, B. S. Lessons in signaling and tumorigenesis from polyomavirus middle T antigen. Microbiol Mol Biol Rev 73, 542-563, Table of Contents, doi:10.1128/MMBR.00009-09 (2009).
- [99] Dawe, C. J. et al. Variations in polyoma virus genotype in relation to tumor induction in mice. Characterization of wild type strains with widely differing tumor profiles. Am J Pathol 127, 243-261 (1987).
- [100] Guy, C. T., Cardiff, R. D. & Muller, W. J. Induction of mammary tumors by expression of polyomavirus middle T oncogene: a transgenic mouse model for metastatic disease. Mol Cell Biol 12, 954-961, doi:10.1128/mcb.12.3.954 (1992).
- [101] Lin, E. Y. et al. Progression to malignancy in the polyoma middle T oncoprotein mouse breast cancer model provides a reliable model for human diseases. Am J Pathol 163, 2113-2126, doi:10.1016/S0002-9440(10)63568-7 (2003).